



Eidgenössische Technische Hochschule Zürich  
Swiss Federal Institute of Technology Zurich



# Optimization and assessment of low-carbon hydrogen supply chains

Master's Thesis

Politecnico di Torino, Dipartimento di Energia  
Corso di Laurea Magistrale  
in Ingegneria Energetica e Nucleare

**Candidate:**

Annalisa Guidolin

**Examiner:**

Prof. Dr. Massimo Santarelli

**Supervision:**

Prof. Dr. Marco Mazzotti  
Dr. Paolo Gabrielli

**Academic Year:**

2018-2019

Submitted on July 12, 2019 to the Department of Energy at Politecnico di Torino in partial fulfillment of the requirements of the Department of Mechanical and Process Engineering at ETH Zurich.

## Abstract

This project was conceived as an extension of a pre-existing optimization tool determining the optimal design of a multi-energy system. The tool determines the optimal selection, sizing and operation of a set of technologies to satisfy the hydrogen demand of an end-user while minimizing the total costs or CO<sub>2</sub> emissions of the system [1]. The main goal is to include the spatial network perspective, with the aim of designing an optimal supply chain at a national scale for the use of hydrogen in the mobility sector. Concerning hydrogen production, a comparative assessment of production technologies for blue and green hydrogen, e.g. Steam Methane Reforming and electrolysis, has been carried out. Furthermore, the trade-off between two different types of biomass as energy source was investigated for two processes: biomass gasification with ‘dry’ biomass and biogas reforming with ‘wet’ biomass. They were selected because they are both very interesting for integrated hydrogen production with CCS towards a negative CO<sub>2</sub> emissions supply-chain. Three economically competitive networks were analyzed for hydrogen transport: namely railway, pipeline and truck. Similarly, dry biomass distribution was also considered for the hydrogen production via gasification. Several model parameters and assumption have been investigated through sensitivity analysis, namely the impact of energy losses, the size effect on the investment cost and the effect on the minimum and maximum energy carried by the different networks.

## Acknowledgement

E' stato un bellissimo e lunghissimo percorso. Non mi sembra vero di essere arrivata alla fine di questo viaggio che in realtà non è altro che un grande nuovo inizio. Ci sarebbero tantissime persone da ringraziare che mi hanno accompagnato in quasi sei anni al Politecnico e, anche se sembrerà banale, voglio iniziare dalle persone senza le quali non sarei qui: mamma e papà. Mamma, tu sei una Donna con la D maiuscola che crede sempre e costantemente in sua figlia. A volte mi infastidisco quando mi dicono che sono uguale a te ma la realtà è che sono super fiera di esserlo! Grazie per essere un esempio da seguire ogni giorno. Papà, devo ringraziarti per la tua generosità e bontà, senza tutti i sacrifici che hai fatto io non potrei essere qui ,in questo momento, a leggere gli 'Acknowledgement' di questa tesi vicino a te; quindi grazie per avermi regalato il bel presente che vivo tutti i giorni. Ringrazio poi le mie sisters, così assurdamente diverse ma che a modo loro entrambe mi hanno sostenuto in questo lungo percorso. Grazie a Fabio, così esterno dal mio mondo ma che ha sempre cercato di starmi vicino nei momenti difficile e gioire nei momenti gloriosi. Grazie alle mie amiche di sempre Groi, Fre, Laure, Ceci che ci siete state dal primo giorno in cui ho messo piede qua dentro all'ultimo. Grazie ai miei compagni, Ila, Paoli, Simo , Mulan, Heddy e Fra con cui ho condiviso sicuramente dolori, ma alla fine anche tante gioie. Gli ultimi ringraziamenti vanno alla persone che hanno fatto parte della mia vita a Zurigo in questi sei mesi di tesi all'estero. Solo a pensare a come sono arrivata ed a come sono uscita mi vengono i brividi. Un'esperienza che mi ha cambiato completamente la vita. Ringrazio Bea, compagna di vita da sempre e che ho riscoperto a Zurigo, talmente inseparabili che l'ETH ci conosce come Annatrice. Ringrazio Paolo, mio supervisor di tesi ma ormai anche amico: penso che tu sia la persona da cui ho imparato di più fino ad oggi: grazie davvero per sopportarmi e per avermi fatto da psicologo costante in questi sei mesi. Ringrazio tutti gli altri ragazzi del lab all'ETH, ognuno di loro mi ha fatto crescere in modo diverso ed unico. Infine, ma non per importanza, ringrazio Marco: grazie per avermi dato l'opportunità più bella della mia vita fino ad oggi. Ti guardo sempre con ammirazione, ricordandomi ogni giorno di quanto sia stata fortunata ad averti come zio, e in seconda veste da professore. La tua professionalità e bontà sono davvero uniche, da grande vorrei essere come te!

Grazie a tutte le persone che fanno parte della mia vita oggi, vi voglio bene.

Annalisa

# Contents

<b>Abstract</b>	<b>I</b>
<b>Acknowledgement</b>	<b>II</b>
<b>1 Introduction</b>	<b>1</b>
1.1 Motivation . . . . .	1
1.2 Aim of the thesis . . . . .	3
<b>2 Configuration of the system</b>	<b>5</b>
2.1 Topology . . . . .	5
2.1.1 Ideal schematic configuration . . . . .	5
2.1.2 Realistic schematic configuration . . . . .	6
2.1.3 Realistic ArcGIS configuration . . . . .	7
2.2 Technology portfolio . . . . .	8
2.3 Network portfolio . . . . .	14
<b>3 Formulation of the optimization problem</b>	<b>15</b>
3.1 Input data . . . . .	15
3.2 Decision variables . . . . .	16
3.3 Constraints . . . . .	16
3.3.1 Conversion technologies and network . . . . .	16
3.3.2 Energy balance between the nodes . . . . .	17
3.4 Objective function . . . . .	18
<b>4 Multi-objective optimization</b>	<b>21</b>
4.1 Optimal competition between the networks . . . . .	23
<b>5 Sensitivity analyses on model parameters</b>	<b>25</b>
5.1 Energy loss coefficient $l$ . . . . .	25
5.1.1 Total energy losses . . . . .	28
5.2 Minimum size of networks . . . . .	30
5.2.1 Minimum railway size . . . . .	30
5.2.2 Minimum truck size . . . . .	33
5.3 Transport pressure . . . . .	35
5.4 Investment cost approximation . . . . .	36
5.4.1 Schematic configuration result . . . . .	38
5.4.2 ArcGIS configuration result . . . . .	39
<b>6 Optimal design of hydrogen supply chains</b>	<b>40</b>
6.1 Competition between SMR and PEME . . . . .	40
6.1.1 Impact of the emission factor of the electricity grid $\epsilon_e$ . . . . .	43
6.2 Role of biomass . . . . .	45
6.2.1 Impact of biomass availability on optimal design . . . . .	45
6.3 Role of carbon capture and storage . . . . .	56
6.3.1 Capture technologies without CO <sub>2</sub> sink . . . . .	56
6.3.2 Capture technologies with CO <sub>2</sub> sink . . . . .	58
<b>7 Conclusions and Outlook</b>	<b>62</b>
7.1 Summary of main results . . . . .	62
7.2 Outlook . . . . .	63
<b>Appendices</b>	<b>64</b>
A Hydrogen demand . . . . .	64
B Energy carriers . . . . .	64
C Technology cost coefficients and performance . . . . .	65
D Network input data . . . . .	66



# 1 Introduction

## 1.1 Motivation

At the Paris climate conference (COP21) in December 2015, 195 countries adopted the first-ever universal, legally binding global climate deal. The agreement sets out a global action plan to put the world on track to avoid dangerous climate change by limiting global warming to well below 2°C and pursuing efforts to limit it to 1.5°C [2]. According to the IPCC Special Report published in October 2018 [?], human activities are estimated to have caused approximately 1.0°C of global warming above pre-industrial levels. Global warming is likely to reach 1.5°C between 2030 and 2052 if it continues to increase at the current rate. Figure 1 shows the general characteristics of the evolution of anthropogenic net emissions of CO<sub>2</sub> pathways limiting global warming to 1.5°C with no or limited overshoot (blue area) and pathways with higher overshoot (grey area). The panels on the right show non-CO<sub>2</sub> emissions ranges for three compounds with large historical forcing and a substantial portion of emissions coming from sources distinct from those central to CO<sub>2</sub> mitigation [3].

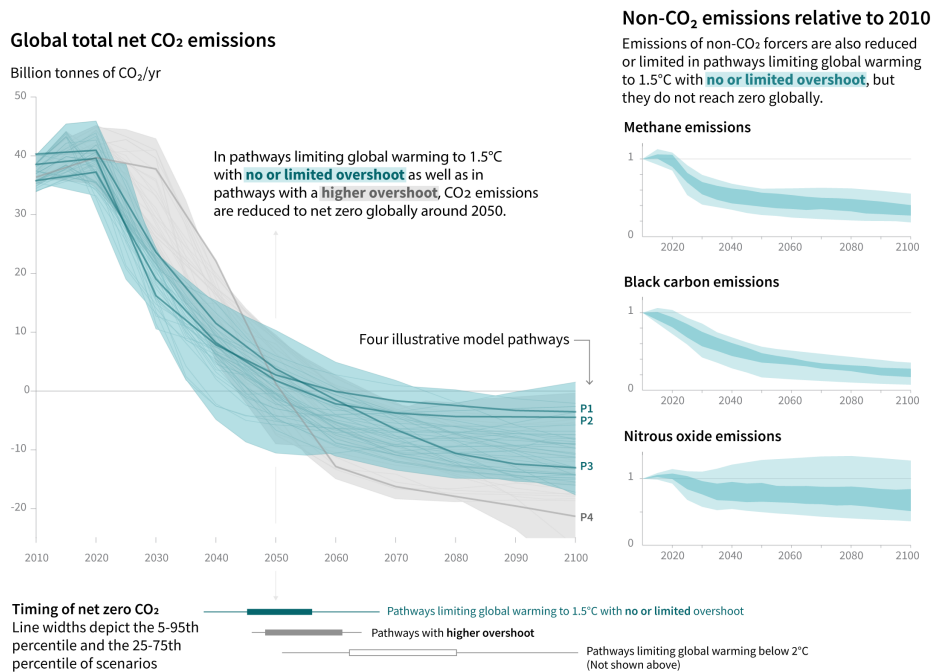


**Figure 1:** Global emissions pathway characteristics [3].

In model pathways with no or limited overshoot of 1.5°C, global net anthropogenic CO<sub>2</sub> emissions decline by about 45% from 2010 levels by 2030, reaching net zero around 2050. For limiting global warming to below 2°C, CO<sub>2</sub> emissions are projected to decline by about 25% by 2030 in most pathways and reach net zero around 2070. CO<sub>2</sub> emissions reductions that limit global warming to 1.5°C with no or limited overshoot can involve different portfolios of mitigation measures.

It is clear that significant changes are requested in many fields of our society. Nowadays, the most CO<sub>2</sub> emitting sectors worldwide are shown in Fig. 2 [4].

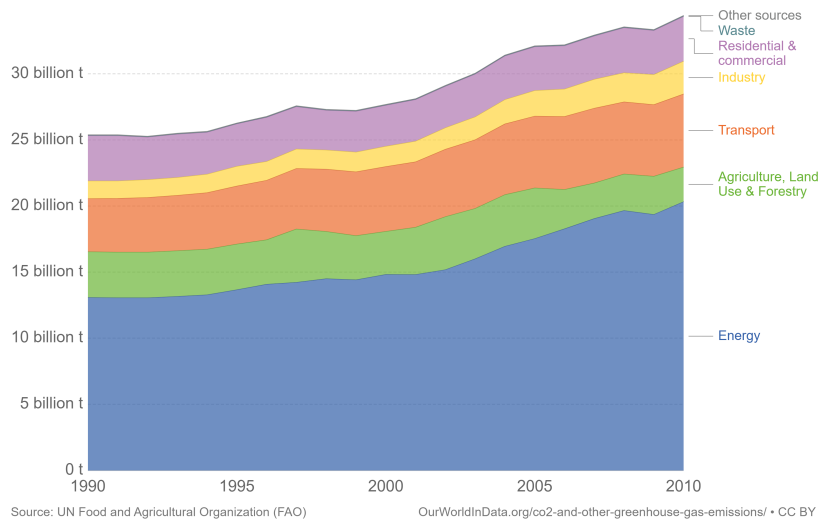


**Figure 2:** Worldwide carbon dioxide emission by sector [4].

The transportation sector is the second world-emitting, bringing it at the centre of the interest for the possibility of decarbonizing the infrastructure. Many efforts are already been done by the industry with the electrification of the mobility sector. Another possibility could be the use of **hydrogen** as an alternative fuel. It is clean and efficient if it is used to power fuel cell propulsion systems, or it can be used directly to fuel the ordinary internal combustion engines. Moreover, hydrogen has the benefits of improving security of fuel supplies since it can be produced from diverse primary energy sources, such as hydrocarbons, wind, biomass, water, or solar energy [5]. It is in this framework that the Elegancy project is inserted. It is a European project funded by DE/TEC (CH), BMWi (DE), RVO (NL), Gassnova (NO), BEIS (UK), Gassco, Equinor and Total, and is cofunded by the European Commission under the Horizon 2020 programme. The project’s primary objective is to decarbonize Europe’s energy system by exploiting the synergies between two key low-carbon technologies: H<sub>2</sub> and CCS (Carbon Capture and Storage) [6]. The integration of CCS in the production chain of hydrogen is fundamental. Currently, around 90% of the feedstock used in the production of hydrogen are from fossil resources, e.g. natural gas. During the conversion process from fossil to hydrogen, a significant amount of carbon dioxide is produced and if not captured, emitted to the atmosphere [7]. If CCS is inserted, it could become a net zero-emissions fuel for transportation, fulfilling perfectly the task of the decarbonization in the transportation sector. The comprehensive ELEGANCY research programme is carried out in six work packages (WP):

1. H<sub>2</sub> supply chain and H<sub>2</sub>-CO<sub>2</sub> separation (WP1)
2. CO<sub>2</sub> transport, injection and storage (WP2)
3. Business case development for H<sub>2</sub>-CCS integrated chains (WP3)
4. H<sub>2</sub>-CCS chain tool and evaluation methodologies for integrated chains (WP4)
5. Case studies (WP5): Switzerland, Netherlands, UK, Germany and Norway.

This Master’s thesis is inserted in the Elegancy framework, sharing most of the goals included in the work packages.

## 1.2 Aim of the thesis

The goal of this Master's thesis is to design and assess a low-carbon hydrogen supply chain through an optimization model. A supply chain is defined as an infrastructure able to produce, transport and distribute the final product, in this case hydrogen. In other words, it consists of a set of hydrogen production technologies and a set of networks able to supply the end-users, in this case the mobility sector. In order to optimize the supply chain, it must be inserted in an optimization framework.

During previous activities, an optimization tool was developed to determine the optimal design of multi-energy systems. The tool determines the optimal selection, sizing and operation of a set of technologies to satisfy the hydrogen demand of an end-user while minimizing the total costs and the CO<sub>2</sub> emissions of the system [1].

In this project, this tool was extended to include the spatial network perspective, with the goal of designing an optimal supply chain at a national scale for the use of hydrogen in the mobility sector. Switzerland has been chosen as the reference territory to which the model is applied, in order to satisfy the requirements of WP5 of Elegancy. The overall configuration of the system is shown in the following Figure 3. The configuration consists on a set of nodes connected between each other. Each of them is

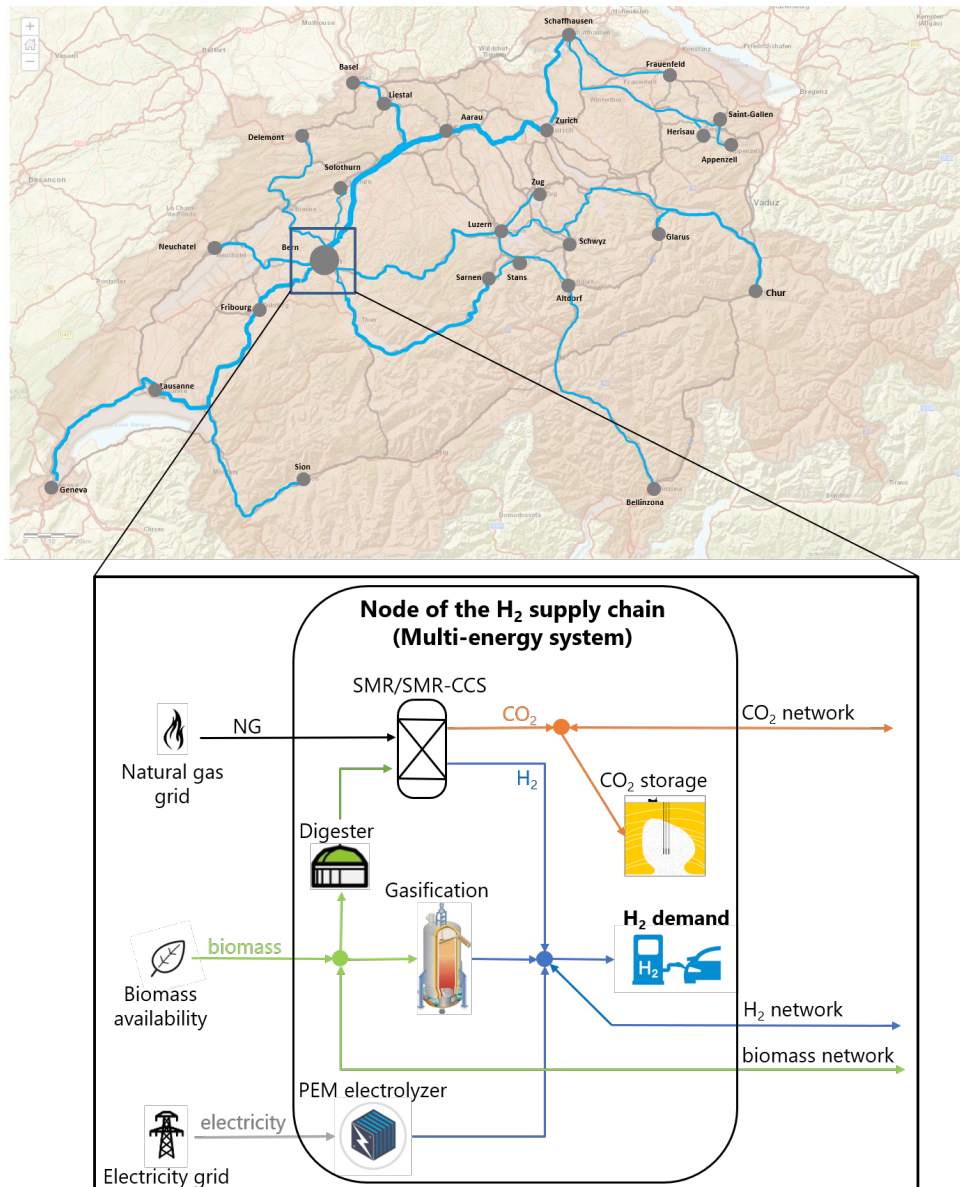


**Figure 3:** Configuration of the overall hydrogen supply-chain system applied to Switzerland.

described with the technology portfolio shown in Fig. 3, referred as a multi-energy system (MES). It consists on the set of technologies which produce hydrogen and CO<sub>2</sub>, both *green hydrogen* technologies, meaning that the energy source exploited is renewable, and *blue hydrogen* technologies, which describe a process which uses fossil-nature energy source. Concerning the first ones, the first typology of technologies are based on biomass, both ligneocellulosic (named *dry biomass*) and wet waste-based (named *wet biomass*). Concerning the first one, a biomass gasification process is analyzed, while for the second a biomethane steam reforming process is considered, having produced the biomethane through a digester. The main product from both of the biomass technologies are hydrogen and CO<sub>2</sub>, the latter originated from the carbonaceous nature of biomass itself and so considered biogenic. The second typology of green hydrogen production pathways is the electrolyzer technology: it separates the water molecule with electricity imported from the grid, which can be renewable, and produces hydrogen and oxygen. Concerning the blue hydrogen production technologies, the steam methane reforming process from natural gas is considered which produces hydrogen and CO<sub>2</sub>, generated from the reforming chemical reaction of methane. The last typology of technologies presented in the portfolio are the CO<sub>2</sub> capture technology. In particular, the steam methane reformer with two different capture processes is considered. The hydrogen produced by the overall MES is satisfying either the hydrogen demand in-*loco* or it is sent to the hydrogen network which transports it towards the end users. In the same way, the CO<sub>2</sub> is either stored in-*loco* or sent to an external storage through the CO<sub>2</sub> network. The goal of this project is firstly to gain a deep understanding on how the model behaves, and for this purpose, a lot of sensitivity analyses are performed to discover and afterwards focus the attention on the main parameters influencing the system. The second main aim consists of the assessment of the competition between the different supply chains producing hydrogen and CO<sub>2</sub> through the optimization problem, minimizing the total costs and the CO<sub>2</sub> emissions of the system and finally to discover their trade-offs varying both of the objective functions.

## 2 Configuration of the system

### 2.1 Topology

The topology of a hydrogen supply chain consists of the subdivision of the territory under investigation in cells, each of them connected to the adjacent ones. It is investigated through three representations: the first defined as ideal schematic, the second realistic schematic and the third realistic.

The advantage to design an optimal supply chain for different configurations is the comparison between the results achieved: the modeling conclusions have to be the same for every configuration.

#### 2.1.1 Ideal schematic configuration

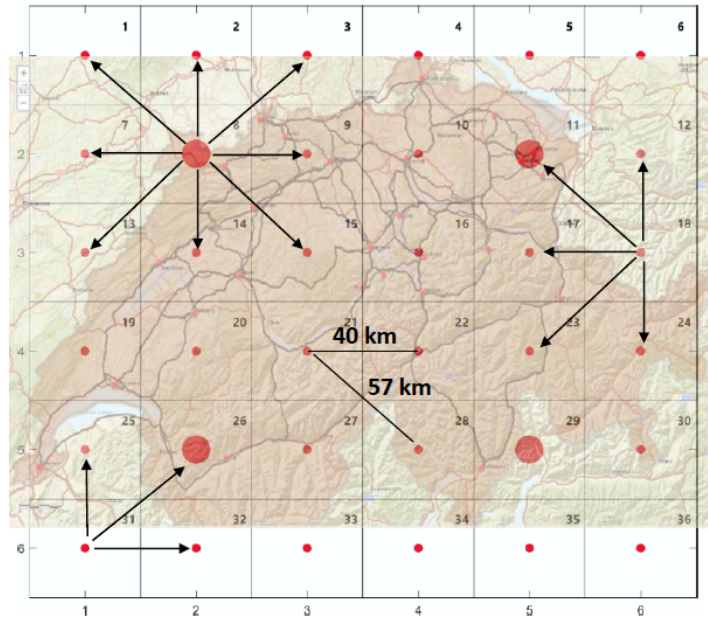


Figure 4: Ideal and schematic configuration of the system.

The choice of a schematic configuration is due to its simplicity: it is very useful to investigate efficiently the impact of the input data on the system configuration. It is constituted by 36 nodes disposed as a 6-by-6 matrix. Each node is representing a fraction of the territory to which the model is applied and is collocated in the centre of each cell. For this reason, the distance between two nodes is  $L$  when considering the vertical and horizontal connection, while  $L\sqrt{2}$  for the diagonal connection (if  $L$  is the side of the square). To be more or less consistent with the dimensions of Switzerland,  $L$  is chosen to be equal to 40 km.

In a modeling perspective, in all the configurations each node is connected with the adjacent ones as shown in Fig. 4 This feature is specified by a so-called connectivity matrix of the nodes.

#### Hydrogen demand

The first characteristic defining each node is the hydrogen demand associated. The methodology used to assign it represents the main difference between the three configurations. In all the analyzed cases the demand is *hourly defined*. In particular, in this first ideal and schematic first representation of the system two values of demand are used:

- **Urban demand:** It represents the main fraction of hydrogen demand associated to the cities. In 4 it is represented by the big four red dots. Basing on population data of the main cities of Switzerland [8], a value equal to 300'000 kWh is set.
- **Rural demand:** It represents the small fraction of hydrogen demand associated to the villages. In 4 it is represented by the 36 little red dots. Basing on the population of a village of Switzerland [8], a value equal to 2'000 kWh is set.

It is of fundamental importance to notice that this configuration is symmetric: there is one distribution of demand (one urban node surrounded by eight rural) which is repeated four times. This gives the possibility to have always four different results which are the same because of symmetry reasons.

### 2.1.2 Realistic schematic configuration

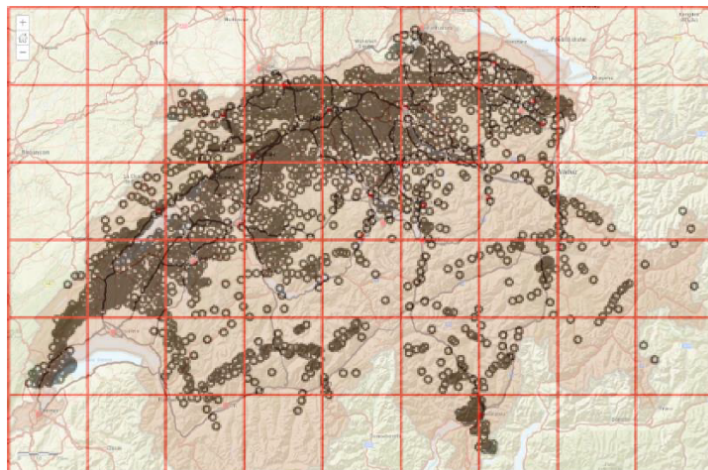


**Figure 5:** Realistic schematic configuration of the system.

The realistic configuration is introduced to resemble the shape of Switzerland and so to head forward the Swiss case study. The other important role it covers is to represent a comparison for the results of the ideal schematic configuration, since the general trends have to be the same. In this case, the system consists of the Swiss communes defined by their latitude and longitude as shown in Fig. 5. These communes are then divided in cells with the same area and a central node, characterized by a population aggregating the communes population of the particular cell. The dimension of the cells remains the same of the previous configuration (40kmx40km), but in this case the matrix becomes a 9-by-6.

### Hydrogen demand

The population data of each cell is then converted in hydrogen demand basing on location specific motorisation rates, national transport statistics and hydrogen car performance [9] [10]. The result is an aggregated hydrogen demand represented in the figure below.

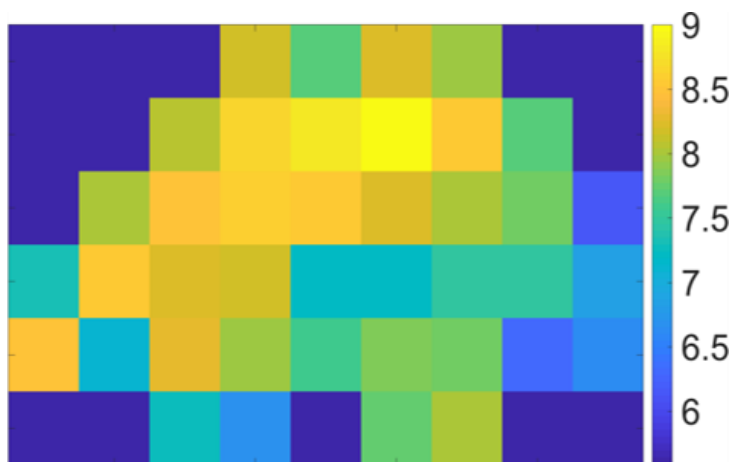


**Figure 6:** Aggregated hydrogen demand for each cell (log10 scale).

### 2.1.3 Realistic ArcGIS configuration

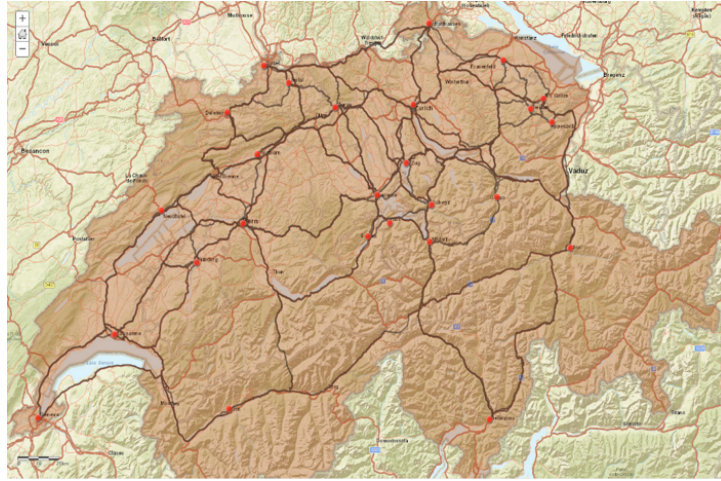


**Figure 7:** ArcGIS configuration of the system.

This third configuration is completely realistic. Therefore, ArcGIS [11], which is a geographical information software, is used to create a map of Switzerland and to extrapolate data from it. The Swiss territory is divided into the 26 cantons, each represented by its capital (red dots in Fig. 7). The set of capitals becomes the nodes of the system introduced into the optimization problem. ArcGIS is capable to calculate the distance between each city and to connect them through the fastest route possible. It is assumed that each capital is connected with the nearest 12 through real roads. It is also possible to select specific means of transport: in this configuration the truck is chosen. In Fig. 7 the red dots represent the location of each capital and the brown lines the connections activated for each of them with the nearest 12.

#### **Hydrogen demand**

Concerning the hydrogen demand, the population for each capital is considered [8] and it is multiplied by an average swiss motorisation factor [10].

## 2.2 Technology portfolio

Independently on the selected configuration, each node is characterized by the same technology portfolio represented in Fig. 8. The one proposed is constituted by green hydrogen production technologies, blue hydrogen production technologies and finally blue hydrogen production technologies with CO<sub>2</sub> capture. In particular, they are:

- Steam methane Reforming Plant (SMR) [12]
- Steam methane Reforming Plant with capture of CO<sub>2</sub> from shifted syngas using MDEA (SMRCCS  $\phi = 0.54$ ) [12]
- Steam Methane Reformer with capture of CO<sub>2</sub> from SMR flue gas using MEA (SMRCCS  $\phi = 0.89$ ) [12]
- Polymer Electrolyte Membrane Electrolyzer (PEME)
- Biomass Gasification
- Steam Biomethane Reforming Plant

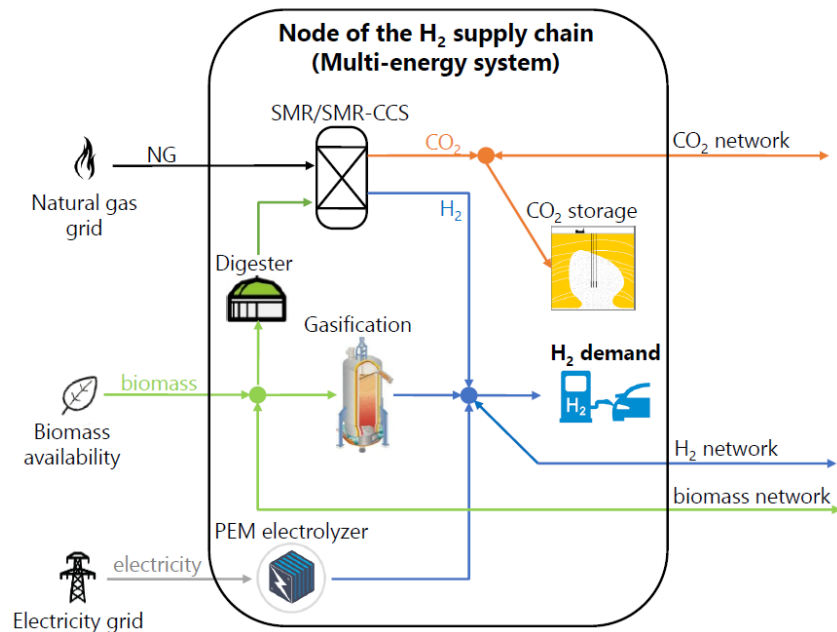


**Figure 8:** Schematic representation of the investigated energy system.

## 1. Steam Methane Reforming (SMR)

Currently, the Steam Methane Reformer is the leading technology for the production of hydrogen from natural gas or light hydrocarbons. This hydrogen is named *blue hydrogen*, referring to its fossil energy source. The reference for the overall process is the Base Case presented in the 2017

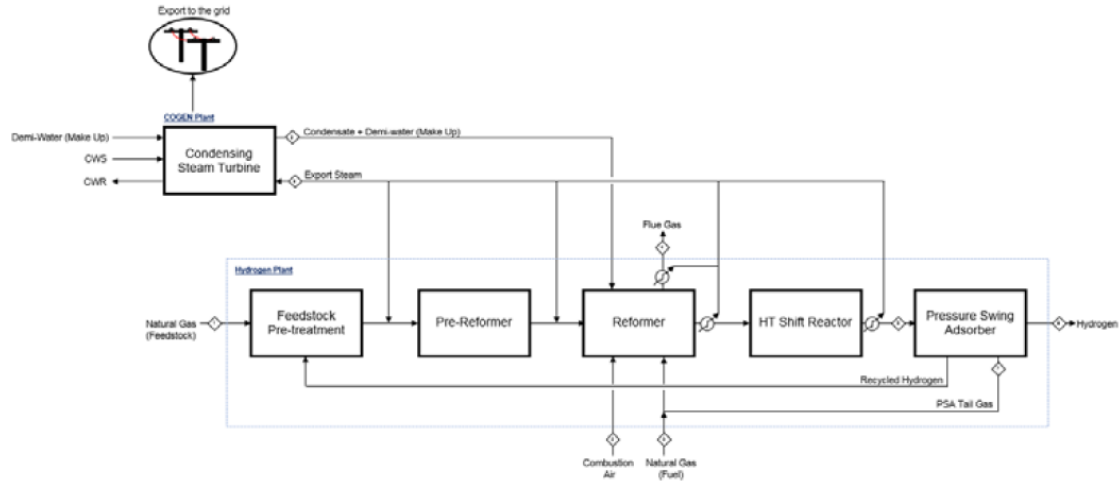


**Figure 9:** Block diagram of a Steam Methane Reforming process [12].

IEAGHG Technical Report [12]. The natural gas is initially pre-treated to remove any sulphur and chlorine present in the feedstock. This prevents any poisoning of the catalyst downstream. This is mixed with process steam and pre-reformed in an adiabatic reactor to convert any light hydrocarbons (mainly converting C2+ and olefines) before being fed into the primary reformer. This component is composed of a tubular reformer with terraced wall firing. The syngas produced should consist of CO<sub>2</sub>, CO, H<sub>2</sub> and residual CH<sub>4</sub>. The syngas produced from the reformer is then fed into the high temperature shift reactor (WGS) to convert the CO to H<sub>2</sub> thus producing a syngas with residual CO of around 2.5-3%v. This is then fed into the PSA where around 85-90% of H<sub>2</sub> with a purity of 99.9+% are recovered. The PSA tail gas is collected and fed into the burners of the SMR as its primary fuel. HP steam is generated by recovering heat from both the convective section of the flue gas and the cooling of the syngas (before and after the shift reactor). Any excess steam is delivered to the power island, which consists of a condensing steam turbine, to generate electricity that is exported to the grid [12].

In this type of SMR plant, all the CO<sub>2</sub> is emitted from the flue gas of the steam reformer. However, it should be noted that the CO<sub>2</sub> is produced from the following processes:

- CO<sub>2</sub> produced during the reforming and water-gas shift reaction;
- CO<sub>2</sub> produced during the combustion of the residual CO in the PSA tail gas and the natural gas (as supplementary fuel) in the SMR furnace.

## 2. Steam Methane Reformer with capture of CO<sub>2</sub> from shifted syngas using MDEA (SMRCCS $\phi = 0.54$ )

This process in Fig. 10 is referring to the technology presented as Case 1A in the 2017 IEAGHG Technical Report [12]. The block diagram shown in Fig. 10 is basically the same presented in Fig. 9 with the added CO<sub>2</sub> capture plant via a MDEA (methyldiethanolamine) absorption process. The syngas exiting the HT Shift Reactor is sent to the CO<sub>2</sub> Capture Plant, which separates the syngas with the CO<sub>2</sub>. The sweet syngas is then sent to a PSA unit to produce pure hydrogen as the product and to recirculate a fraction to the de-sulphurization, while the PSA tail gas is recirculated to the reformer to sustain the chemical reaction as a fuel. The CO<sub>2</sub> is instead sent to a compression and dehydration unit and then sent to the pipeline. The capture process is applied only on the syngas exiting the HT Shift Reactor, while the CO<sub>2</sub> from the flue gas of the reformer is emitted to the atmosphere. For this reason, the capture rate  $\phi$  of this technology is relatively low and equal to 0.54.

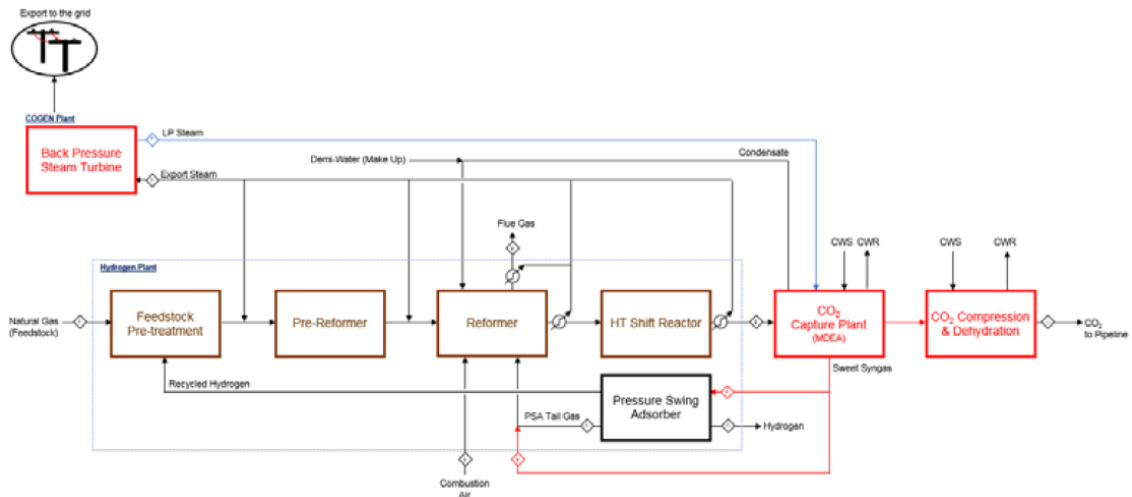


Figure 10: Block diagram an SMR with capture of CO<sub>2</sub> from shifted syngas using MDEA [12].

### 3. Steam Methane Reformer with capture of CO<sub>2</sub> from SMR flue gas using MEA (SM-RCCS $\phi = 0.89$ )

This process is referring to the technology presented as Case 3 in the 2017 IEAGHGT technical

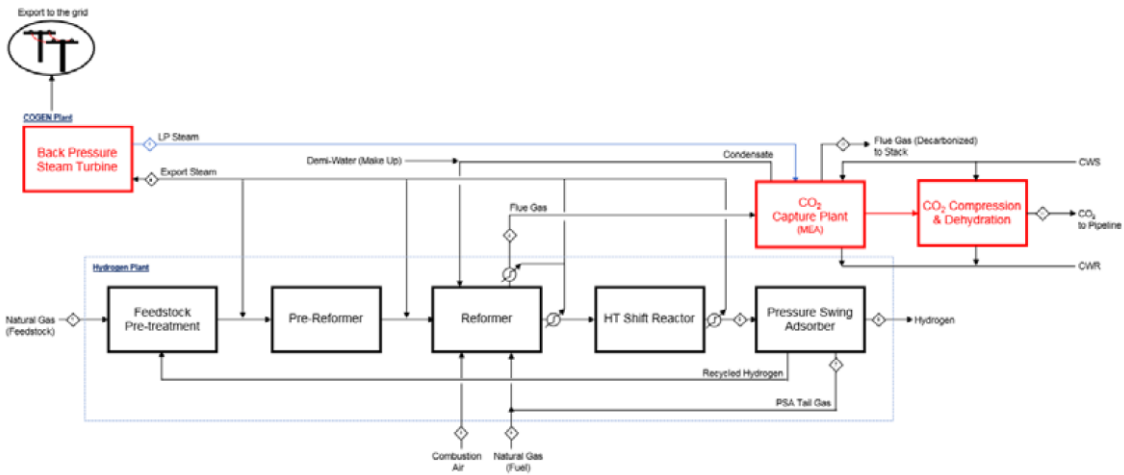
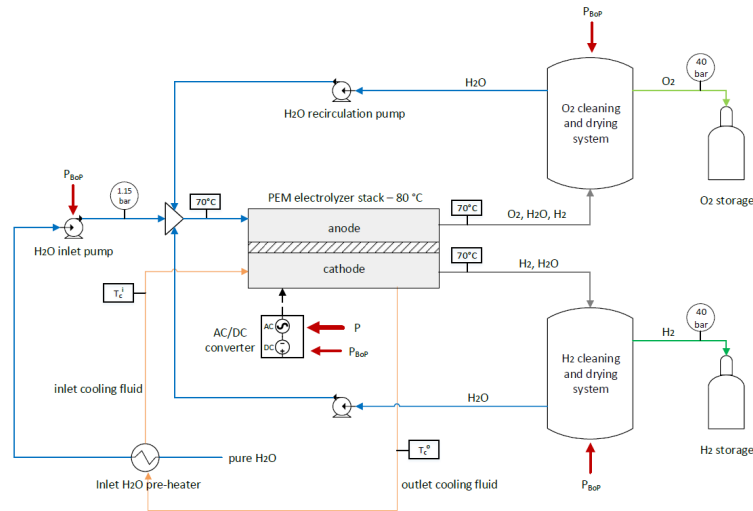


Figure 11: Block diagram an SMR with capture of CO<sub>2</sub> from from SMR flue gas using MEA [12].

report [12]. This process consists of a post-combustion capture technology based on a MEA (Monoethanolamine) absorption technology. The flue gas exiting the reformer is sent to the CO<sub>2</sub> plant where the CO<sub>2</sub> is captured. The PSA is the unit which separates the hydrogen and the remaining CO<sub>2</sub> is contained in the PSA tail gas, which is recirculated to the reformer. The overall flow of the CO<sub>2</sub> is almost closed, consequently the overall process has a much higher capture ratio with respect to SMR Case 1A, equal to 0.89.

#### 4. Polymer Electrolyte Membrane Electrolyzer (PEME)

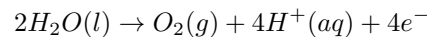
The electrolysis is an alternative option for hydrogen production from renewable resources. For this reason, it is named *green hydrogen*. Electrolysis process consists of using electricity to split the water molecule into hydrogen and oxygen. Electrolyzers can range in size from small, appliance-size equipment that is well-suited for small-scale distributed hydrogen production to large-scale, central production facilities which could be directly tied to renewable forms of electricity production. Hydrogen production via electrolysis may offer opportunities of synergies with variable power generation, which is characteristics of some renewable energy technology [13]. In this project, the



**Figure 12:** Block diagram of a Polymer Electrolyte Membrane Electrolyzer process [14].

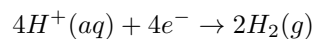
Proton Exchange Membrane (PEM) electrolysis is chosen as the reference process shown in Fig. 12. It consists of the electrolysis of water in a cell equipped with a solid polymer electrolyte that is responsible for the conduction of protons from the anode to the cathode while insulating the electrodes electrically. Under standard conditions the enthalpy required for the formation of water is 285.9 kJ/mol. A portion of the required energy to sustain the eletrolysis reaction is supplied by thermal energy and the remainder is supplied through electrical energy. One of the main advantages of the PEM electrolyzer over the concurring Solid Oxide electrolyzer (SOE) is the low temperature operation, in the range of 50-80°C [15].

- Anode reaction



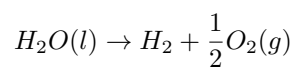
At the anode, the liquid water reactant is supplied to catalyst where the supplied water is oxidized to oxygen, protons and electrons.

- Cathode reaction



At the cathode, the supplied electrons arrive through the external circuit while the protons are conducted through the solid membrane. Here, they are combined to create gaseous hydrogen.

Finally, the overall cell reaction becomes:



The final products are hydrogen at the cathode, oxygen and excess of water at the anode. In order to fully exploit the pure oxygen produced, a O<sub>2</sub> separator is needed, while the warm water is recycled at the inlet of the anode. A make-up of water, heated up by an external thermal energy source, is needed to cover the amount converted into hydrogen.





## 2.3 Network portfolio

In a practical perspective, there are three means of transport available to carry the hydrogen from the production nodes to the end-users, from here referred as *networks*:

- Truck
- Railway
- Pipeline

In the optimization problem, each network is chosen independently in each connection of the configuration depending on their characteristics. The main hypothesis here is that the hydrogen is transported in the gaseous form in every network. Consequently, the liquefaction process and the energy consumption correlated is not considered.

### 1. **Truck**

The main constraint about compressed hydrogen transportation is its low capacity. For this reason, it is more suitable to supply the low demand nodes and for short distances to minimize the losses. On the other side, the investment cost per unit is the lowest in comparison with the other two. The operational cost is connected with the price of the fuel, while the CO<sub>2</sub> emissions are the highest due to the fossil nature of the fuel. The big advantage of the truck is the adaptability: it could reach any demand node as long as there is a road available.

### 2. **Railway**

Nowadays hydrogen transportation via railway is not yet applied. In this project it is chosen as the more sustainable option in terms of CO<sub>2</sub> emissions in comparison to truck. Of course, it depends on the electricity grid emission factor, a parameter changing for each country. Taken Switzerland as the reference, the electricity is produced mainly by hydroelectric and nuclear power, so the emission factor of the grid is very low. Hence, it has sense to consider the railway network as the sustainable option. Moreover, the capacity of a unit (carriage) is about twice the truck unit. For these reasons, it is more suitable to supply high hydrogen demand nodes and for long distances. This network has a lower adaptability with respect to the truck, it can be applied as long as the freight transport by rail is permitted.

### 3. **Pipeline**

Hydrogen transportation by pipeline seems the option permitting the broadest range of distances [20]. Naturally, the investment cost is the highest among the three. However, the real advantage is that the operational cost is nearly zero. The CO<sub>2</sub> emissions are also the lowest, taking also into account the indirect one. The big constraint of the pipeline is the territory feasibility and secondly the social acceptability.

### 3 Formulation of the optimization problem

The energy hub considered for the production of hydrogen has the primary objective of supplying the energy demanded by the users. In every node, the energy hub is connected to the gas and to the electrical grid and includes all the technology presented in the technology portfolio.

The primary energy prices, the emissions factors of the grids, the demand values, the network topology and cost and technology cost and performance are the set of inputs to the optimization problem. The model returns the optimal system design in terms of technology selection, location and size and the energy flows between the nodes. An other output is the imported/exported energy from/to the grid.

The problem is mathematically formulated as a MILP (Mixed Integer Linear Program), where binary variables are introduced to model the capital cost of the technologies. The MILP can be written in general form as

$$\begin{aligned}
 & \min_{\mathbf{x}, \mathbf{y}} (\mathbf{c}_1^T \mathbf{x} + \mathbf{c}_2^T \mathbf{y}) \\
 & \text{s.t.} \\
 & \mathbf{A}_1 \mathbf{x} = \mathbf{b}_1, \quad \mathbf{A}_2 \mathbf{y} = \mathbf{b}_2 \\
 & \mathbf{x} \geq \mathbf{0} \in \mathbb{R}^X, \quad \mathbf{y} \in \{0, 1\}^Y
 \end{aligned} \tag{1}$$

where  $\mathbf{c}_1$  and  $\mathbf{c}_2$  represent the cost vectors associated to the continuous and binary decision variables,  $\mathbf{x}$  and  $\mathbf{y}$ , respectively;  $\mathbf{A}_1$  and  $\mathbf{A}_2$  are the corresponding constraint matrices, with  $\mathbf{b}_1$  and  $\mathbf{b}_2$  being the corresponding constraint known-term;  $X$  and  $Y$  indicate the dimensions of  $\mathbf{x}$  and  $\mathbf{y}$ , respectively. Here, both continuous and binary variables are optimized, with the latter being introduced to model the nonlinearities arising within the optimization problem, which are related to the performance and the capital costs of the considered technologies, as well as to the presence of network connections. The formulation of the optimization problem is based on previously presented work [1], which is expanded to consider the spatial dimension of the hydrogen supply chain. In the following, all aspects of the optimization problem are described in detail, namely input data, decision variables, constraints, and objective function.

#### 3.1 Input data

The following input data are given to the optimization problem:

- Primary energy prices and emission factors
- Energy and mass carrier availability
- Technology cost coefficients and performance: Each technology is characterized by a piece-wise affine approximation of the investment cost. Increasing the size, the unit cost ( $m$ ), expressed in €/kW, decreases and the fixed cost ( $q$ ) in € increases. Concerning the performance, each technology is characterized by an energetic efficiency taken from the literature (see 7.2).
- Network minimum, maximum size and costs coefficients
- Network losses
- Network topology and H<sub>2</sub> demand: The system configuration described in 2.1 as well as the H<sub>2</sub> demand are given as input to the optimization problem. In particular,  $N$  number of nodes, the connectivity matrix, the distance between them and one value of H<sub>2</sub> demand associated for each node.
- Location of the CO<sub>2</sub> storage

Constant prices are considered for the different carriers, independently of the specific technology. Concerning availability, electricity and natural gas are assumed to be available with no limitation at any location of the HSC, as the optimal design of the corresponding grids is beyond the scope of this work. In contrast, limited availability is considered for biomass, hydrogen must be produced starting from the other carriers, and CO<sub>2</sub> is captured from the NG-based SMR processes. While the formulation of the optimization problem holds for any set of input data, the specific values used to determine the optimal HSC design are reported and discussed in the Appendix.

## 3.2 Decision variables

The following decision variables are returned:

- The selection, location of the technologies and the corresponding size,  $\mathbf{S} \in \mathbb{R}^M$ .
- The input power,  $F \in \mathbb{R}^M$ , and output power  $P \in \mathbb{R}^M$  of the conversion technologies.
- The selection and location of the networks.
- The energy flow between the nodes,  $G \in \mathbb{R}^N$ .
- The imported electrical and gas power,  $\mathbf{U}_e$  and  $\mathbf{U}_g$ ,  $U \in \mathbb{R}$  respectively, and the exported electrical power,  $V_e \in \mathbb{R}^M$ .

It is worth noticing that, while the mathematical structure of the proposed optimization framework allows it, the time evolution of the aforementioned decision variables is not investigated, as the study focuses on the design features of hydrogen supply chains.

## 3.3 Constraints

The constraints of the optimization problem can be divided into two categories: (i) conversion technologies and networks (ii) energy balances between the nodes.

### 3.3.1 Conversion technologies and network

The set of available technologies is indicated with  $M$  and includes all the technologies described in the energy hub. In the following equations,  $S$  refers to the size of the technology considered, i.e the rated input power. For each technology  $i \in M$ ,  $S_i$  must vary between a minimum and a maximum value,  $S_i^{\min}$  and  $S_i^{\max}$  respectively.

$$S_i^{\min} x_i \leq S_i \leq S_i^{\max} x_i \quad (2)$$

where the binary variable  $x_i \in \{0,1\}$  indicates whether the  $i$ -th technology is installed. Every technology is described through this very simple equation:

$$P = \eta F \quad (3)$$

where

$$S_i^{\min} x_i \leq F \leq S \quad (4)$$

The equation (3) is characterizing each technology with a linear efficiency. In all the cases, the size effect on the efficiency is not considered.  $P$  is the energy produced and  $F$  is the energy in input to each technology.

The set of available networks is indicated with  $Z$  and they are all described by (2) and (4), where  $S$  is the size in kW of each network and  $F$  is the energy transported in kWh.

### 3.3.2 Energy balance between the nodes

The set of considered energy and mass streams within the overall system is indicated with  $C$  and includes:

- Hydrogen ( $H_2$ ): it is produced by of all the conversion technologies in the system and then exchanged between the nodes in order to satisfy the demand of the end users.
- Electricity (e): it can be consumed and generated by the technologies, i.e consumed by the PEME and produced as secondary product by the SMR.
- Natural gas (g): it can be imported from the grid and consumed by the conversion technologies.
- Dry biomass ( $B_d$ ): it can be available in some nodes of the system and consumed by the conversion technologies. There is also the possibility to exchange it from where it is available to where it is consumed.
- Wet biomass ( $B_w$ ): it can be available in some nodes of the system and consumed by the conversion technologies. In this case, there is not the possibility to exchange it between the nodes.
- Carbon dioxide ( $CO_2$ ): it is produced by some technologies and can be exchanged between the nodes of the system and, where there is the possibility, stored.

The overall energy balance is of fundamental importance in our system because it links all the nodes creating the network itself. The mathematical notation used is the following:  $\mathcal{N} = [1, \dots, N]$  is the set of nodes in the system, where  $N$  is the number of nodes,  $\mathcal{C} = [1, \dots, C]$  is the set of energy carriers, where  $C$  is the number of energy carriers,  $\mathcal{M} = [1, \dots, M]$  is the set of technologies, where  $M$  is the number of technologies and finally  $\mathcal{Z} = [1, \dots, Z]$  is the set of available networks, where  $Z$  is the number of available networks.

$$\forall i \in \mathcal{N}, \forall c \in \mathcal{C} : \sum_{m=1}^M R_{m,i,c} + \sum_{z=1}^Z \left[ \sum_{j=1, j \neq i}^N G_{j,i,z,c}(1 - ld_{j,i}) - \sum_{j=1, j \neq i}^N (G_{i,j,z,c}) \right] = D_{i,c} \quad (5)$$

where

$$\forall i \in \mathcal{N}, \forall c \in \mathcal{C}, \forall m \in \mathcal{M} : R_{m,i,c} = P_{m,i,c} - F_{m,i,c'} \quad (6)$$

where

$$\forall i \in \mathcal{N}, \forall c \in \mathcal{C}, \forall m \in \mathcal{M}, c \neq c' : P_{m,i,c} = \eta_m F_{m,i,c'} \quad (7)$$

Equation (7) underlines that the produced energy  $P$  is referred to the output carrier  $c$ , while the input energy  $F$  is referred to the input carrier  $c'$  and are always different. This means that in the expression of the variable  $R$  (6), that represents the net energy converted in each node, either  $P \neq 0$  or  $F \neq 0$ , because it is written for the same energy or mass carrier. Consequently, in equation (5), the first summation is representing the total net energy produced within a node for all the technologies for each energy or mass carrier. The second term consists on the summation of every network of the amount of energy which arrives to each node. It consists of the energy which leaves the previous node  $G$  reduced by a factor which takes into account the energy losses  $l$  over the distance  $d$ . The third term takes into account the amount of energy which leaves every node  $G$ , indicated as a negative contribution, always counted for each network  $z$ . The algebraic sum of these three terms is equal to the demand of each node  $D$  for the investigated carrier.

### 3.4 Objective function

The objective function of the optimization problem is the total cost of the system given by the sum of two contributions: the technology total cost and the network total cost.

- **Technology total cost  $J_m$ :** It is given by the sum of three contributions, the technology investment cost  $J_I$ , the technology operational cost  $J_O$  and the technology maintenance cost  $J_M$ . The investment cost is expressed as:

$$\forall i \in \mathcal{N} : J_I, i = \sum_{m=1}^M \left\{ \sum_{w=1}^W [ (m_{m,w} S_m, i + q_{m,w}) u_{m,w,i} ] \right\} a_m \quad (8)$$

where

$$\sum_{w=1}^W u_{w,i} \leq 1 \quad (9)$$

$$\sum_{w=1}^W (u_w S_i^{\min}) \leq S_i \leq \sum_{w=1}^W (u_w S_i^{\max}) \quad (10)$$

The variables  $m_m$  and  $q_m$  represent the variable and fixed cost coefficients for the  $m$ -th technology.  $S_m$  indicates the size, i.e the rated input power for each conversion technology. To compute the annual investment cost, the annuity factor  $a$  is included, which is calculated using the standard definition and based on an interest rate of 6%. As previously stated, a piecewise affine approximation is implemented to model the size dependency of the investment cost. For each technology  $m \in M$  a binary variable  $u \in \{0, 1\}^W$  is defined specifying the active line segment for the investment cost calculation, where  $W$  is the total number of line segments. The size  $S$  of the  $m$ -technology is defined between a minimum and a maximum of every line segments  $w$  considered, reported in equation (10). Since the capital cost must be minimized, and due to the concavity of the curve, a binary variable for each line segment is required to identify the active linear approximation, as shown in equation (9). The operational cost  $J_O$  of each technology is expressed as difference between the imported and the exported energy carriers multiplied by the corresponding energy price for each node:

$$\forall i \in \mathcal{N} : J_O, i = \sum_{c=1}^C \sum_{m=1}^M (u_{c,m} U_{c,m,i} - v_{c,m} V_{c,m,i}) \quad (11)$$

where  $u$  is the import price of every energy carrier input to the every technology and  $v$  is the export price;  $U$  and  $V$  are the energy quantity imported and exported in kWh.

The maintenance cost  $J_M$  is given as a fraction  $\psi$  of the annual investment cost:

$$\forall i \in \mathcal{N} : J_M, i = \sum_{m=1}^M \psi_m J_{c,m,i} \quad (12)$$

$\phi$  is a parameter indicated for each technology which can be found in the Appendix.

- **Network total cost  $J_z$ :** It is given by the sum of two contributions: network investment cost and network operational cost.

The investment cost for the truck and railway network is expressed as:

$$J_{I,T,R} = \alpha_{T,R} a \sum_{j=1}^N \sum_{i=1, i \neq j}^N (S_{i,j}) \quad (13)$$

Where  $a$  is the annuity factor and  $\alpha_{T,R}$  is the investment cost coefficient for the truck and the railway expressed in [€/kWh] introduced in section 3.1.2.

The investment cost for the pipeline network is expressed as:

$$J_{I,P} = \alpha_P a \sum_{j=1}^N \sum_{i=1, i \neq j}^N (S_{i,j} d_{i,j}) \quad (14)$$

where  $\alpha_P$  is the investment cost coefficient for the pipeline expressed in [€/kWh m] and  $d$  is the distance between the nodes.

The operational cost for the  $z$ -th network is expressed as:

$$\forall z \in Z : J_O = \beta \sum_{j=1}^N \sum_{i=1, i \neq j}^N (G_{i,j} d_{i,j}) \quad (15)$$

where  $\beta$  is the operational cost coefficient expressed in [€/kWh m] and  $G$  is the energy flow between the nodes in kWh.

The **total cost**  $J$  of the system becomes:

$$J = \sum_{i=1}^N \sum_{m=1}^M (J_{I,i,m} + J_{O,i,m} + J_{M,i,m}) + \sum_{z=1}^Z (J_{I,z} + J_{O,z}) \quad (16)$$

As previously stated, the system is also optimized for the total CO<sub>2</sub> emissions of the system. This multi-objective optimization is performed by means of the  $\epsilon$ -constraint method. This translates into a minimum-cost optimization problem, where the CO<sub>2</sub> emissions are constrained below a maximum value [1]. The total emissions are calculated as the sum of two terms: the CO<sub>2</sub> emissions from the technologies and the CO<sub>2</sub> emissions from the networks.

$$e = \sum_{i=1}^N \sum_{c=1}^C \sum_{m=1}^M (\lambda_c F_{m,i,c}) + \sum_{z=1}^Z (e_z) \quad (17)$$

where  $\lambda$  is the emissions factors referred to the input energy  $F$  to each technology, introduced in section 3.1.1.

The emissions from the networks  $e_z$  are given by:

$$e_z = \gamma \sum_{i=1}^N \sum_{j=1, j \neq i}^N (G_{i,j} d_{i,j}) \quad (18)$$

where  $\gamma$  is the CO<sub>2</sub> emission coefficient for each network expressed in [ton<sub>CO<sub>2</sub></sub>/kWh m]. The emissions referred to the network are proportional to the distance covered times the energy transported.

## 4 Multi-objective optimization

The result of a multi-objective optimization problem is the Pareto front. It is the set of the optimal solutions of the system: from these points, the solutions cannot be improved in any of the objectives without degrading at least one of them.

The first results shown below are based on the following assumption:

- Technology portfolio: SMR
- Network portfolio: Truck, Railway and Pipeline

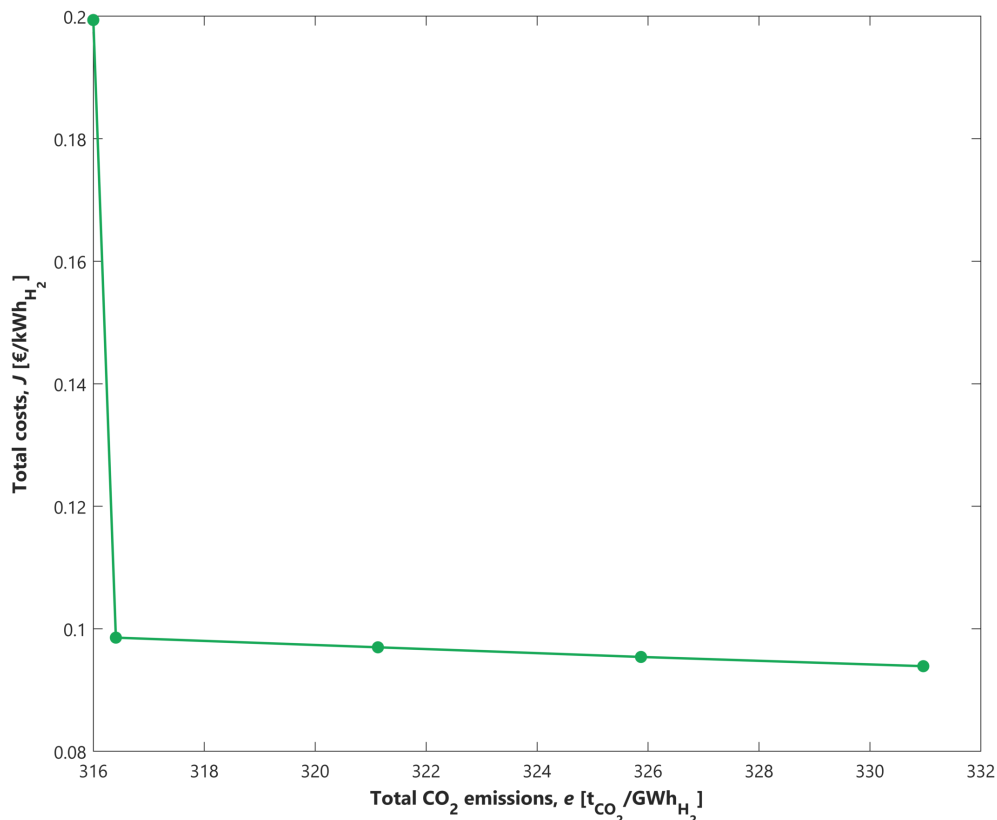


**Figure 15:** Pareto front.

In all the result shown in this thesis the discussion is always headed from the minimum cost point of the Pareto front, the first on the right-hand side of Fig. 15, to the minimum emission point, the first from the left-hand side. Looking at Fig. 15 in this way, it shows the increase of the total costs of the system decreasing the total CO<sub>2</sub> emissions. In this specific case, the total CO<sub>2</sub> emissions are decreased by 5% from the first to the last point of the Pareto while the total cost double. The CO<sub>2</sub> emissions variation is very small because the only technology available, the SMR, has also the highest emission factor due to the fossil energy in input.

Each Pareto point represents a specific configuration of the system whose total cost are minimized and the total emissions are constrained below a maximum threshold set according to the  $\epsilon$ -constraint method. The network configurations for some specific Pareto points are shown in Fig. 16.

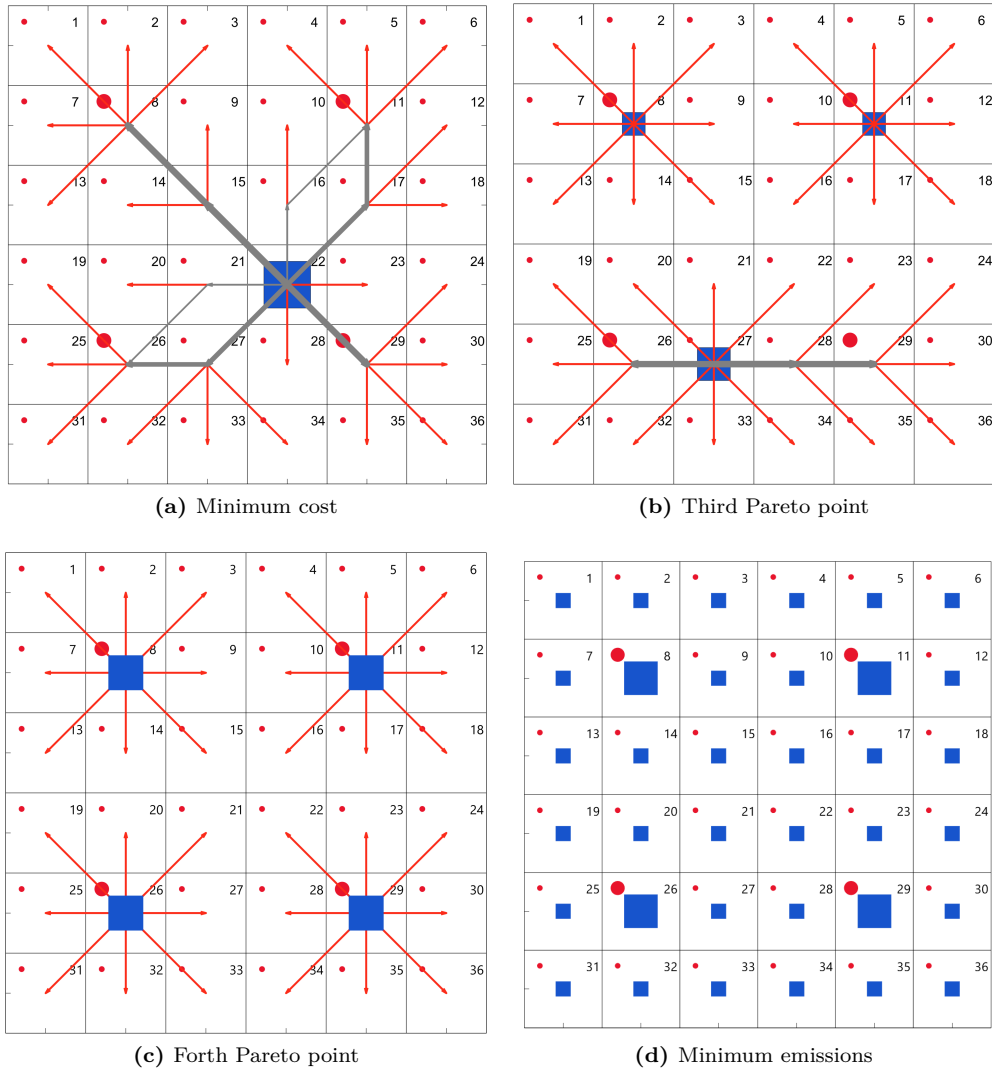


**Figure 16:** Network configuration in different Pareto points.

The minimum cost configuration presents one big SMR in node 21 which is one of the four central nodes in this schematic configuration. As previously stated, the possible configurations are always four because of the symmetry of the system. For example in this configuration, if the SMR is installed in node 15, 16 or 22 the result is exactly the same. While heading towards the minimum emissions, the CO<sub>2</sub> emissions are reduced progressively: this is achieved by lowering the overall number of connections activated, so basically reducing the total network. This is an effect of the presence of the network energy losses: more connections activated means more losses, so more energy to be produced at the production nodes and finally more CO<sub>2</sub> emitted. Lowering the emissions brings to the last configuration, minimum emissions, that nullifies totally the network. The consequent effect is on the technologies installed: their number increase as the network is limited, so more technologies are needed to satisfy the demand. In the minimum emissions configuration one technology per node is installed, which is the reason why the total costs, which are more or less constant in the previous configuration, increase dramatically almost doubling. The minimum cost (a) presents only one technology consequently of the PWA approximation of the investment cost: one big-sized SMR is convenient because it presents a lower unit cost in [€/kW], while small-sized SMRs present higher unit cost and is the reason why configuration (d) is the most expensive.

## 4.1 Optimal competition between the networks

The main aspect to be noticed in 16 is that in every configuration the pipeline network is not installed. This is due to the high investment cost of the pipeline with respect to the truck and railway, making it not cost competitive. The two networks installed, the truck and railway, supply different nodes: the railway is transporting the hydrogen towards the urban nodes, while the truck is supplying the rural nodes. This is because in the case of the railway network, the specific investment cost for transportation are lower than the one assigned to the truck (see Appendix): the result is that it is convenient to transport big amount of energy by railway and small amounts by truck.

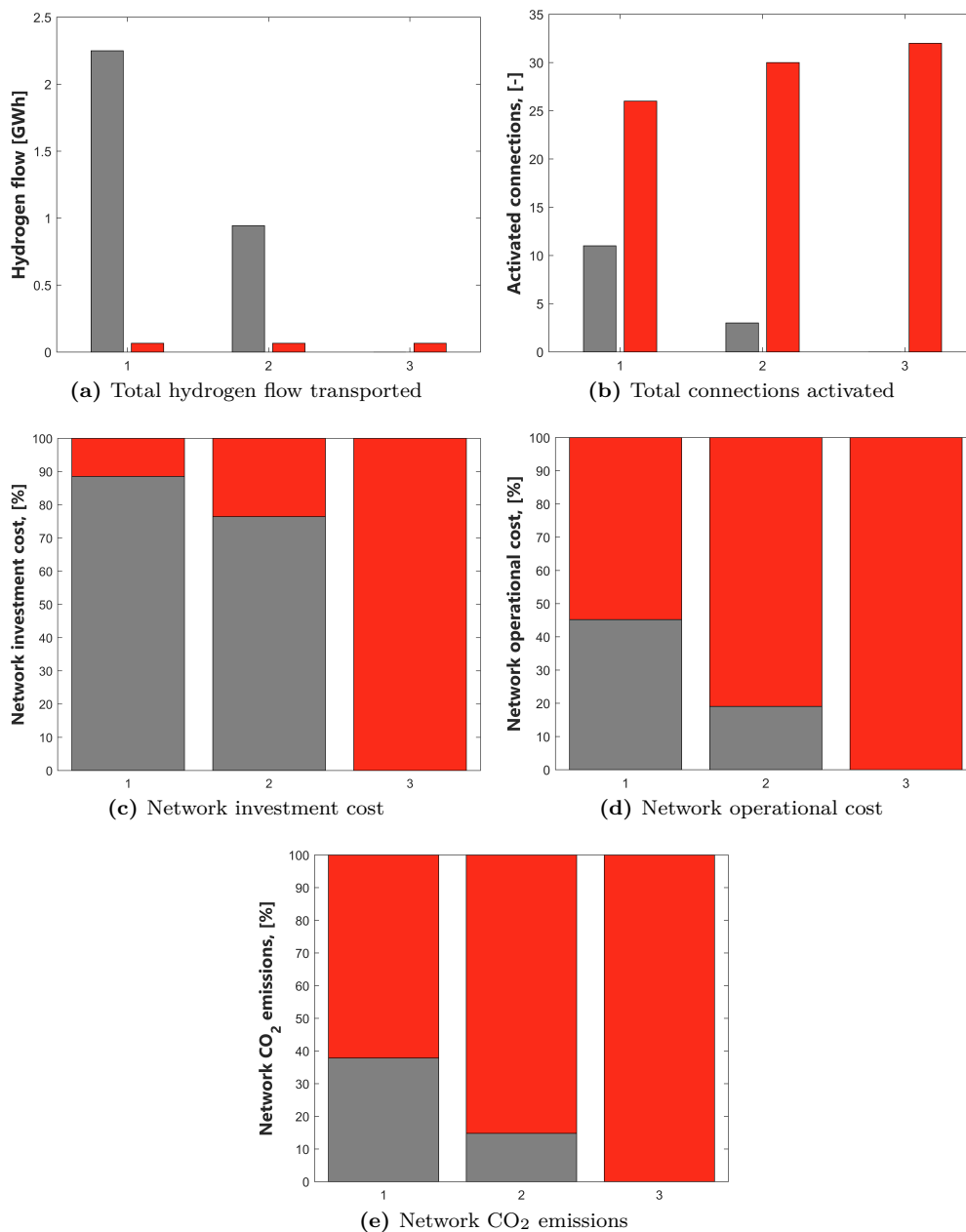


Figure 17: Network competition in three different Pareto points.

In the above figures it is shown how the different networks compete in terms of investment cost, operational cost and on CO<sub>2</sub> emissions in the configurations (a), (b) and (c) represented in Fig. 16. The minimum emissions configuration (d) is not considered as it does not present networks. It is impressive to notice that the total network cost in the minimum cost configuration is only the 3% of the total costs, which includes also the technologies cost. The three Pareto points investigated are referred as 1, 2, 3 in Fig. 17, referring to the configurations (a), (b) and (c) of Fig. 16 respectively.

The first bar plot (a) represents the total hydrogen flow transported: in the minimum emission configuration the main fraction is supplied by the railway, as it transports towards the urban node, while the truck fraction is small due to the transportation towards the rural nodes. In configuration 2 the hydrogen transported by railway decreases as the technologies start to be installed in the urban nodes, and consequently they do not need to be supplied anymore. In configuration 3 the railway network totally disappears, as four SMRs are installed in the urban nodes.

The second bar plot (b) represents the number of the total connections activated in each investigated configuration. The truck always presents the majority of connections due to the fact that the rural nodes are 32, while the railway connections are less as the urban nodes are four.

The bar plots (c) and (d) represent the percentage of the investment cost and of the operational cost over the total network cost. As the investment cost scales with the amount of energy transported, it is higher for the railway in the first two cases. On the opposite, the operational cost is higher for the truck as it scales with the energy transported but also with the distance covered, which is much more for the truck network.

The final bar plot (e) shows the partition of the CO<sub>2</sub> emissions, which is mainly dominated by the truck network because of the distance covered, and also because it is the most CO<sub>2</sub> emitting network, as indicated by its emission coefficient  $\gamma_T$  (see Appendix).

## 5 Sensitivity analyses on model parameters

The goal of these set of analyses is to understand better the behaviour of the model while changing some design parameters. Consequently, these parameters are selected depending on the impact they have on the optimal design of the system. A minimum cost optimization is performed and selected to study in detail these aspects as the one presenting the maximum network installed. In Fig.18 is shown a minimum cost configuration of the system with the following assumptions:

- Technology portfolio: SMR
- Network portfolio: Truck, Railway and Pipeline

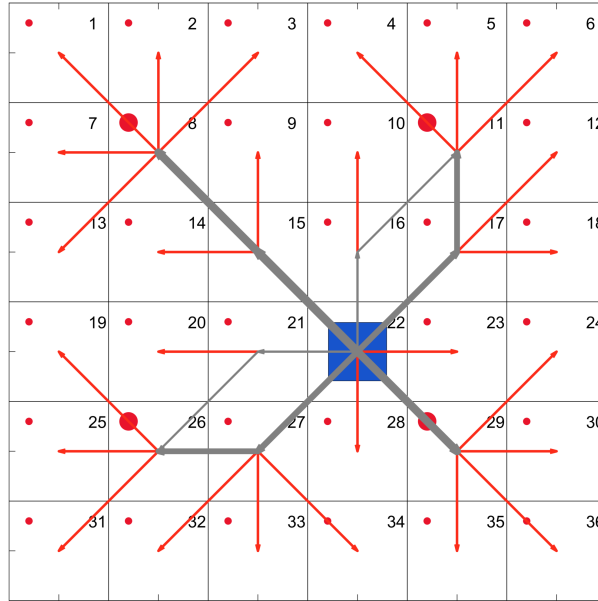


**Figure 18:** Minimum cost configuration of the system.

It presents one SMR installed in one of the central nodes (22) supplying hydrogen for the the end users. In particular, the railway network, always referred with the grey color, connects the urban nodes while the truck network, referred with the red color, connects the rural nodes. The pipeline network is not selected as not competitive in terms of investment cost.

### 5.1 Energy loss coefficient $l$

As previously stated, the equation (5) is the fundamental equation of the model, since it connects the energy transported between the different nodes of the system. In this energy balance the parameter  $l$ , measured in  $[1/m]$ , plays an important role, as it is setting the amount of energy lost in every connection of the system which multiplies the distance covered in every connections. In the following analysis this parameter is varied to see how it impacts the minimum cost configuration of the system, which is the most indicated as it presents the widest network installed. The loss parameter is varied from  $5 \times 10^{-7} [1/m]$  to  $1.8 \times 10^{-5} [1/m]$ , which corresponds respectively to 0.05% and 1.8% of the energy lost over a kilometer.

In Fig. 19 the results are summarized with the following assumptions:

- Technology portfolio: SMR
- Network portfolio: no specific network is selected (light blue color), meaning it has no limitations in size

In the first (a) and second (b) configurations the network remains unaffected: one SMR installed and all the hydrogen transported to the end users. The first aspect to be noticed is the visible increase of the network size, due to the losses coefficient increase. Basically, the energy transported by the network increases, due to more losses in the connection between the nodes. Consequently, the technology size installed is bigger as more energy is needed to satisfy the total demand.

In the third (c) and fourth (d) configurations the technologies installed becomes two: it is no more convenient to convert all the energy in one single technology because the size is too big (due to the increasing losses coefficient) and for that too costly. For this reason, in the first configuration, the optimizer chooses two technologies. These are situated in the middle between the nearest two urban nodes available to supply. From (c) to (d) the network size still increases for the same reason previously explained and consequently also the size of the technologies.

The last configuration (e) presents four SMRs in the urban nodes and the diagonal connection towards the rural nodes is no more selected, so that some nodes are reached through a secondary connection. This is because the energy losses increase in primary connection is lower compared to the one which would be on the diagonal, whose length is higher: 56 km instead of 40 km.

**Conclusion** The conclusion of this analysis is that it is visible that this parameter has a huge impact on the resulting configuration of the system and consequently it has to be chosen with attention. According to literature, a value of  $A$  value of  $1.25 \times 10^{-7}$  [1/m], which is lower than the first value selected for this analysis shown in configuration (a), is selected to be not impacting on the results. This value corresponds to 0.01% of the energy lost over a kilometer.

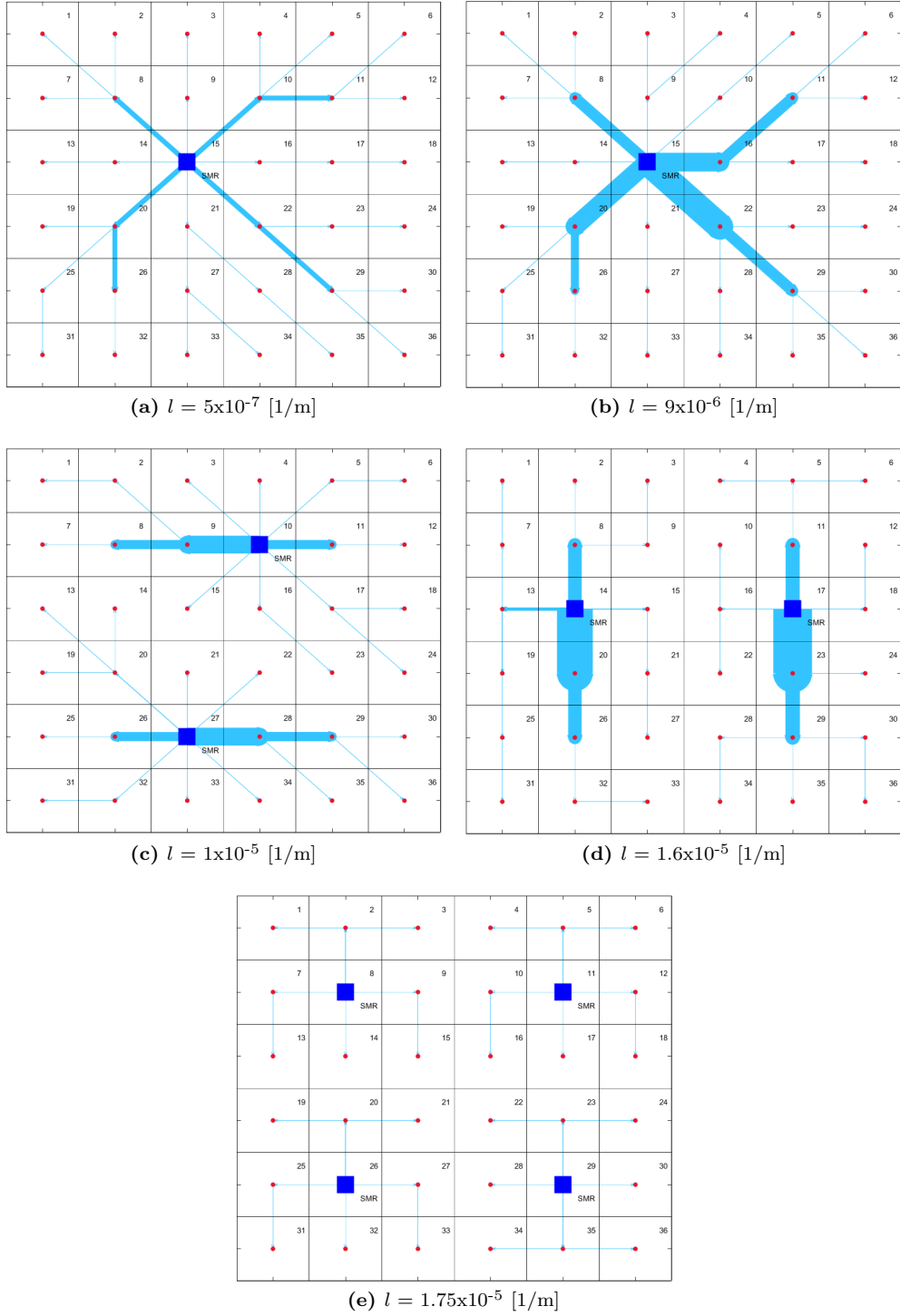


**Figure 19:** Sensitivity analysis on the energy loss parameter  $l$ .

### 5.1.1 Total energy losses

In Fig.19 are chosen to be shown only five more interesting configurations out of the ten available. In the following analysis all them are investigated in order to evaluate the evolution of the total energy losses of the system while increasing the losses coefficient. In Fig. 20 the total energy losses for each

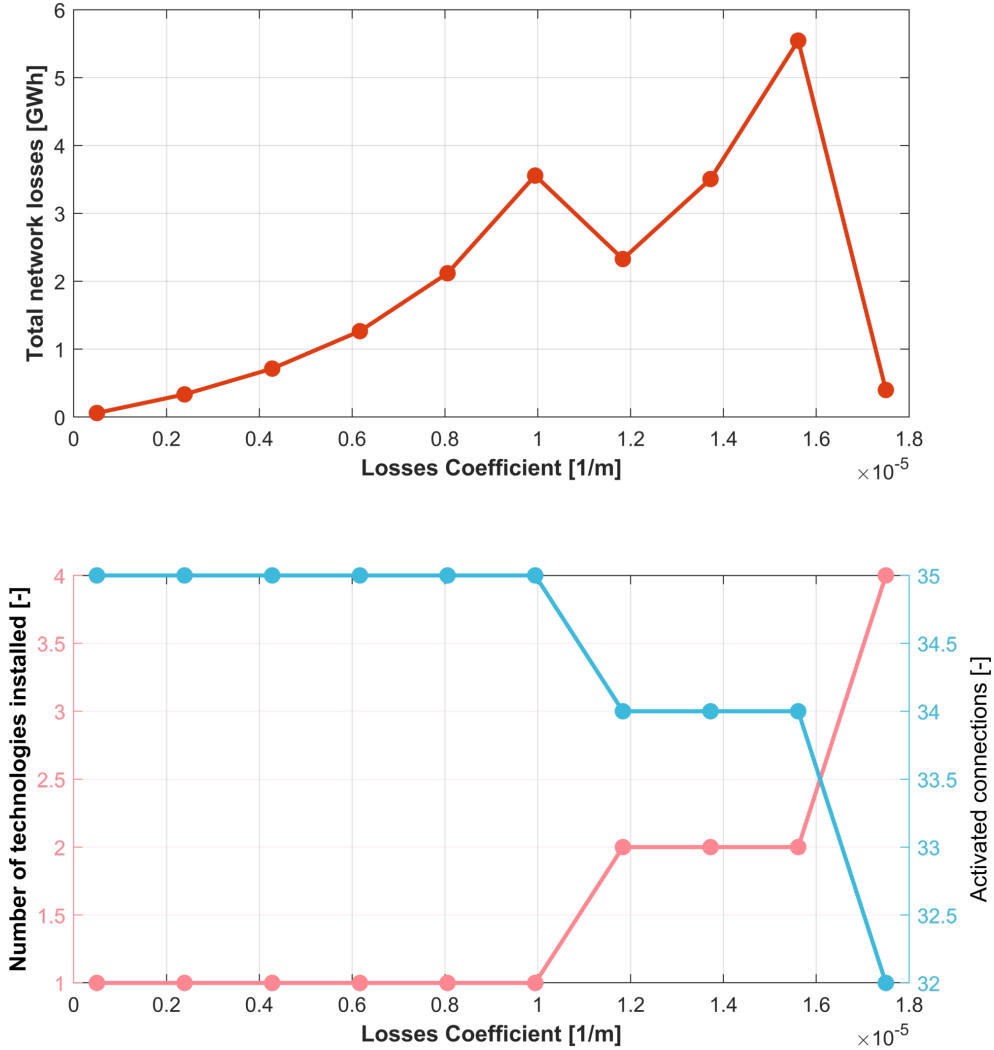


**Figure 20:** Total energy losses evolution of the system increasing the energy loss coefficient  $l$ .

configuration are shown. In the first six simulations the technology installed is only one, the activated connections stay constant (35) and therefore the energy losses are increasing until a local maximum. In the seventh configuration the technologies installed become two therefore the connections decrease by one and the total energy losses as well. Then, they increase again until the absolute maximum, as the number of connections (34) and the technologies (2) remain constant. From there, the losses have a quick decrease as four technologies are installed and so the connections are reduced as well.

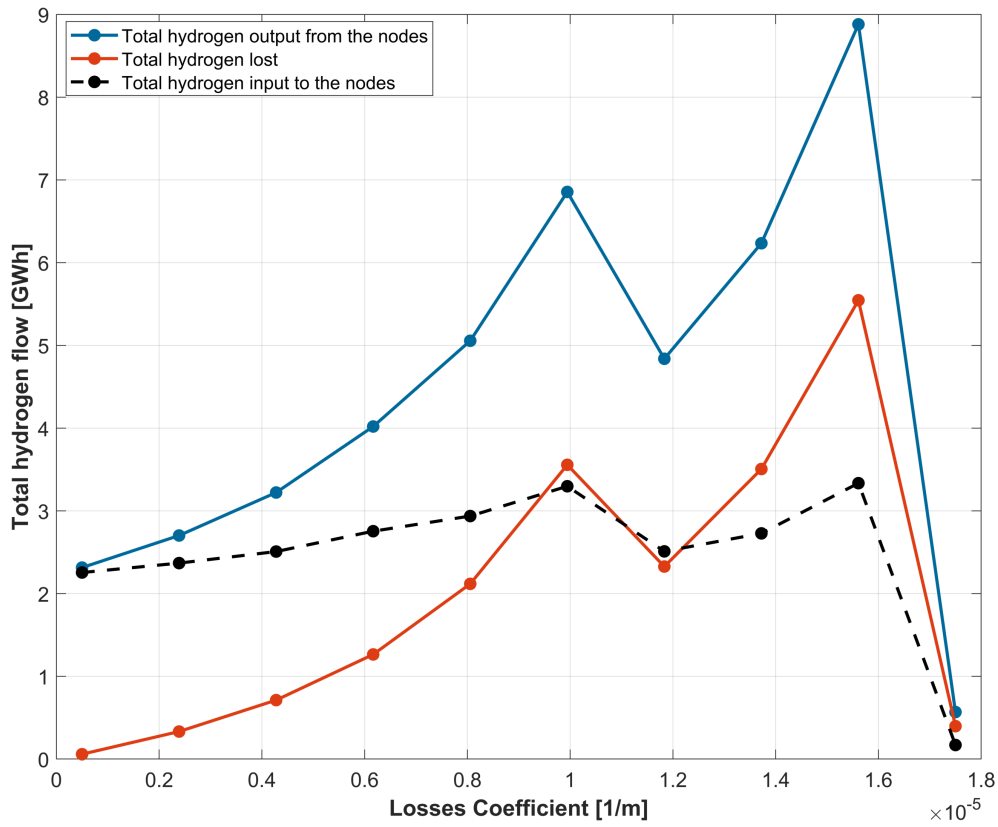


Figure 21: Total H<sub>2</sub> flow transported.

Fig. 21 shows the evolution of the total hydrogen flow in the system, which is increasing when in the different configurations the number of technologies remains the same and decreasing when it changes. The red curve is the total hydrogen lost in the system, which has exactly the same trend as the total but of course in every configuration is lower. The difference between the two is the net hydrogen flowing in the network.

## 5.2 Minimum size of networks

The goal of this second analysis is to understand the impact of networks minimum size on the resulting system configuration. In particular, the minimum size of the truck and of the railway network is increased and analyzed with respect to the hydrogen demand of the the rural nodes and of the urban nodes respectively. For this purpose, two ratios are introduced:

$$r_R = \frac{\text{Minimum size railway}}{\text{Urban hydrogen demand}}; r_T = \frac{\text{Minimum size truck}}{\text{Rural hydrogen demand}}$$

Two analyses are performed concerning the two networks, where these ratios  $r_R$  and  $r_T$  are varied to see the resulting relations with the hydrogen demands.

As the hydrogen demand is defined hourly, the minimum size of the network is set as units sent per day, where the amount of energy carried by each unit varies for each network (see Appendix).

### 5.2.1 Minimum railway size

The following assumptions are made for the railway sensitivity analysis:

- Technology portfolio: SMR
- Network portfolio: Truck, Railway and Pipeline network
- The Railway minimum size is varied from one to four unit/day, which in terms of energy transported corresponds to 85'248 kWh to 340'992 kWh of hydrogen, which is more than the maximum demand 300,000 kWh. The maximum size is set not to be limiting for the analysis
- The minimum and the maximum size for both truck and pipeline is not limiting

#### One unit per day ( $r_R=0.3$ )

The peculiarity of this configuration is that the optimizer chooses to deliver the energy to the two urban nodes 11 and 26 through two different pathways: one with the largest fraction of the energy (22-17-11/22-27-26) and the other with the smaller fraction (21-16-11/22-21-26). In the two low energy branches, the last connection brings an energy equal to one unit/day. Therefore, this is how the configuration is influenced by the minimum size constraint.

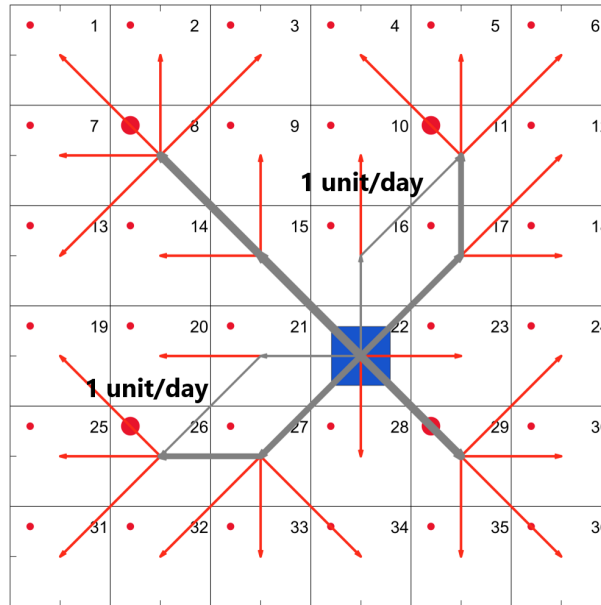


**Figure 22:** Configuration of the system with one unit/day as minimum railway size.

To understand why it works in this way, we have to compare the investment cost of the configuration shown in Fig.22 to a configuration where the second ‘small’ pathway is not possible to select. Consequently, by changing the connectivity matrix, the result presents the the same configuration as Fig. 22 but without the additional branches.

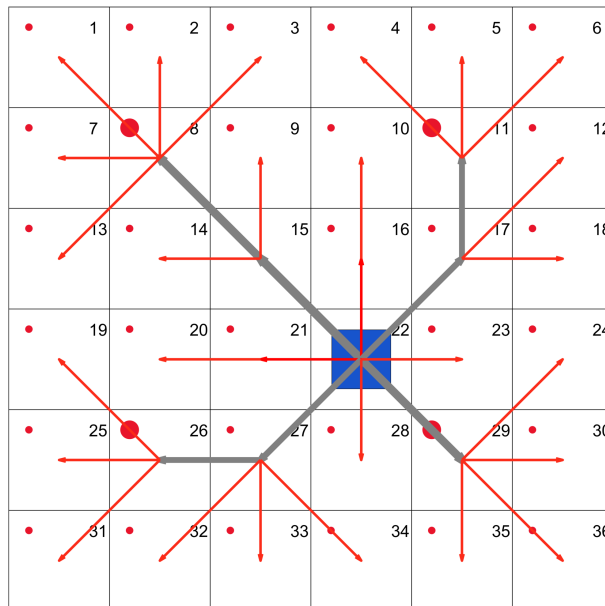


**Figure 23:** Configuration of the system with one unit/day as minimum railway size with modified connectivity matrix.

The total cost of the two configurations is represented in the following bar plot.

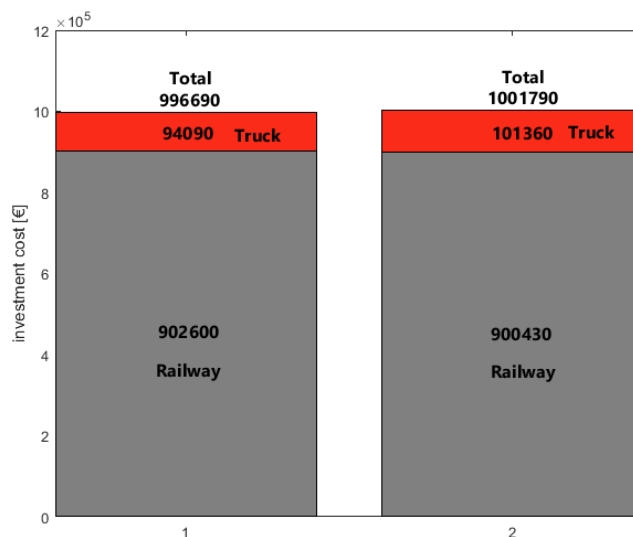


**Figure 24:** Configuration of the system with one carriage as minimum railway size changed the connectivity matrix.

In the first configuration, the railway investment cost of the first configuration is 902600 €, while for the truck 94090 €. In the second one, the investment cost for the railway is decreased to 900430, as the ‘second pathway’ is not installed anymore, but the truck is increased until 101360 €. Therefore, the total cost of the second configuration results to be higher than the first for the contribution of the additional

two truck connections activated. In the end, the decrease in the investment cost of the railway is lower with respect to the increase of the truck investment cost, which is why the optimizer chooses the first configuration. The second reason is due to the energy losses: the energy loss in the two branches is lower because less hydrogen is transported. In Fig. 23 more hydrogen is transported towards the urban nodes, consequently the energy losses are higher.

### Two and three units per day ( $r_R = 0.5$ , $r_R = 0.8$ )

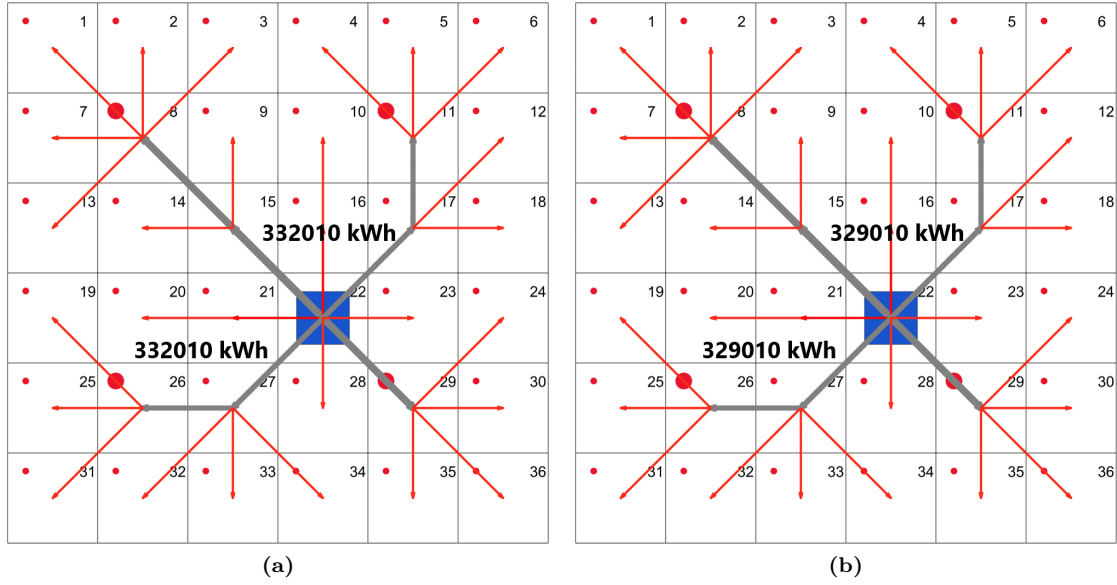


**Figure 25:** (a) two unit/day as minimum size, (b) three unit/day as minimum size

In configuration (a) the minimum energy transported by railway in this case is 170496 kWh, which corresponds to 57% of the maximum demand. The configuration is equal to the one in Fig. 23. In this case, the optimizer is obliged to transport the largest quantity of energy by railway, and so the second pathway to reach the high demand node is not possible anymore. In configuration (b) the minimum energy transported by railway in this case is 255744 kWh, which corresponds to 85% of the maximum demand. The minimum energy constraint has the same effect. In this case, the energy quantity carried in the two branches is identical: this is only related to the quantity of small demand nodes supplied by that big connection.

### Four units per day ( $r_R = 1.1$ )

The minimum energy transported by railway in this case is 340992 kWh, which is higher than the maximum demand (300000 kWh) and consequently  $r_R$  is bigger than one. This constraint on the minimum size has a big impact in the configuration. Firstly, the optimizer is forced to bring all the energy contained in the four units directly to the main demand nodes by railway, and consequently is not satisfying the demand of the intermediate nodes that it encounters. How this is satisfied is seen in the truck configuration plot in Fig.?? (a). This demand is satisfied by truck, which leaves the urban nodes, pass through the intermediate ones, and arrives in the production node to supply further energy to be transported. Consequently, it is cheaper to transport the energy to the production node by truck rather than installing a bigger plant there.

Size of the SMR installed: 1772800 kW

Energy output of the plant:  $1772800 \times 0.75 = 1329600$  kWh

Energy sent by railway:  $4 \times 340992 = 1363968$  kWh

The energy that has to be supplied by truck is the difference between the two, 34368 kWh.

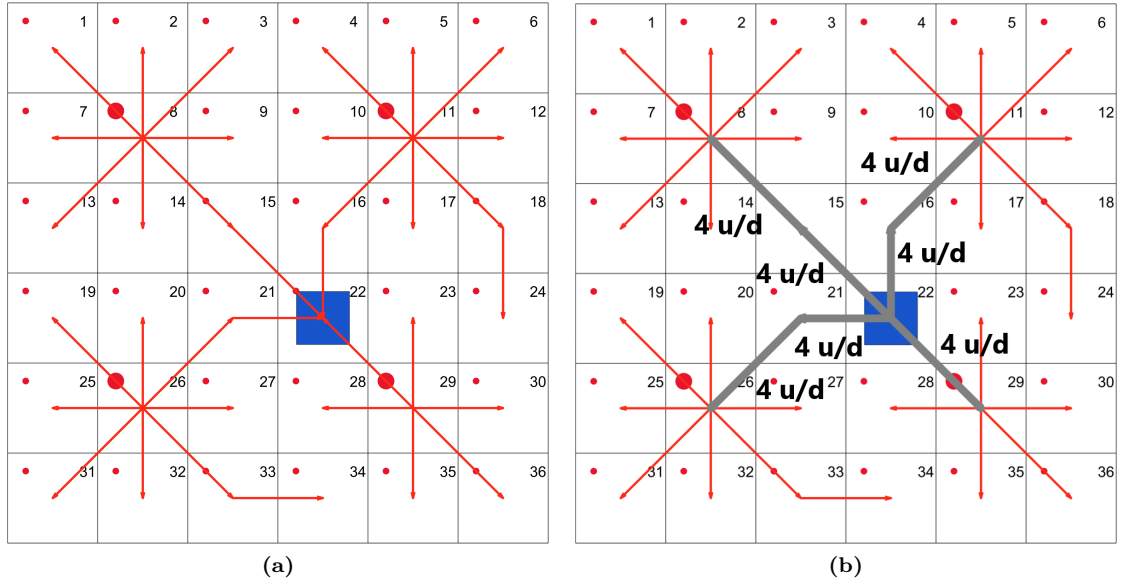


**Figure 26:** (a) Truck network with four units/day minimum size, (b) Total network with four/units as minimum size

### Conclusion

The conclusion of this analysis is that the ratio  $r_R$  is a very impacting parameter on the system configuration. In order to have results which are not affected by the value of the minimum size the inequality

$$r_R \leq 1$$

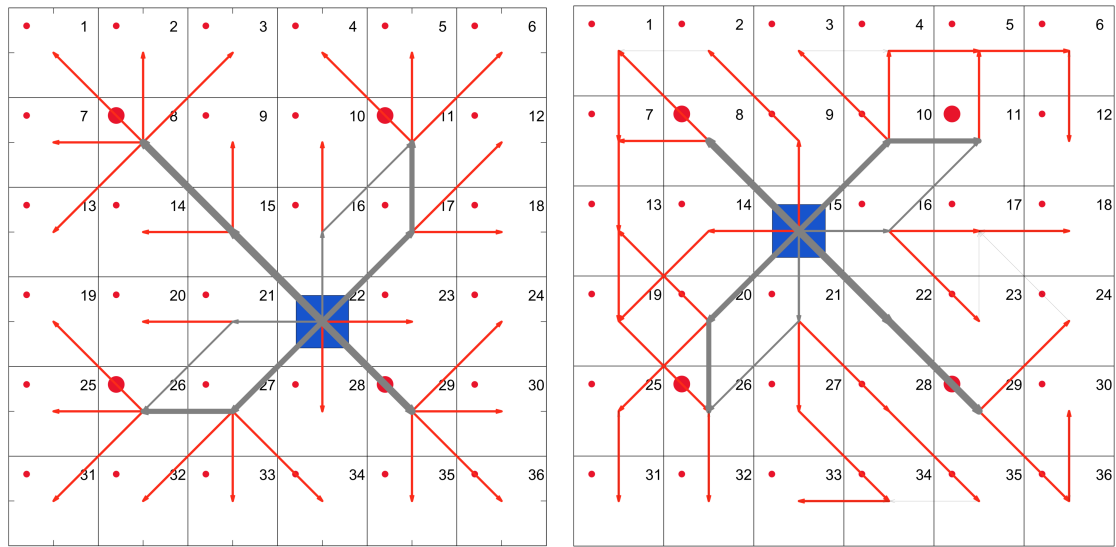
has to be respected. The consequence is that the urban demand must be bigger or equal to the minimum railway size.

### 5.2.2 Minimum truck size

The second analysis is focused on the minimum size for the truck network. The  $r_R$  is varied to understand in detail the relation between the minimum size and in the case the rural demand, as the truck supplies those nodes. The following assumptions are made:

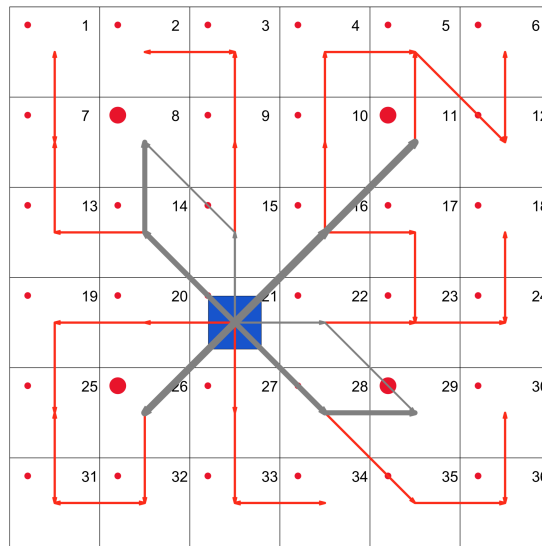
- Technology portfolio: SMR
- Network portfolio: Truck, Railway and Pipeline
- Truck minimum size is varied from one unit per day to four units per day, which respectively corresponds to 1690 kWh and 6438 kWh of energy transported, the maximum sizes is not limiting
- Railway and pipeline minimum and maximum size are not limiting

In the first configuration (a) in Fig.27, the minimum size is one unit per day and lower than the rural demand, for this reason the configuration is unaffected and is identical to the reference one in Fig. 18. The configuration with two units per days as minimum size is not shown as identical to the first one, underlying even more the fact that if the minimum size is lower than the rural demand, the network is not affected. In configuration (b) represents the first case where this is not valid anymore. It is visible that the connections where the truck is installed increase, and some strange circles underlines the particular behaviour of this result. The reason is that there is too much energy to distribute, and consequently more connections are activated to close these energy balances for all the nodes. Increasing even more



(a) One unit per day as minimum size ( $r_R=0.8$ ).

(b) Three units per day as minimum size ( $r_R=2.4$ ).



(c) Four units per day as minimum size ( $r_R=2.4$ ).

**Figure 27:** Sensitivity analysis on the truck minimum size.

the minimum size over the rural demand this behaviour is again visible, even with connections which are activated twice with the truck.

### Conclusion

Similarly to the previous analysis, the  $r_T$  is an important parameter for the analysis. In order to have a result not affected by the minimum truck size, the inequality

$$r_T \leq 1$$

has to be respected. In a real case, the minimum size of a network is fixed, the variable is the  $H_2$  demand of the end users. This sets a threshold for the minimum demand that can be satisfied: under this value, the demand of that node is transferred to the adjacent node with the highest demand.

### 5.3 Transport pressure

In all the previous analyses the transport pressure of hydrogen is not considered, so it is not discriminatory between the different networks. This analysis sets a different transport pressure to each network, corresponding to an electrical energy penalty of the compressor needed. The goal is to see the impact of this additional energy consumption on the resulting configuration of the system.

As previously stated, all the hydrogen is assumed to be transported in the gaseous form. The following assumptions are made for the analysis:

- Technology portfolio: SMR
- Network portfolio: Truck, Railway and Pipeline
- SMR exit pressure: 30 bar
- Truck and Railway transport pressure: 300 bar
- Pipeline transport pressure: 30 bar

The difference between the exit pressure of the SMR and the transport pressure of each network corresponds to the specific work that the compressor has to perform. From the literature (cita articolo fuel cell), data referring to the compressor specific work with respect to the pressure ratio are extrapolated in Fig. 28.

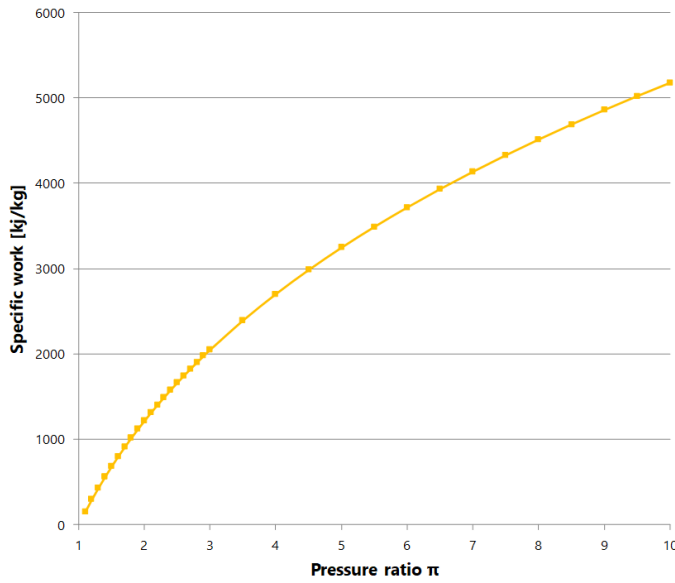


**Figure 28:** Specific work of a compressor as a function of the pressure ratio  $\pi$  [14].

According to the assumptions, for the truck and railway networks  $\pi$  is the same and equal to 10; this corresponds to a specific work equal to 5177  $\text{kJ}_{\text{el}}/\text{kg}_{\text{H}_2}$ . Concerning the pipeline network,  $\pi$  is equal to one, consequently the energy penalty corresponding to the compression does not have an impact. The resulting minimum cost configuration is shown in Fig. 29.

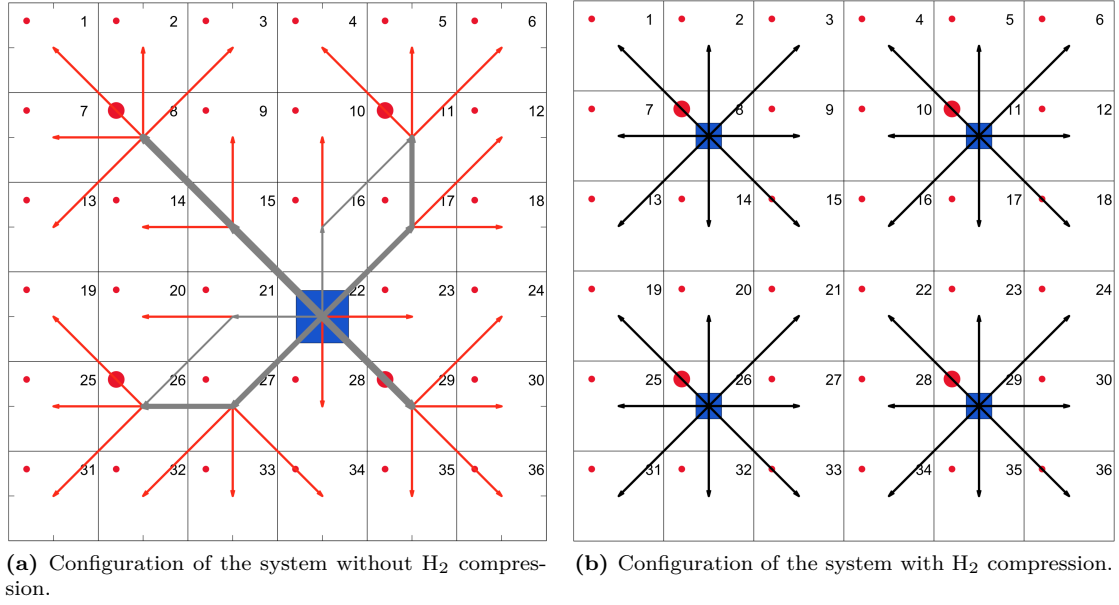


**Figure 29:** Minimum cost configuration with and without H<sub>2</sub> compression.

It is visible that the energy consumption due to H<sub>2</sub> compression has a big impact on the resulting configuration. In particular, two effects are underlined:

- **Network:** the pipeline network is installed rather than the truck and the railway. The H<sub>2</sub> compression is not applied in the case of this network, so the cost correlated to this electrical energy is not accounted. For this reason, the pipeline network is the one selected and so becomes cost competitive.
- **Technologies:** the number of SMRs installed varies from one to four. Being the network with the highest investment cost, less connections are activated. In particular, the four technologies are installed in the urban nodes to avoid the transportation to the nodes with the highest hydrogen demand.

Concerning the model, the hydrogen compression has an impact on two aspects: the operational cost of to the electrical energy needed to compress and the correlated CO<sub>2</sub> emissions of the electricity grid. In the minimum cost configuration, the influence on these two aspects is shown in Fig. 30. The largest variation is on the operational cost of the configuration which increases by 20%, while the CO<sub>2</sub> emissions increase by 3%, as the emissions of the pipeline network are the lowest of the three networks.

## 5.4 Investment cost approximation

The goal of this analysis is to understand the impact of the investment cost approximation on the system configuration. In particular, two cost approximations are analyzed:

- Piece-wise affine approximation
- Linear approximation

The investment cost is a fraction of the total cost of the system, which is the objective function of the optimization problem. The mathematical expression of the piece-wise affine approximation of the investment cost is expressed in equation (8). For each node  $i$  of the system, the linear cost approximation is otherwise expressed as:

$$\forall i \in N : J_I, i = \sum_{m=1}^M (c_m S_{m, i}) a_m \quad (19)$$

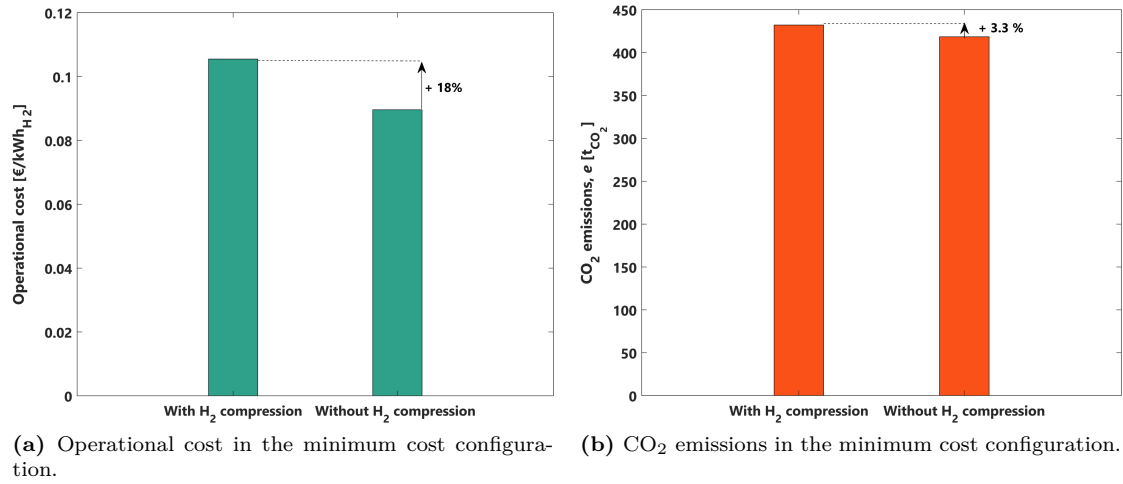


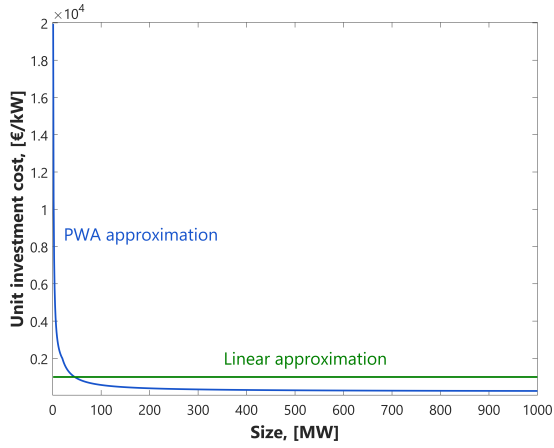
**Figure 30:** Influence of the H<sub>2</sub> compression on the operational cost and on the CO<sub>2</sub> emissions.

where  $c$  is the unit cost in [€/kW] of each  $m$ -th technology which is constant for all the size values  $S$  and  $a$  is the annuity factor, calculated with the general expression. In Fig. 31 the difference between these two approximations are shown in terms of investment cost in [€] and of unit cost in [€/kW]. In the PWA approximation, the unit cost decreases asymptotically; for bigger technologies sizes, the unit cost is lower and the opposite stands for small sizes. Consequently, the investment cost presents a steeper trend for small sizes, where the unit cost is higher and the fixed costs are lower, and a flatter trend for big sizes, where the unit cost is lower and the fixed cost are higher.

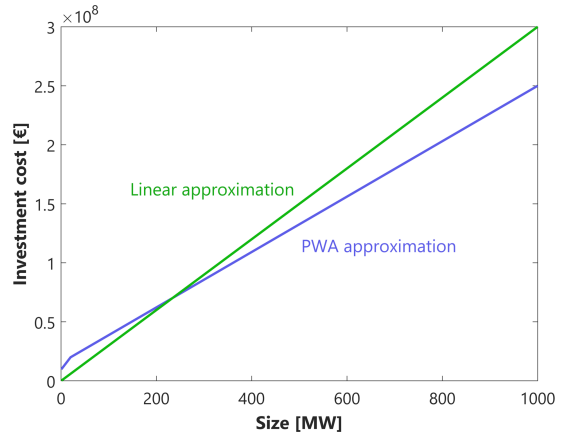
Concerning the linear approximation, the unit cost is constant for all the technology sizes. Consequently, only one straight line through the origin is describing the investment cost.

The analysis is performed in two different configurations of the system with the following assumptions:

- Technology portfolio: SMR
- Network portfolio: Truck, Railway and Pipeline
- Transport pressure not considered

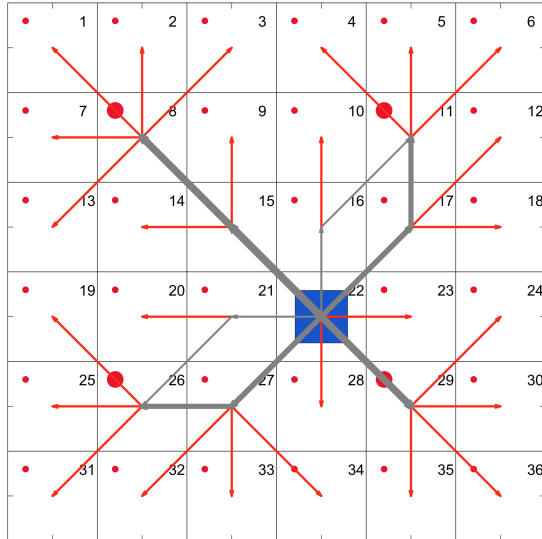


(a) Piece-wise affine and linear unit cost.

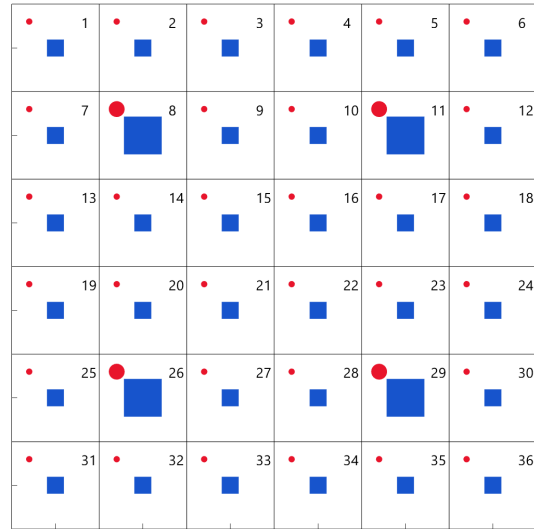


(b) Piece-wise affine and linear investment cost.

**Figure 31:** Linear and piece-wise affine approximation of the investment cost.



(a) Minimum cost configuration with a piece-wise approximation of the investment cost.



(b) Minimum cost configuration with a linear approximation of the investment cost.

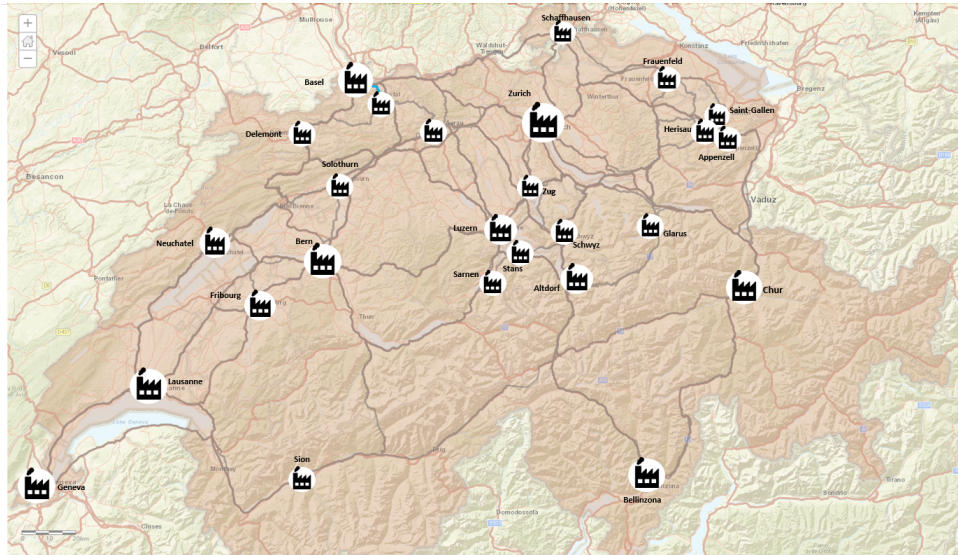
**Figure 32:** Minimum cost configuration with a piece-wise affine and linear approximation of the investment cost.

#### 5.4.1 Schematic configuration result

The fact that the two configurations shown in 32 are completely different shows the big impact that the investment cost approximation has on the optimal design. In (a) the PWA approximation is used and one single SMR is installed, so the total centralization of the system is the preferred. The reason stays in the unit cost trend, which is lower for big sizes and so it is convenient to have one big technology and all the hydrogen transported to the end users. On the other hand, in (b) the opposite configuration is shown. One technology is installed in each node and the system is so completely decentralized. In this case the advantage to have big-sized technologies is completely nullified, so every SMR is supplying the local demand and there is no reason to have a hydrogen network.



(a) Minimum cost configuration with a piece-wise approximation of the investment cost.



(b) Minimum cost configuration with a linear approximation of the investment cost.

**Figure 33:** Minimum cost configuration with a piece-wise affine and linear approximation of the investment cost.

#### 5.4.2 ArcGIS configuration result

The configuration (a) in Fig. 33 is to be compared with configuration (a) in Fig. 32. It is visible that the result is conceptually the same: one big-sized SMR installed and the largest network to supply all the other capitals. Also the position of the technology is similar: the SMR is located in Bern which is geographically in the middle between the high demand capitals: Geneva and Lausanne on the western part and Zurich Basel on the eastern part. In the schematic configuration the technology is installed in node 22, which is one of the four in the centre in order to be the nearest possible the high demand nodes.

The configuration (b) in Fig. 33 is instead to be compared with configuration (b) in Fig. 32. Also in this case the optimal design is conceptually the same: each SMR is supplying the hydrogen for the capital where it is installed and the network is totally nullified.

The result is very important because it underlines a modeling conclusion: the result is general and can be applied to any configuration.

## 6 Optimal design of hydrogen supply chains

Until this point a more modeling prospective of the hydrogen supply chain has been proposed: the influence of some important input data to the optimization problem now is known and it is possible to proceed to the overall final result. In this chapter, the optimal design of the hydrogen supply chain is finally proposed and discussed.

### 6.1 Competition between SMR and PEME

In this first analysis, the competition between a blue hydrogen production technology, SMR, and a green hydrogen production technology, the electrolyzer, is investigated along the Pareto front. The following assumptions are made:

- Technology portfolio: SMR and PEME
- Network portfolio: Truck, Railway and Pipeline
- Transport pressure considered
- PWA approximation of the investment cost

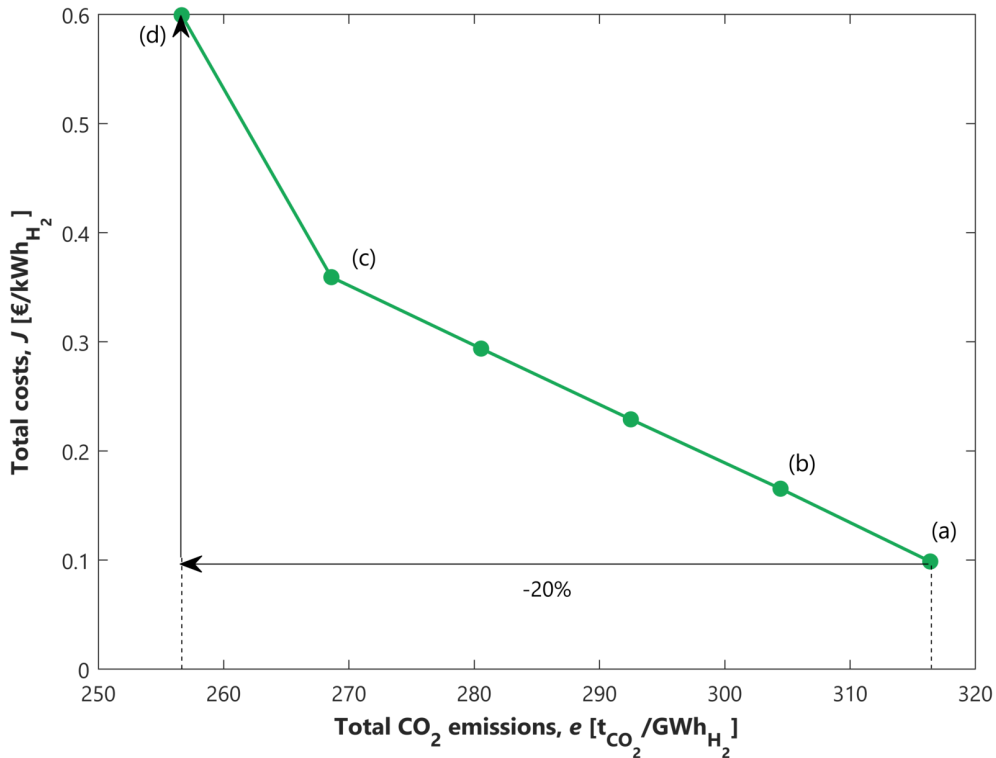


**Figure 34:** Pareto front with SMR and PEME technologies.

In the above Pareto front the overall CO<sub>2</sub> emissions are reduced by 20% from the minimum cost point, named with (a), to the minimum emissions point, named with (d). The emissions reduction is due to the PEME technology that is installed, and has lower emission factor connected to the electricity grid in comparison to the one of the natural gas grid.

Concerning the total cost of the system, they increase by four times from (a) to (d) due to the cost of the electrolyzer, which has a higher unit cost than the SMR (see Appendix). In Fig. 35 the configuration of the system of some relevant Pareto points are shown.

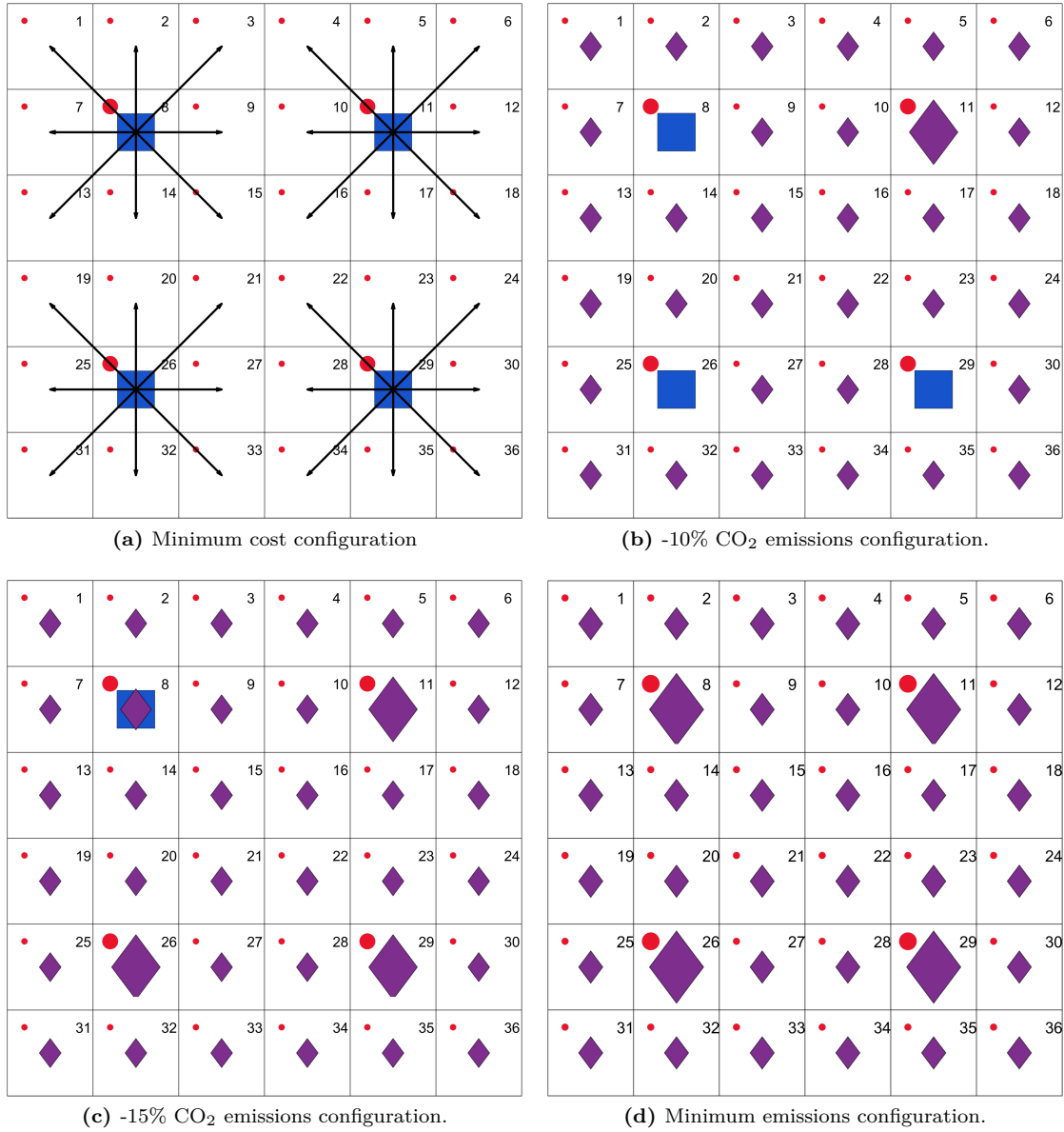


**Figure 35:** Optimal configurations of the system along the Pareto front.

As the transport pressure is accounted, the minimum cost configuration of the system is the same as 29 (b): four technologies installed in the urban nodes and hydrogen transported to the rural nodes by pipeline. As the CO<sub>2</sub> emissions decrease, the configuration shown in (b) presents the small-sized electrolyzer technologies installed in the rural nodes and one big-sized in one urban node. The emissions are decreased due to the removal of the network already in the second Pareto point and because of the electrolyzer, which has an emission factor connected to the electricity grid of 0.137 ton<sub>CO<sub>2</sub></sub>/MWh which is lower in comparison to the one of the natural gas grid, of 0.237 ton<sub>CO<sub>2</sub></sub>/MWh. In configuration (c) the emissions are decreased by 15%, so in the urban nodes three big-sized SMRs are installed rather than the SMR. In the fourth urban node both of the technologies are installed medium-sized. The minimum emission configuration shown in (d) present an electrolyzer technology for each node, so the SMR is not selected anymore.

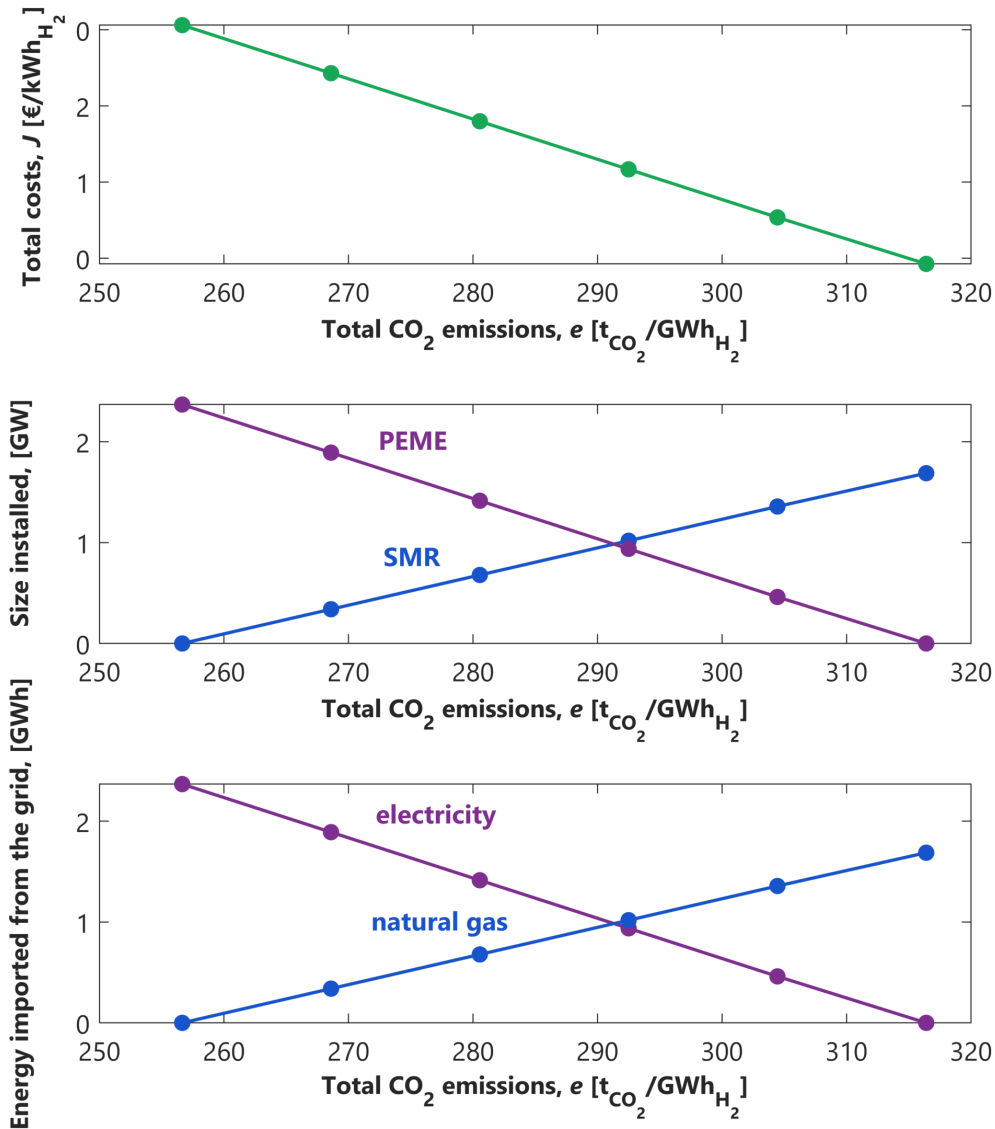


**Figure 36:** Size of the technologies and energy imported from the grids along the Pareto front.

In the first plot of Fig. 36 the size of the two technologies along the Pareto front is shown. As already explained, it is visible that the size of the SMR technology decreases linearly towards zero in the minimum emission configuration. On the other hand, the size of the electrolyzer increases linearly from zero to its maximum size in the last Pareto point. In particular, in the third Pareto point the total sizes of the two technologies are approximately the same. An important aspect to notice is that the size of SMR installed in the minimum cost point, which presents only SMRs, is lower than the size installed of electrolyzers in the minimum emission point, where only PEME are installed. This is due to the fact that the SMR efficiency is higher than the PEME efficiency, so a total smaller size is needed to satisfy the total hydrogen demand.

The energy imported from the electricity and gas grid has the same trend of the technology sizes. The electricity imported increases linearly as the PEME size, while the natural gas imported decreases linearly as the SMR size.

### 6.1.1 Impact of the emission factor of the electricity grid $\epsilon_e$

In the following analysis the emission factor of the electricity grid is increased to understand better its influence over the optimal result. The minimum emission configuration is the most suitable as the one which uses that highest quantity of electrical energy from the grid, having one electrolyzer installed in every node. Starting from the top, the total CO<sub>2</sub> emissions trend with respect to the emission factor is

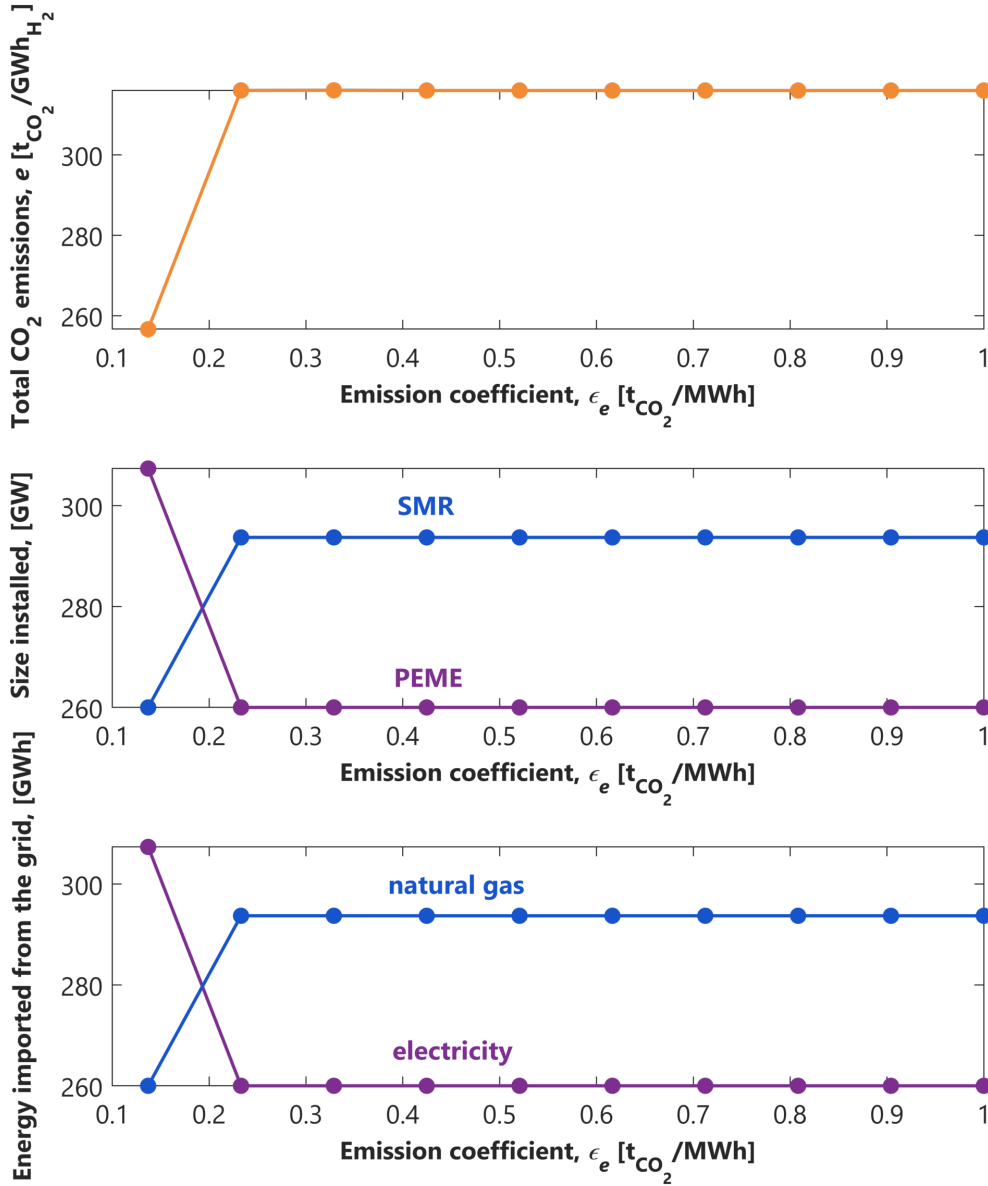


**Figure 37:** Impact of the emission factor of the electricity grid  $\epsilon_e$  in the minimum emission configuration.

shown: naturally, they increase as the emission factor of the grid increases. In the second plot, the size of the technologies show an interesting trend as  $\epsilon_e$  increases: from one particular value of  $\epsilon_e$ , the SMR is installed instead of the PEME. This happens because the emissions related to the grid increase, and consequently the SMR becomes the technology less impacting on the total emissions. This threshold is expected to be when

$$\epsilon_e = \epsilon_g$$

Instead, in Fig. 37 is visible that the technology switch happens for a lower value of  $\epsilon_e$ . Performing a zoom on the plot it is possible to find out the exact value, shown in Fig. 38.

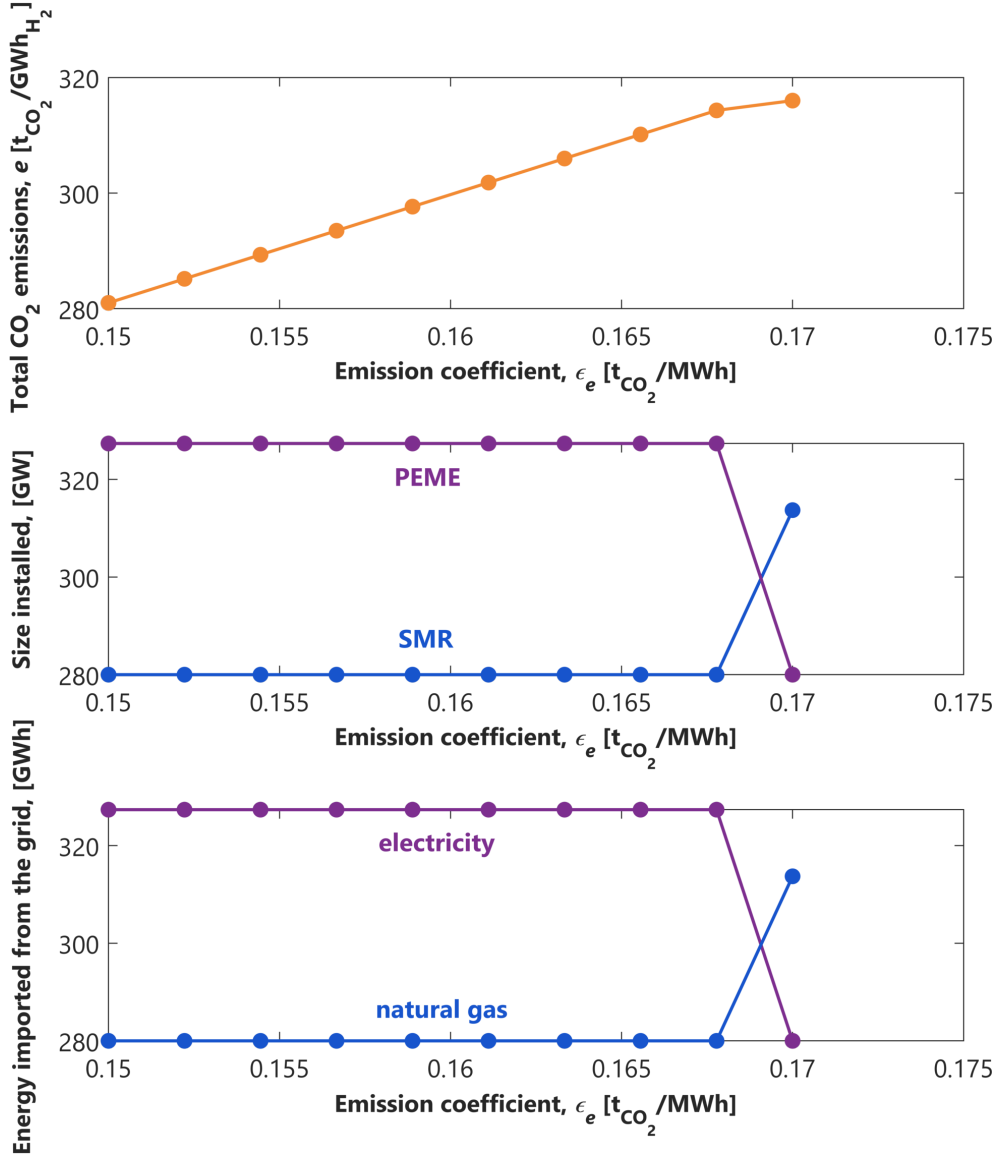


**Figure 38:** Impact of the emission factor of the electricity grid  $\epsilon_e$  in the minimum emission configuration.

The exact value where the two curves intersect is between 0.165 and 0.170  $\text{tonCO}_2/\text{MWh}$ . It is possible to calculate the exact threshold with the following expression:

$$\epsilon_e = \epsilon_g \frac{\eta_{\text{PEME}}}{\eta_{\text{SMR}}} = 0.169 \frac{\text{tonCO}_2}{\text{MWh}}$$

This result is interesting because shows that for decreasing the total emission of the system, not only the direct and indirect emissions of the single technology play a role, but also the efficiency has an impact.

## 6.2 Role of biomass

This section presents the final result of the optimal design of the hydrogen supply chain. In particular, the biomass technologies are introduced in the technology portfolio as an alternative green hydrogen production pathway to the electrolyzer. Those are compared with the blue hydrogen production technology, the SMR. Finally, the competition among all the technologies and all the networks is analyzed to give a conclusive result on the optimal design of a low-carbon hydrogen supply chain.

### 6.2.1 Impact of biomass availability on optimal design

#### Modeling of biomass technologies

The biomass technologies introduced uses two different types of biomass as energy source:

- Steam Biomethane Reforming (named *wet biomass*): uses waste residues such as manure, waste water and municipal solid waste.
- Biomass Gasification (named *dry biomass*): uses charcoal, wood and wood waste as well as a multitude of agricultural residues.

The wet biomass input to the Steam Biomethane Reformer is assumed to be available only in the rural nodes without the possibility to transport it. Consequently, the technology is forced to be installed directly in the rural node.

The dry biomass input to the gasification process is assumed to be also only available in the rural nodes but with the possibility of transport it via the truck network. In this case, the technology can be installed in every node of the system: in-loco in the rural nodes, or in the urban nodes with the biomass truck network supplying the energy source. This network presents the following characteristics: The cost

Network	Minimum size [kWh]	Maximum size [kWh]	Loss coefficient $l$ [1/m]
Truck	4344	104250[ref]	$5 \times 10^{-12}$

**Table 1:** Truck network input parameters for dry biomass.

coefficients for the dry biomass truck are equal to the ones referred to the hydrogen truck, summarized in table 7. The CO<sub>2</sub> emission coefficient  $\gamma$  is set equal to zero for both biomass technologies. This is because all the CO<sub>2</sub> emitted is considered biogenic, so already contained in the molecular structure of biomass and consequently it is not considered as an additional emission (see Appendix).

The availability of biomass  $B$  in [kWh] is modelled to be equally distributed among all the rural nodes  $n$  of the system and to entirely satisfy the hydrogen demand of the system. The availability for the  $i$ -th rural node is expressed with the following expression , where  $\mathcal{N}_r = (1, \dots, n)$  is the set of rural nodes of the system:

$$\forall i \in \mathcal{N}_r : B_i = (r \cdot n + \frac{U}{1 - ld} N) \frac{(F)}{n\eta}$$

In the expression,  $r$  is the rural hydrogen demand which is multiplied by the number of rural nodes,  $U$  is the urban hydrogen demand divided by the fraction of energy lost from rural to urban nodes multiplied by the total number  $N$  of urban nodes. This first factor represents the total energy to be produced in order to satisfy entirely the hydrogen demand. Diving then by  $n$  and  $\eta$ , the efficiency of the biomass technologies, becomes the total energy required for each rural node in input to the technologies.  $F$  is the factor which sets the fraction of hydrogen demand which can be satisfied by the biomass technologies.

#### Research question

*How is the hydrogen network influenced by the quantity of biomass available to satisfy the demand?*

The practical implementation of this question is the variation of the parameter  $F$ . If  $F$  is equal to 1, the overall biomass technologies are able to satisfy 100% of the total demand, half by steam biomethane reforming and half by biomass gasification. If  $F$  is equal to 0.5, the hydrogen demand is satisfied by wet biomass technologies for 25% and by dry biomass technologies for the other 25%.

The end goal of the analysis is to vary the biomass availability in the system and to see the impact on the optimal result, in terms of technologies and networks installed.

### Result: Total H<sub>2</sub> demand satisfied by biomass potential

In Fig. 39 it is immediately visible that the Pareto front goes from approximately 316 to zero ton<sub>CO<sub>2</sub></sub>.

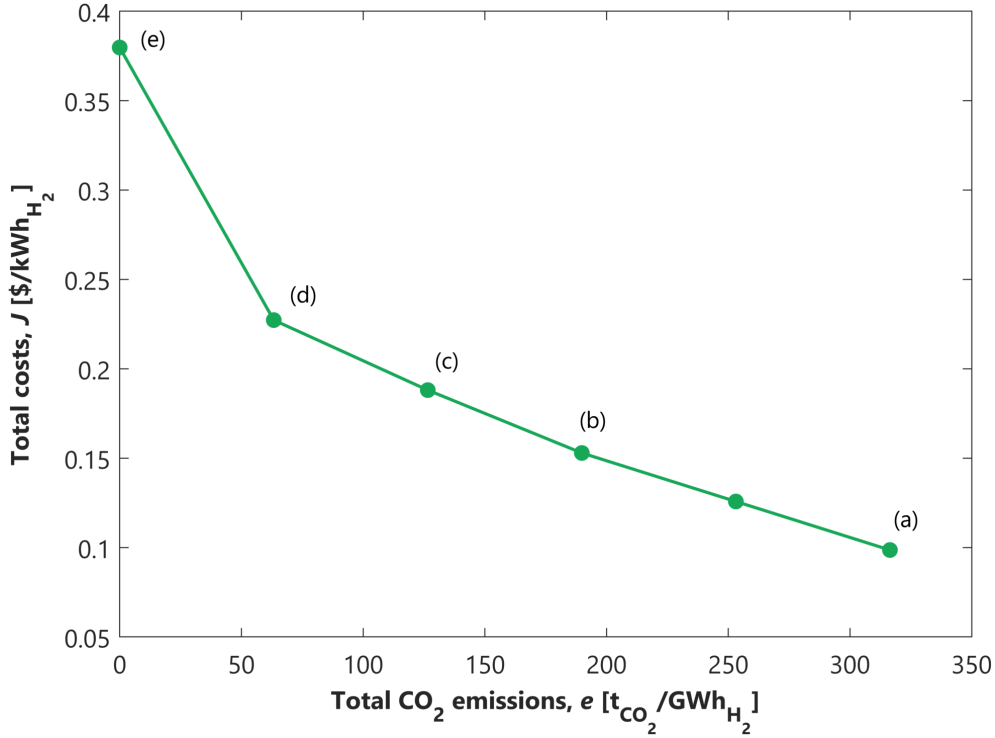


**Figure 39:** Pareto front with total H<sub>2</sub> demand satisfied by biomass potential.

This is the effect of setting the emission coefficient  $\gamma$  equal to zero. The costs are almost multiplied by four from (a), minimum cost configuration, to (d) minimum emissions configuration. In Fig. 40 the corresponding network configuration are shown in the underlined Pareto points.

Starting from the minimum cost configuration (a), four SMRs in the urban nodes are chosen, supplying hydrogen to the nearest rural nodes by pipeline. From the second configuration (b) the gasifier starts to be installed in two of the urban nodes available and consequently the truck network transporting biomass is activated (indicated with the yellow color), bringing the energy source from the rural nodes, where it is available, to the urban nodes. The hydrogen produced by the gasifier is then transported by pipeline to the rural nodes. In the others two the SMR is still installed, and the pipeline network transport the hydrogen to the remained rural nodes. The emissions are lowered because of the zero emission factor of the gasifier, which permits to lower much the emissions installing even more network, which in the previous cases analyzed is the first element eliminated along the Pareto front. The gasifier is selected rather than the biomethane reformer, as less efficient, but also as less expensive technology.

In configuration (c) and (d) the CO<sub>2</sub> emissions are decreased by 55% and then 80% and they present a decentralisation of the technologies towards the rural nodes with the biomethane reformer installed, firstly in (c) and then more evident in (d). The circuits of dry biomass are needed to supply the energy source towards to the gasifiers installed in the urban nodes. The gasifiers are supplying the hydrogen to the urban nodes, so locally, but also to some rural nodes in which it is not present the bio-reformer. The number of SMRs is decreased from two to one as they are substituted with biomass technologies emitting less CO<sub>2</sub>.

In the minimum emission configuration (e) the system is totally decentralized. Locally in each rural node one gasifier and one bio-reformer are installed to supply the hydrogen in loco and also to transport it towards the urban node via pipeline. This configuration is chosen rather than the one with four gasifiers in the urban nodes and with the biomass truck network activated because of the emission coefficient  $\gamma$ , which is lower in the case of the pipeline.

In Fig. 41 are summarized some important variables of the system along the Pareto. In the first plot, it is visible that the activated connections of the truck network transporting biomass (named bio-truck) increase along the Pareto as the gasifier also increases, visible in the third plot. The pipeline network remains almost constant, used in the firsts configurations to supply hydrogen to the rural nodes from the gasifiers and SMRs localized in the urban nodes. In the last configuration the pipeline is used by the bio-SMR as well, supplying the urban nodes. It is important to notice that the railway and the hydrogen ruck are not installed, because not anymore competitive with the pipeline is the hydrogen compression is activated.

The majority of the energy flow is carried by the bio-truck as energy input to a technology which is also the less efficient in the technology portfolio. The energy carried by the pipeline is always lower as it connects urban to rural nodes, and in the last configuration it increases because the technologies in the rural nodes are totally supplying the urban nodes.

In Fig. 42 (a) the decentralisation coefficient  $D$  is shown along the Pareto front. This parameter quantifies the tendency of the system to go from the technologies only installed in the urban nodes ( $D = 0\%$ ), to only installed in the rural nodes ( $D = 100\%$ ), in the minimum emission configuration.  $D$  is expressed as:

$$D = \frac{|(t - T)|}{t} \cdot 100$$

where  $T$  and  $t$  are the number of technologies installed in the urban nodes and the number of technologies installed in the rural nodes respectively.

The biomass exploitation coefficient is the total amount of biomass used with respect to the total available in the specific configuration. It is visible that the dry biomass technology is firstly installed, while the wet is exploited from the fourth Pareto point on. In all the points of the Pareto front, the dry biomass is more exploited than the wet as a less expensive technology, and also because of its flexibility to be also installed in the urban nodes. In the last configuration, both of the biomass technologies exploit the total amount of energy available and are able to satisfy the total hydrogen demand because of the assumption made at the beginning.

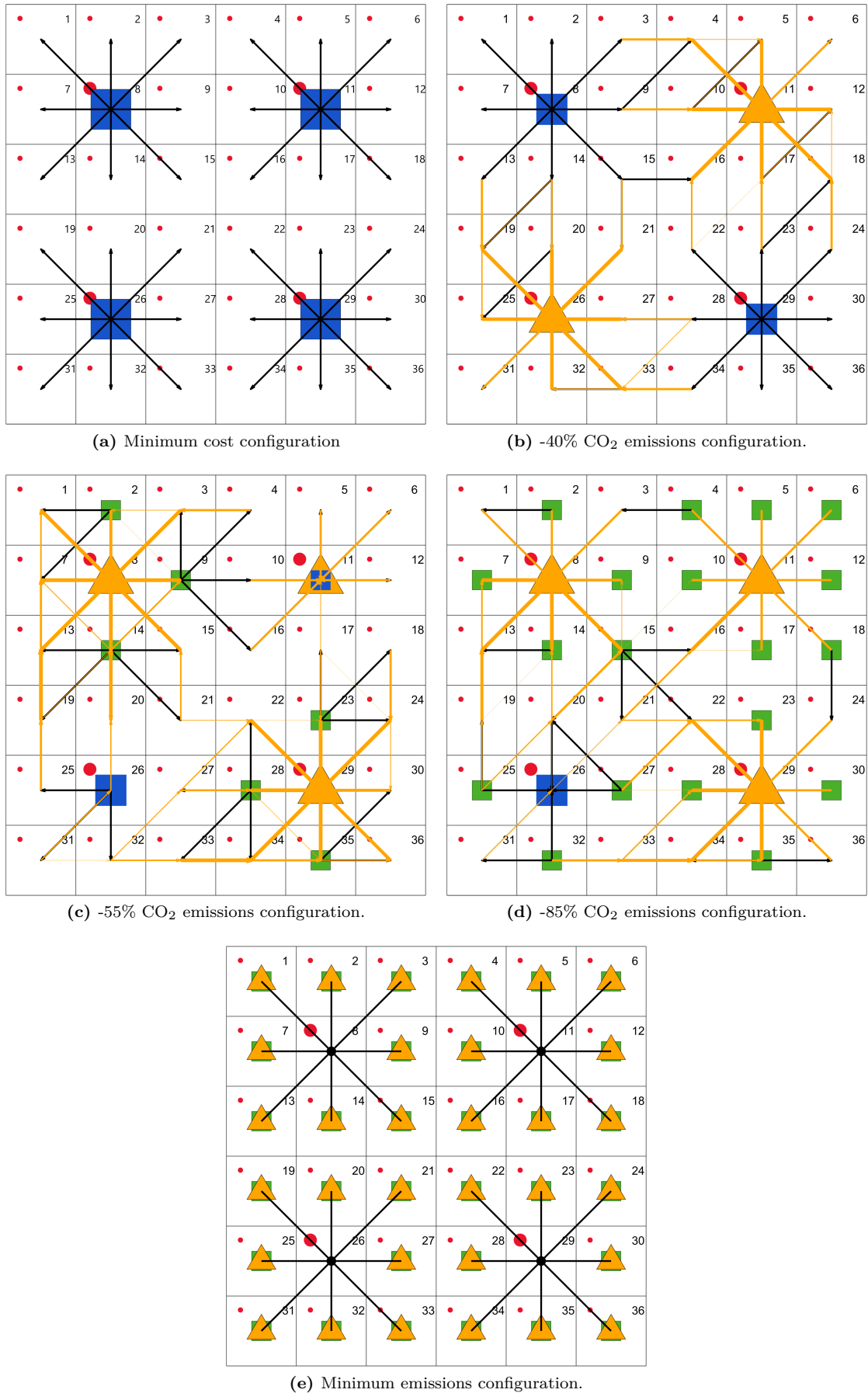


**Figure 40:** Optimal configurations of the system along the Pareto front when the total H<sub>2</sub> demand can be satisfied by biomass technologies.

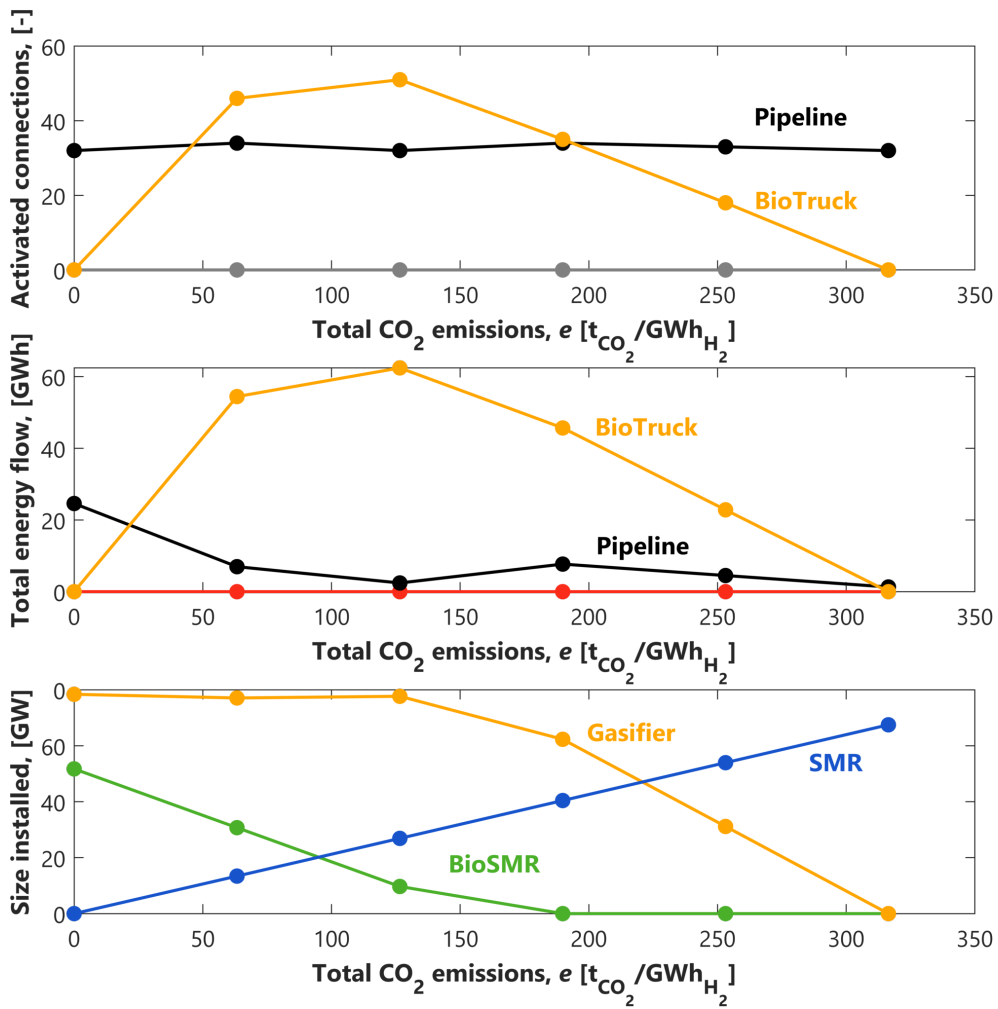
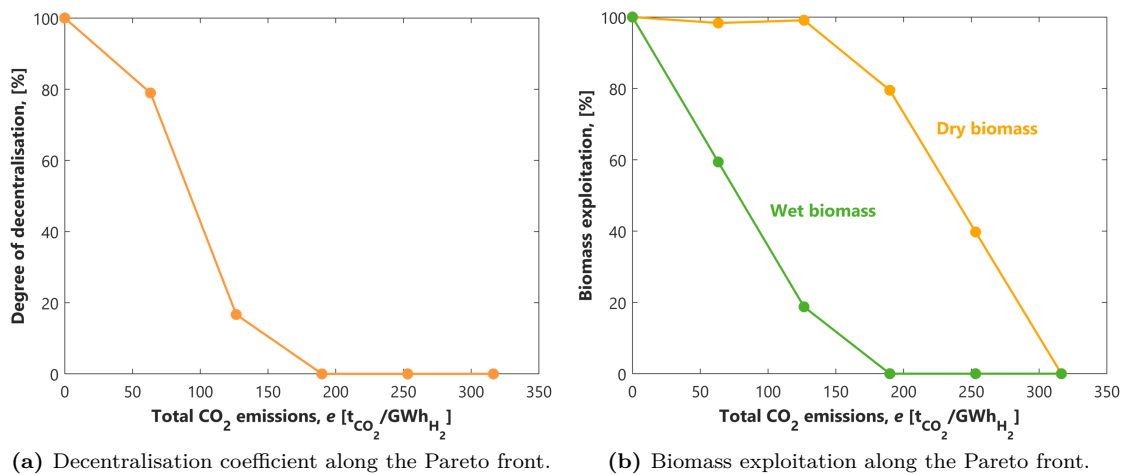


**Figure 41:** Activated connections, hydrogen flow and size of the installed technologies along the Pareto front with total H<sub>2</sub> demand satisfied by biomass technologies.



(a) Decentralisation coefficient along the Pareto front.

(b) Biomass exploitation along the Pareto front.

**Figure 42:** Biomass exploitation and decentralisation along the Pareto front.

**Result: 20% of H<sub>2</sub> demand satisfied by biomass potential**

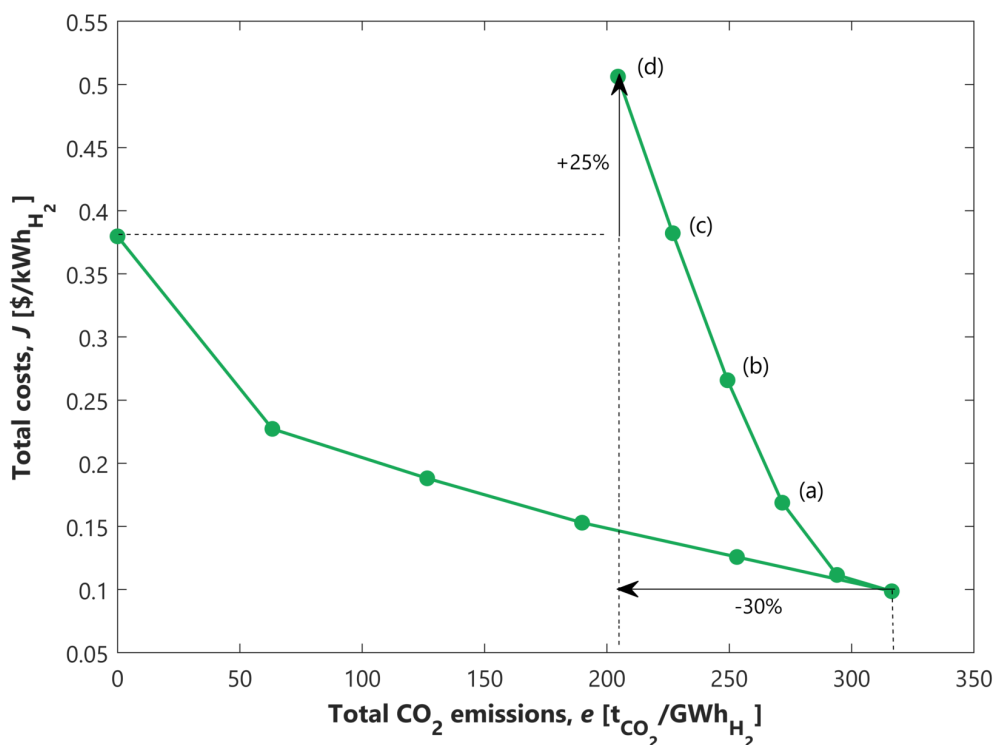


**Figure 43:** Pareto front with 20% of H<sub>2</sub> demand satisfied by biomass potential.

In Fig. 43 the new Pareto front is added to the one shown in Fig. 39. When the biomass potential is only able to satisfy 20% of the total hydrogen demand, it is clear that the emission cannot be brought to zero as in the first case: they are decreased by 30% from the minimum cost to the minimum emission configuration. In every point of this Pareto, the total costs of the system are higher in comparison to the first Pareto front. In particular, in the minimum emission configuration the costs increase by 25%. This is due to the electrolyzer technology which is installed over the new Pareto in order to help the emissions decrease, which cannot be totally performed by the biomass technologies anymore. In the following Fig. 44 the configurations of the system over this Pareto are shown.

The minimum cost configuration and the second Pareto point are no more shown because similar to the ones in the previous analysis. In particular, in the second Pareto point one small-sized gasifier is installed in one urban node with one big-sized SMR; the total cost do not have a considerable increase. From the third point (a), the costs are higher as the system starts to decentralize with some biom-reformers installed in the rural nodes supplying hydrogen to rural neighboring nodes, but still with the same amount of technologies installed in the urban nodes, which makes the cost increase even more. In the fourth Pareto point (b) the system is already completely decentralize and for the first time a small-sized electrolyzer technology is installed in one rural node to help decrease the emissions. Of course, this cause a step increase on the total costs of the system as it is the most expensive technology; all the other technologies still are installed in the urban nodes.

The configuration (c) presents still the configuration completely decentralized with the wet biomass technology, but with two big-sized electrolyzers in two urban nodes, and only one big-sized SMR remains. In the minimum emissions configuration (d) both of the biomass are totally exploited and the electrolyzer technology is installed in three of four rural nodes. The SMR technology is removed: all the hydrogen demand is satisfied by green production pathways, with 25% higher total costs from the minimum emission configuration analyzed in the previous analysis, because of the electrolyzer technology which satisfies the demand that cannot be covered by the biomass technologies, as in this analysis their potential is limited.

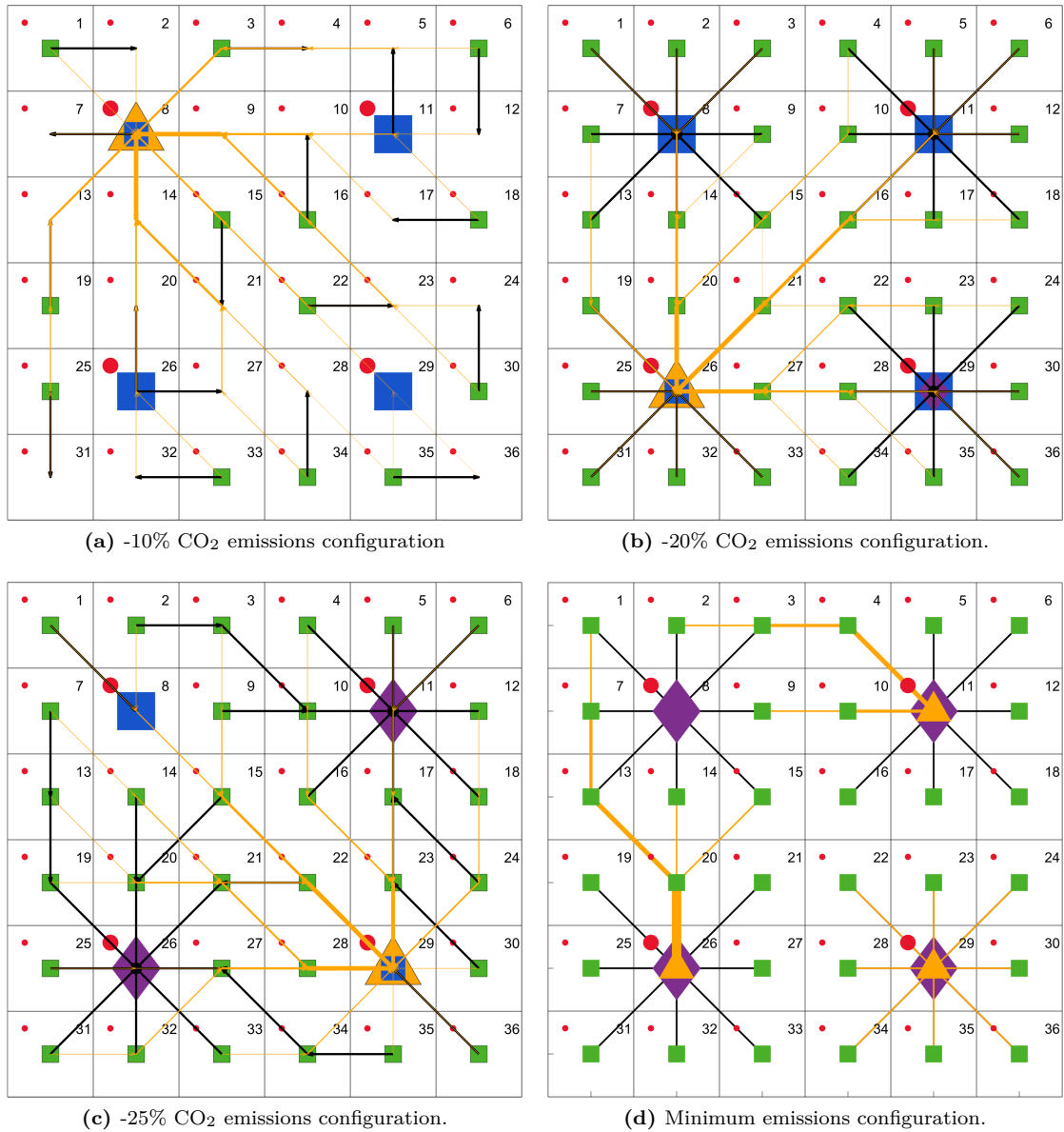


**Figure 44:** Optimal configurations of the system along the Pareto front when the 20% of H<sub>2</sub> demand can be satisfied by biomass technologies.

In this second analysis, the decentralisation coefficient shown in Fig. 45 (a) increase until it saturates the number  $f$  urban nodes available already in the fourth Pareto point. In that point  $D$  is not equal to 100% because there are still technologies installed in the urban nodes, shown in configuration (b) in Fig. 44, in particular six, four SMRs, one gasifier and one electrolyzer. In the following Pareto point, configuration (c), the decentralisation is still at its maximum, but  $D$  increases again as five technologies are left in the urban nodes, particularly one big-sized SMR is substituted with one big-sized electrolyzer. This is the same reason why in the minimum emissions configuration (d) the decentralisation coefficient decreases, as seven technologies are installed in the urban nodes: four big-sized electrolyzers and three big-sized gasifiers.

Similar conclusions are extrapolated by the biomass exploitation plot shown in 45 (b): the dry biomass technology is exploited always before along the pareto front with respect to the wet technology. The comparison with Fig. 42 (b) is that the biomass potential is saturated totally before along the Pareto curve: the dry biomass is totally used from the third Point while before was from the fourth, instead the

wet biomass potential is exploited totally already from the fourth Pareto point while before it reached 100% only in the minimum emission configuration.

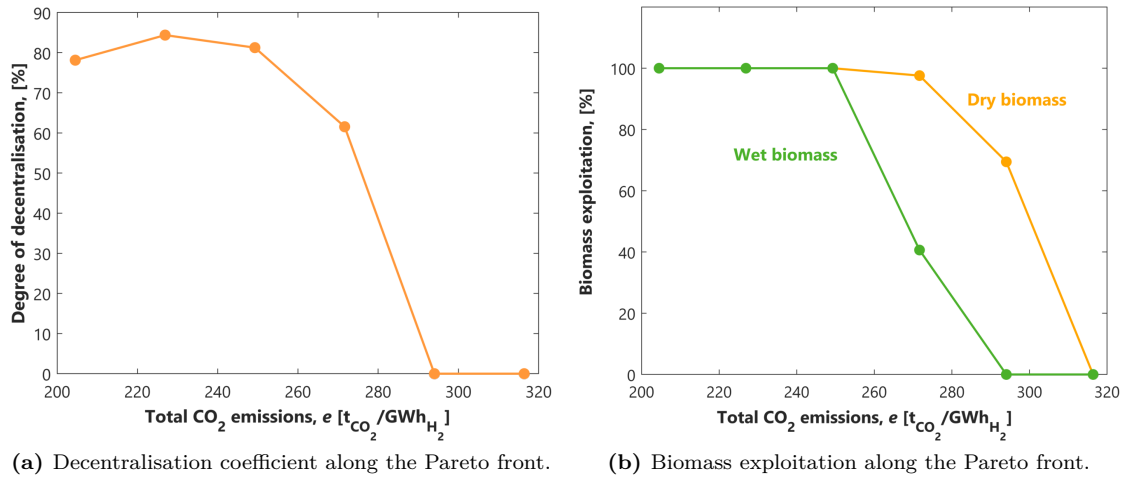


Figure 45: Biomass exploitation and decentralisation along the Pareto front.

Result: 0% H<sub>2</sub> demand satisfied by biomass potential

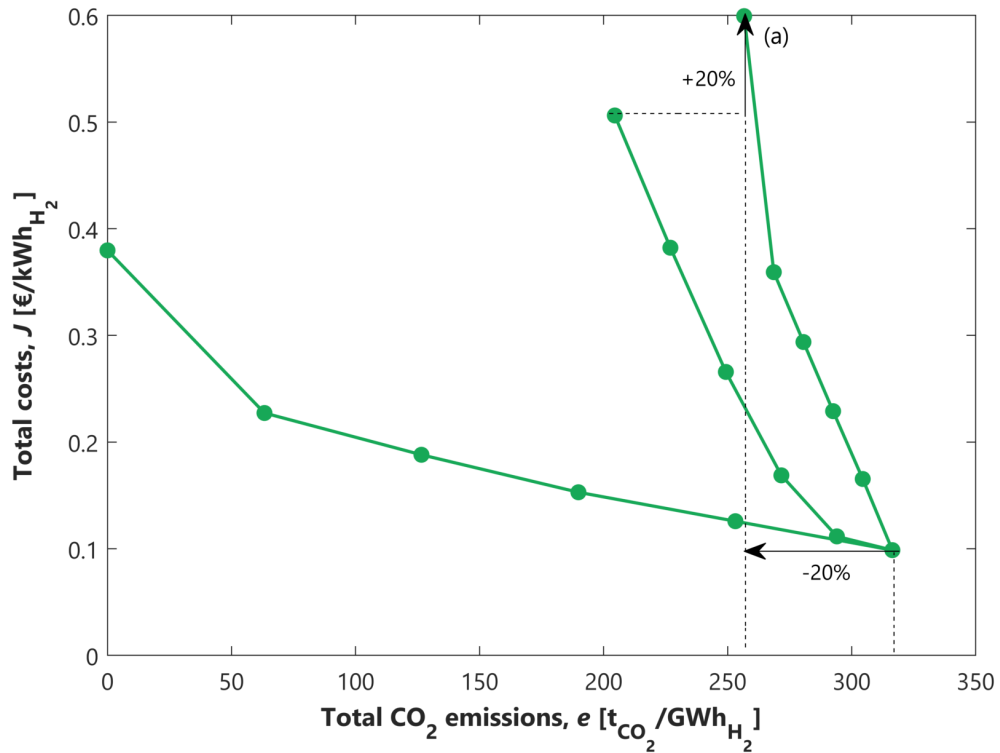
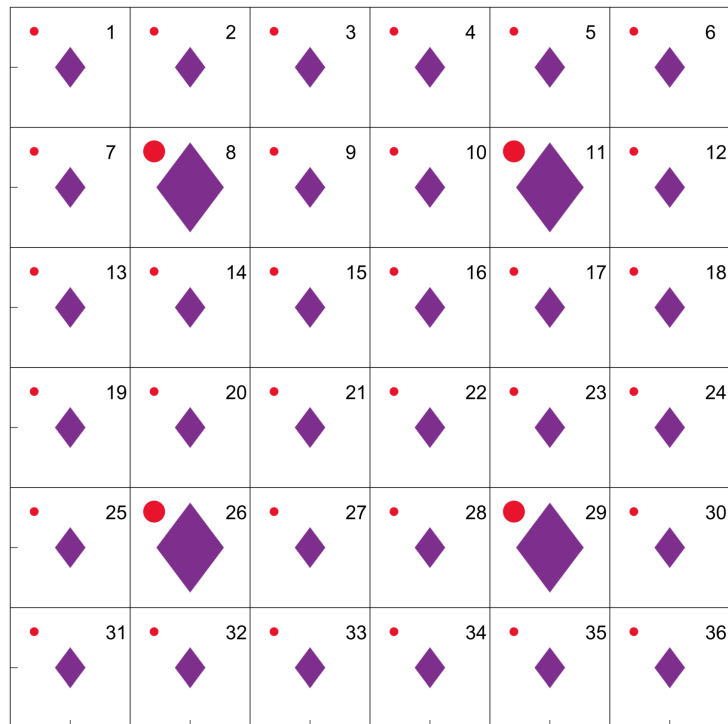


Figure 46: Pareto front with 0% of H<sub>2</sub> demand satisfied by biomass potential.

In this third analysis, the biomass potential both for the wet and for the dry biomass technologies is set to zero. Consequently, the technology portfolio is limited only to two technologies: the SMR and the electrolyzer. The competition between these two technologies is already been discussed in section 6.1; the Pareto front is consequently the same as in Fig. 34. However, the interesting added value is the comparison with the Pareto front of the previous analysis: the total emissions of the system are decreased of 20% from the minum cost to the minum emissions configuration, less than the previous Pareto front which decreased by 30%. The reason, of course, is the absence of the biomass technologies in the portfolio. The electrolyzer is the only technology which is installed along the Pareto to decrease the total CO<sub>2</sub> emissions of the system. The total costs in all the configurations is higher with respect to the previous Pareto fronts shown, due to the high cost associated with the electrolyzer technology. In particular, from the fifth to the minimum emission point a huge increase in the costs is visible, because of one electrolyzer is installed in every node in the system, rural and urban. This minimum emission configuration is shown in the following figure, point (a) in the Pareto front.



**Figure 47:** Minimum emissions configuration with 0% of H<sub>2</sub> demand satisfied by biomass potential.

**Result: 0% H<sub>2</sub> demand satisfied by biomass potential, without PEME**

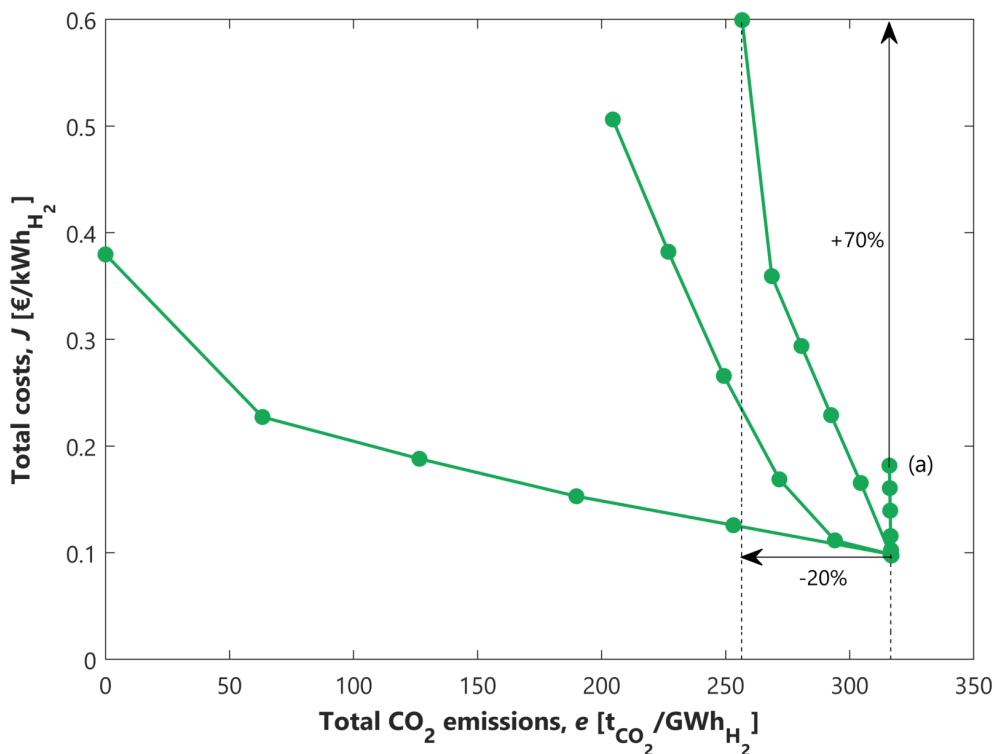


**Figure 48:** Pareto front with 0% of H<sub>2</sub> demand satisfied by biomass potential and with no PEME available.

The additional Pareto front shown in Fig. 48 presents only the SMR as technology available. It is clear that the emissions are almost not decreased along the Pareto, they go from 316.8 to 316.1  $\text{ton}_{\text{CO}_2}/\text{GWh}_{\text{H}_2}$ . The minimum emission configuration (a) shown in Fig. 49 presents one SMR installed per node. In this case, the decrease in the CO<sub>2</sub> emissions is performed only by the elimination of the pipeline network, whose emissions coefficient  $\gamma$  is way less impacting the result in comparison to the emissions from a technology, as previously discussed; this is why the Pareto stays almost vertical. The interesting aspect to notice is that from configuration (a) to the minimum emissions of the previous Pareto front in which only electrolyzers were installed, an increase in 70% on the total cost is performed, which is able to decrease the total emissions only by 20%.

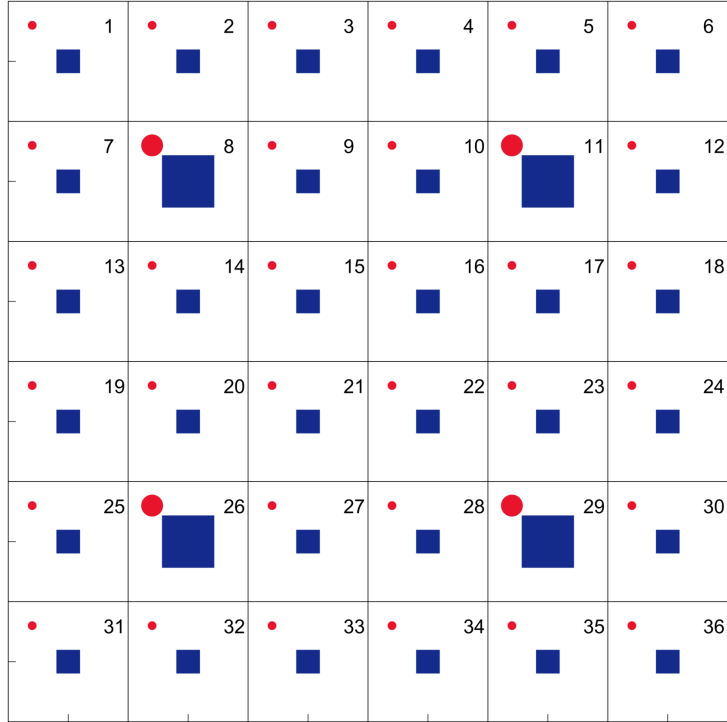


**Figure 49:** Minimum emissions configuration with 0% of H<sub>2</sub> demand satisfied by biomass potential, without PEME.

### Conclusions

This analysis was performed to achieve a deeper understanding of the competition between the various hydrogen production pathways from renewable energy sources: biomass gasification, steam biomethane reforming and the electrolyzer. The assumption that the CO<sub>2</sub> emitted from the biosources is considered biogenic, has a strong influence on the conclusions on this analysis. Firstly, both of the biomass technologies are able to decrease more considerably the emissions in comparison to the electrolyzer, which reaches only 20% of reduction in the minimum emission configuration of the Pareto. This is because the emission factor related to the Swiss electricity grid, which is already very low since the majority of energy is produced by hydropower and nuclear technologies. The other considerable drawback of the electrolyzer is that it is much more expensive than the others green hydrogen production pathways, and its efficiency is approximately equal to the steam biomethane reforming process.

The optimal design of a low-carbon supply chain would mean to couple to a blue hydrogen production pathway such as the SMR with one or more of the green technologies previously described. The conclusion of this analysis is that if the electrolyzer alone is the choice, not a significant impact can be achieved on the overall system concerning the sustainability. Instead, if it is coupled with biosources technology, a significant decrease on the overall emissions can be achieved. Moreover and even more importantly, the total cost of this type of hydrogen supply chain will be lower, as shows the comparison between the third and fourth Pareto fronts in Fig. 48.

### 6.3 Role of carbon capture and storage

In Fig. 46 is visible how the SMR technology alone is not able to compete with the other green hydrogen production pathways in terms of CO<sub>2</sub> emissions reduction along the Pareto. For this reason, in order to achieve a lower carbon intensity in the overall supply chain with this technology, the two capture technologies SMRCCS  $\phi = 0.54$  and SMRCCS  $\phi = 0.89$  are inserted in the technology portfolio and the competition between the two of them with the SMR is analyzed.

In this analysis, the configuration of the system changes from the ideal schematic and symmetric case (2.1.1) to the realistic schematic configuration (2.1.2).

#### Research question

*How is the H<sub>2</sub> network influenced by the addition of carbon capture technologies and storage infrastructure?*

#### 6.3.1 Capture technologies without CO<sub>2</sub> sink

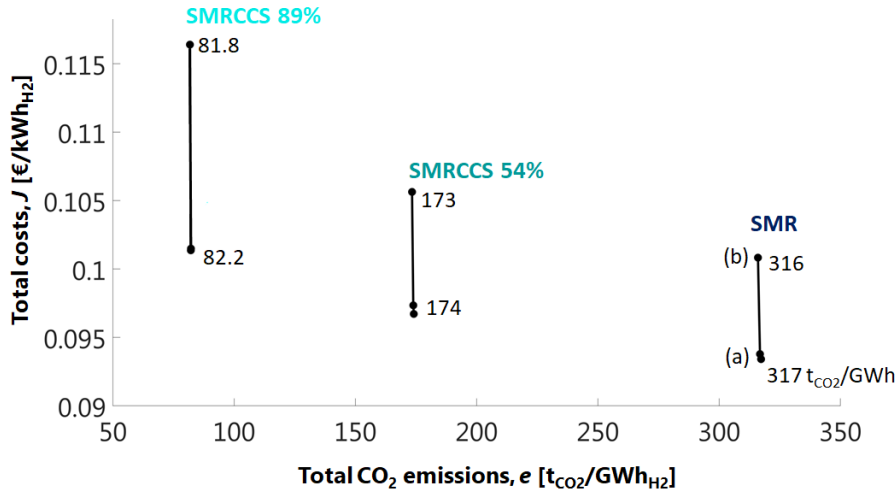


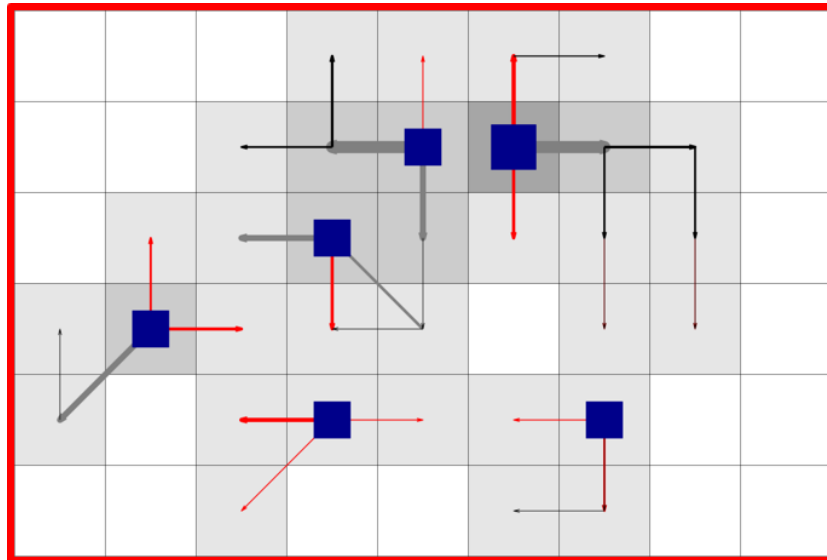
**Figure 50:** Pareto fronts with the SMR technology, the SMR SMRCCS  $\phi = 0.54$  and the SMRCCS  $\phi = 0.89$ .

In this first analysis, the capture technologies produces hydrogen and carbon dioxide: the latter is stored in a fictitious CO<sub>2</sub> storage in-loc, located in the same node where the technology is installed. The aim here is only to understand the impacts on the total emissions reduction and on the total cost increase on the overall supply chain due to the capture technologies.

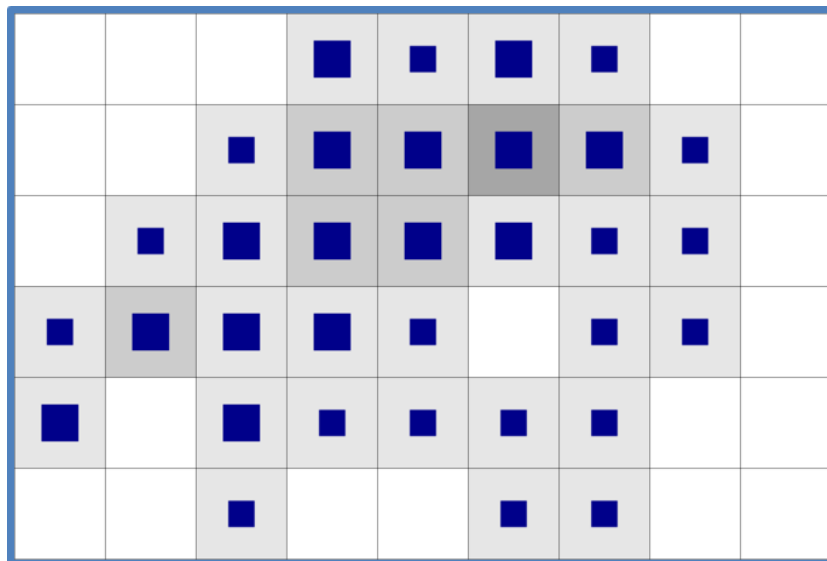
As it is visible in Fig. 50, the first Pareto from the right is identical to the one presented in the previous biomass analysis with only the SMR and it represents the reference fossil-nature Pareto based. The second Pareto presents as technology portfolio only the SMRCCS  $\phi = 0.54$  and the total emissions of the sistem from the first Pareto are already decreased by 45%. Having only one technology available, all the Pareto fronts presented are almost vertical, as the decrease in the total CO<sub>2</sub> emissions are only due the elimination of the network, from a centralised configuration to a completely decentralised configuration, an effect noticed many times in the previous results. As already discussed, the network has a small impact on the total costs of the system, that is the reason why the total costs are decreased of a very small percentage from the minimum cost point to the minimum emission point. Naturally, the total costs of the system increase, due to the addition of the capture plant to the SMR process. The costs describing the SMRCCS  $\phi = 0.54$  technology are reported in the ???. In particular, the costs of the SMR plant are multiplied by a factor of 1.2, so 20% higher.

Concerning the second capture technology SMRCCS  $\phi = 0.89$ , the Pareto front presents the overall CO<sub>2</sub> emissions decreased by a factor of 75% from the only SMR case. Naturally, this is due to a higher capture rate  $\phi$ , due to the post combustion capture of the technology presented in section represented in Fig 11. The Pareto front is vertical as the previous ones described, presenting only the decentralisation of the

single technology as an effect to minimize the total emissions. In this case the costs of the technology are increased of 80%, due to a more complex capture plant which results in a higher capture rate. In the following figures the minimum cost configuration of the SMR Pareto and the minimum emission configuration are shown, whose characteristics are exactly the same as the ones achieved with the ideal schematic representation of the system. Minimum cost has a centralized shape, while minimum emissions presents a totally decentralized configuration.



(a) Minimum cost configuration of the SMR Pareto front.



(b) Minimum emissions configuration of the SMR Pareto front.

**Figure 51:** Optimal configurations of the system along the Pareto front when the 20% of  $H_2$  demand can be satisfied by biomass technologies.

### 6.3.2 Capture technologies with CO<sub>2</sub> sink

In this second analysis, the main assumption is to add to the system the possibility to store the CO<sub>2</sub> produced by the capture technologies in two different sinks, localised in two cities of Switzerland:

- **Bern:** being a central Swiss city, it represents the Swiss CO<sub>2</sub> storage of the supply chain.
- **Basel:** being a Swiss city on the border, it represents the CO<sub>2</sub> storage abroad of the supply chain.

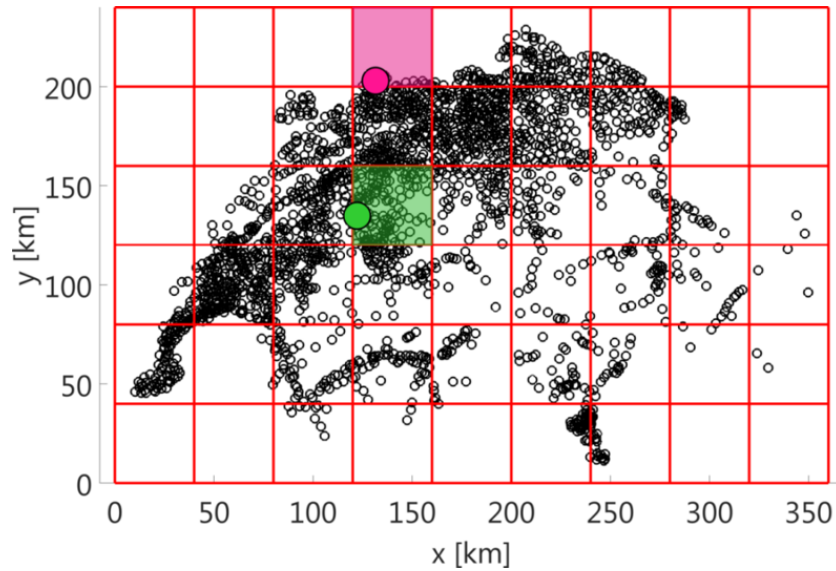


**Figure 52:** Realistic schematic configuration with the location of the two storages: the green color refers to Bern, while the pink color refers to Basel.

The comparison between these two storages is connected with the concept behind: the storage in Bern represents a possible storage in Switzerland, which is very improbable to be created as an infrastructure, while the storage in Basel represents the possibility to store the CO<sub>2</sub> abroad, for example in Norway, as it is already done nowadays.

Naturally, a storage infrastructure also includes the CO<sub>2</sub> network associated, indicated with the orange color. In particular, the pipeline is selected and described with the input parameters summarized in ???. The CO<sub>2</sub> storage instead, is described as any other technology with an efficiency  $\eta$  equal to zero, so presenting only the CO<sub>2</sub> as an mass flow entering, but nothing which exits ???.

The final goal of this analysis is the understanding of the impact of the location of the storages in the overall supply chain, together with the competition of the different capture technologies with respect to the SMR as the reference fossil-based technology.

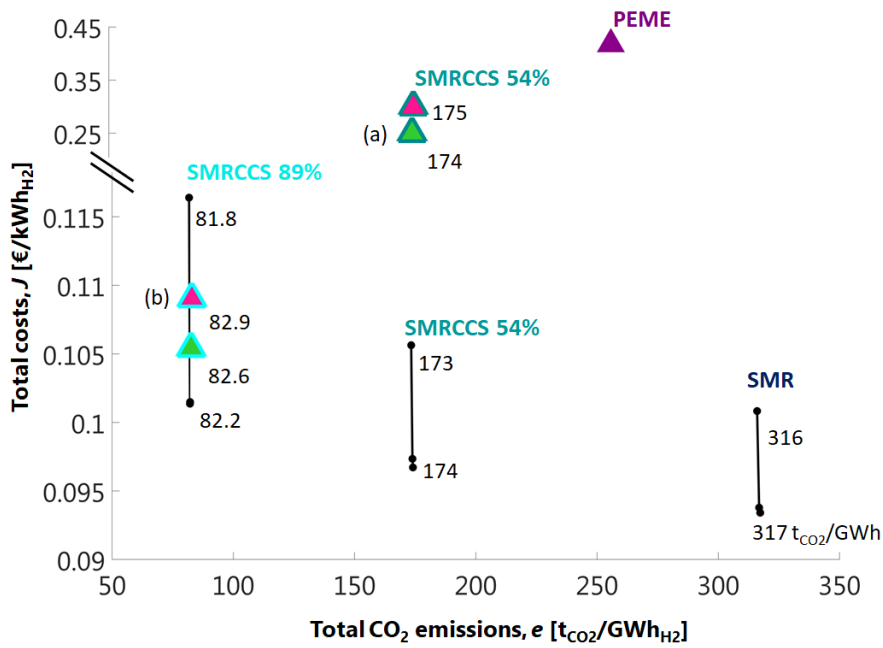


**Figure 53:** Pareto fronts with and without the possibility to store CO<sub>2</sub> in external storages.

In the above Fig. 53, it is represented the comparison between the Pareto fronts without the CO<sub>2</sub> sink, already shown in Fig. 50, and the minimum emissions points of the new Pareto which considers also the CO<sub>2</sub> storage, both for the SMRCCS  $\phi = 0.54$  and the SMRCCS  $\phi = 0.89$ , represented with the triangle marker. The green one is referred to the CO<sub>2</sub> storage in Bern, while the pink one to the CO<sub>2</sub> storage in Basel.

Starting from the SMRCCS  $\phi = 0.54$ , the the resulting configuration is shown in Fig. 54, referred as (a) in total plot. In Fig. 54, the minimum emission configuration of the system is shown with the SMRCCS

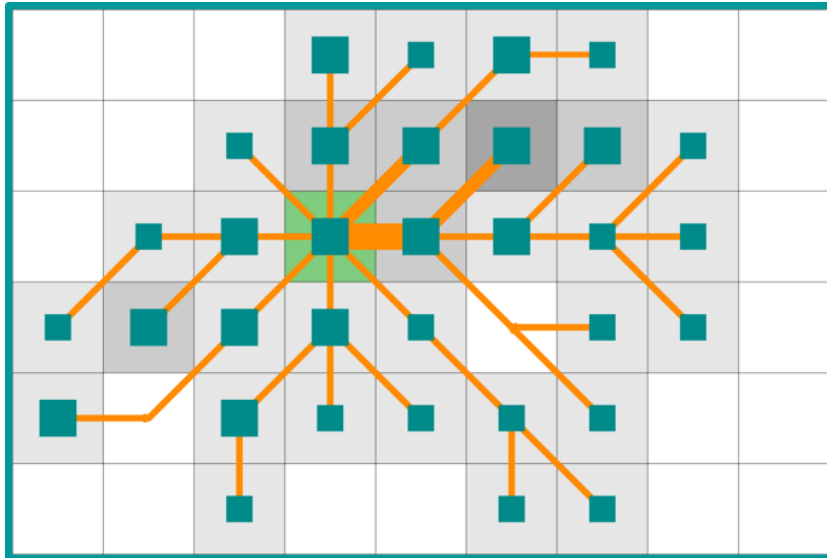


**Figure 54:** Minimum emissions configuration of the system with the CO<sub>2</sub> storage located in Bern, with SMRCCS  $\phi = 0.54$  as the capture technology.

$\phi = 0.54$  technology as the only one available. The configuration is totally decentralised, one SMRCCS is installed per node and all the CO<sub>2</sub> captured is sent to the Swiss central storage in Bern. The total costs of this system are approximately twice in comparison to the minimum emission point of the SMRCCS  $\phi = 0.54$  Pareto front without the CO<sub>2</sub> storage. This is due to the fact that the CO<sub>2</sub> is installed in

every connection of the system, with the associated costs, while in the minimum emission point of the previous Pareto front no network is installed because the emission are stored directly in loco. The pink triangle above the green is representing the minimum emission configuration of the system with the CO<sub>2</sub> storage located in Basel. The total costs are a bit higher due to the fact that it is not central anymore, consequently the connections which comes from far away present more energy losses to overcome and so the costs increase as more carbon dioxide has to be sent.

Concerning the second capture technology SMRCCS  $\phi = 0.89$ , the minimum emissions points shown in Fig. 53 with the CO<sub>2</sub> storage presents completely different features with respect to the previous ones. The minimum emissions configuration is shown in Fig. 55. In this case is visible how the system presents

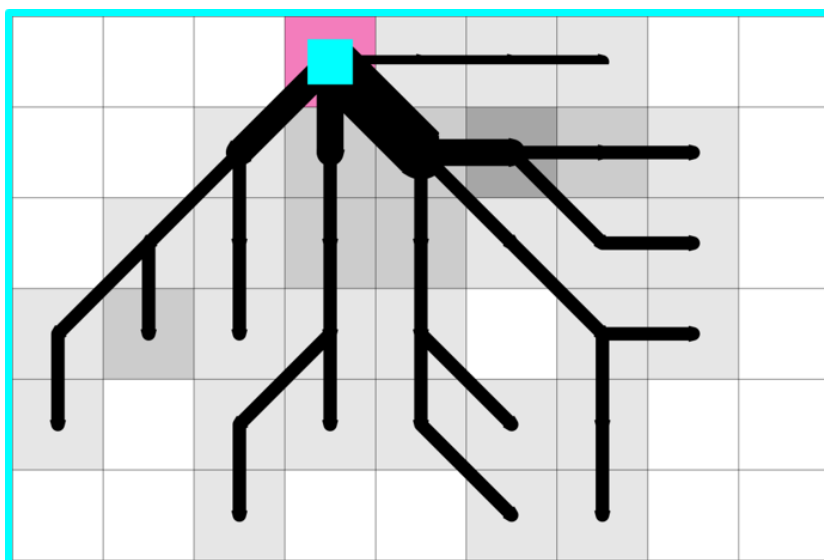


**Figure 55:** Minimum emissions configuration of the system with the CO<sub>2</sub> storage located in Basel, with SMRCCS  $\phi = 0.89$  as the capture technology.

a completely opposite configuration with the one with the SMRCCS  $\phi = 0.54$  technology in Fig. 54. First of all, the technology installed is one in the minimum emissions configuration: a characteristics that is never been encountered in all the previous analyses performed. This SMRCCS  $\phi = 0.89$  is installed exactly in the node where the CO<sub>2</sub> storage is available, capturing the all 89% of the emissions from this big-sized SMR and storing directly the CO<sub>2</sub> in the available storage. For this reason, a CO<sub>2</sub> network has no need to exist, and all the hydrogen produced is transported towards the end users by the pipeline network, the least emitting one of the networks available. The reason for this deep change on the supply chain design is correlated to the amount of CO<sub>2</sub> that is captured. The SMRCCS  $\phi = 0.54$  captures 54% of the emissions, so in the minimum emissions configuration the costs are high as already discussed, but still the optimization chooses the CO<sub>2</sub> network instead of the H<sub>2</sub> network. The SMRCCS  $\phi = 0.89$  instead, captured almost 90% of the emissions from the technology which would result in much higher costs to be encountered if the carbon dioxide is transported, as the mass flow is significantly higher. This is because the CO<sub>2</sub> network is completely eliminated, and the SMRCCS is installed directly in the node where there is the storage availability.

Another important characteristic to notice is that the cost of the minimum emissions configuration in the case of the SMRCCS  $\phi = 0.89$  with the CO<sub>2</sub> storage is lower than the minimum emissions configuration of the previous Pareto front with no storage availability. This is interesting and it consists simply on another example of the size-effect on the investment cost already discussed in 5.4. One big-sized plant has a lower unit cost with respect to a small-sized plant, which are the one installed in the previous minimum emissions configuration. In the end, as already discussed for the SMRCCS  $\phi = 0.54$ , the minimum emissions configuration with the storage available in Bern has a lower overall costs for the same reason (green triangle on the Pareto).

## Conclusions

Both of these analyses are very interesting since they propose another option for a low-carbon hydrogen

supply chain which can compete with the biomass-based chain proposed in section 6.2. In this case, the competition encountered is network-based: hydrogen vs CO<sub>2</sub> network. For low capture rates, the CO<sub>2</sub> network is chosen as the mass flow transported is not so high; after a certain limit of capture rate, the configuration switches to a total H<sub>2</sub> network, installing the one big-sized technology in the node where the storage is available.

## 7 Conclusions and Outlook

### 7.1 Summary of main results

The first part of this thesis has modeling perspective: the aim was to gain a deeper understanding on the model describing the hydrogen supply chain, performing many sensitivity analyses to focus the attention on the main parameters influencing the system. The results from those studies have permitted to choose with attention the input data to the optimization problem, knowing the impact they would have on the final design of the supply chain. The second part of the thesis concerns applying these conclusions in order to design the final optimal design.

The two main results concern two different but equally important features of the optimal design: the technology competition on one side and the network competition on the other.

Concerning the first, the goal of the biomass analysis was to perform an overall comparison between the four hydrogen supply chains in the technology portfolio, while varying the wet and dry biomass availability of the system (48). From the analysis of the final results, this parameter influences the system significantly and represents a discriminatory between the technologies. This conclusion may be similar to a real case study: in many countries biomass as an energy source is limited or not available at all, so other technologies have to supply the energy to the end-users.

The competition between the two biomass-based hydrogen production pathways is already very interesting to analyze. The biomass gasification is the cheapest and also the less efficient between the two: in the configurations on the Pareto front with low total costs of the overall system, it is always the one selected and installed in the urban nodes. The centralization of the biomass gasification technology means that the biomass truck network associated is also active with the associated emissions, this because the biomass has to be brought from the rural nodes where it is available to the urban nodes. The configuration changes as along the Pareto the CO<sub>2</sub> are decreased, the biomethane reformer is also installed in the rural nodes, supplying the energy demand in-loco or even transporting it towards the urban nodes. For this reason the costs increase, being the more expensive option. The decentralisation of the system continues to increase and in the minimum emissions configuration, both of the technologies are decentralized and the hydrogen is supplied to the main nodes.

When the system has to decrease the emissions below a certain threshold the truck transporting biomass is substituted with the pipeline to supply hydrogen from the decentralized node.

When the total biomass availability is more constrained, it is interesting to see that the system saturates the biomass and the electrolyzer hydrogen production pathway is selected, being the other green technology in the portfolio. Taking the electricity from the grid, it has an emission factor associated and the reduction of the emissions induced on the system is far less in comparison to the biomass-based technologies, whose emissions are considered biogenic. Moreover, the costs of the overall system is significantly higher due to the fact that the electrolyzer is still the most expensive option. This impact of the electrolyzer cost is even clearer when it is competing only with the SMR technology, and without the possibility to exploit any of the two biomass energies also the total CO<sub>2</sub> emissions increase.

In order to couple a fossil-based technology as the SMR with a green hydrogen production pathway, the biomass-based technologies seem a very promising choice. The costs are way lower than the electrolyzer and the overall emission reduction is way more impacting the the optimized design of the hydrogen supply chain.

Concerning the second analysis, other two low-carbon hydrogen production pathways are analyzed: the SMR capture technologies with two very different capture rates,  $\phi = 0.89$  and  $\phi = 0.54$ . The interesting result is achieved when there is possibility to transport and store the CO<sub>2</sub> in an underground storage in two possible location: one centralized (Bern) and one decentralized (Basel). This feature causes the surprising competition between the two networks available, the hydrogen and the CO<sub>2</sub> networks. If the CO<sub>2</sub> captured is only 54%, the minimum emissions configuration of the system presents the total decentralisation of the capture technology and consequently the maximum size of the CO<sub>2</sub> network installed, which is all transported to the underground storage, either in Bern or Basel. This configuration causes a significant increase in the costs of the system. Otherwise, considering the second capture technology  $\phi = 0.89$ , a much higher fraction of emissions is captured. The impact on the configuration

are surprisingly huge: in the minimum emissions configuration only one big-sized technology is installed exactly in the node when there is the storage availability. For this reason, there is no need to install a CO<sub>2</sub> network associated. All the emissions are captured in-loco, and the hydrogen is transported from there towards all the end users. Moreover and even more importantly, the costs of the system is lower in comparison to a case where the CO<sub>2</sub> emissions are captured with a smaller fraction. The technology capturing more is surely more expensive, but the size effect of the investment costs is more impacting: consequently, a one big-sized technology capturing more is way less expensive than many small-sized technologies capturing less. For this reason, the localised capture at the source seems to be the preferred option for the overall optimal sustainability of the hydrogen supply chain.

## 7.2 Outlook

The following steps in this project can be multiple and all of them seem very attractive and interesting. Surely, the achievement of a zero-emissions hydrogen supply chain seems the most probable option, meaning the competition between the capture technologies and the biomass technologies. Secondly, the CO<sub>2</sub> storage in Basel is symbolically referring to a possible storage abroad: the most probable option could be Norway. In that case, to analyze a European case study would be surely interesting, in order to see if the results achieved from Swiss case study also reflect on broader configurations of the system.

# Appendix

## A Hydrogen demand

The hydrogen demand for the realistic configuration is defined by collecting data on population and motorization rate for all municipalities in Switzerland [21], which are aggregated based on their geographic location, according to a given spatial resolution explained in 2.1.2. Then, based on average Swiss values of car occupancy, distance traveled, and consumption of fuel cell vehicles, the average hourly hydrogen demand,  $D$ , is defined as follows:

$$D = p \frac{m}{o} l \eta \quad (20)$$

where  $p$  is the cell-dependent aggregated population,  $m$  the cell-dependent motorization rate (having the units of cars per person),  $o$  the average car occupancy in Switzerland (having the units of people per car),  $l$  the average distance traveled per hour in Switzerland (having the units of meters per hour),  $\eta$  the H<sub>2</sub> fuel consumption under the US EPA test conditions (having the units of kWh per meter). The values of such parameters are reported in table 2.

**Table 2:** Parameters used to calculate hydrogen demand required for Swiss mobility within the realistic system configuration.

Average car occupancy, $o$	[p/car]	1.57 [21]
Average distance traveled per hour, $l$	[m/(h p)]	992 [22]
Average fuel consumption fuel cell vehicles, $\eta$	[kWh/m]	$3.3 \cdot 10^{-4}$ [23]

## B Energy carriers

The carrier prices and carbon intensity are summarized in table 3. The import gas price is considered equal to 0.06 €/kWh [24], while a value of 0.2 €/kWh is considered for the electricity import price as an average value for industry use. A carbon intensity of 237 g<sub>CO<sub>2</sub></sub>/kWh is considered for the natural gas grid, whereas a value of 137 g<sub>CO<sub>2</sub></sub>/kWh is considered for the electricity grid [25, ?]. It is worth noting that in Switzerland the carbon intensity of the electricity grid is relatively low due to the major fraction of hydro and nuclear power, which add up to about 95% of the installed Swiss capacity [26]. Finally, although CO<sub>2</sub> emissions are associated to the consumption of biomass, this is assumed to be carbon-neutral due to the carbon offset occurring during the biomass lifecycle.

**Table 3:** Carrier prices and carbon intensity.

Carrier	$u$ [€/kWh]	$v$ [€/kWh]	$\epsilon$ [gCO <sub>2</sub> eq/kWh]
Natural gas	0.06 [24]	–	237
Electricity	0.2	–	137
Wet biomass	0.005 [17]	–	0
Dry biomass	0.07 [17]	–	0

## C Technology cost coefficients and performance

Each technology is characterized by a piece-wise affine approximation of the investment cost. Increasing the size, the unit cost ( $m$ ), expressed in €/kW, decreases and the fixed cost ( $q$ ) in € increases. Concerning the performance, each technology is characterized by an energetic efficiency taken from the literature.

**Table 4:** Parameters describing the conversion performance of production technologies.

Technology	Conversion	$\eta$	$S^{\min}$ [kW]	$S^{\max}$ [kW]
PEME [?]	$e \rightarrow H_2$	0.53	0	$10^8$
SMR <sup>[12]</sup>	$NG \rightarrow H_2$	0.75	1000	$10^8$
	$NG \rightarrow e$	0.03		
SMR-CCS, $\phi = 0.54$	<sup>[12]</sup> $NG \rightarrow H_2$	0.75	1000	$10^8$
	$NG \rightarrow e$	0.004		
	$NG \rightarrow CO_2$	0.001 ton/kWh		
SMR-CCS, $\phi = 0.90$	<sup>[12]</sup> $NG \rightarrow H_2$	0.75	1000	$10^8$
	$NG \rightarrow e$	0.001		
	$NG \rightarrow CO_2$	0.002 ton/kWh		
Bio-SMR <sup>[19]</sup>	$b \rightarrow H_2$	0.50	1000	$10^8$
Gasifier <sup>[18]</sup>	$B \rightarrow H_2$	0.33	1000	$10^8$
CO <sub>2</sub> storage	$CO_2 \rightarrow CO_2$	0	0 ton	$10^9$ ton

**Table 5:** Parameters describing the cost coefficients of production technologies.

Technology	Conversion	$m_1, m_2$ [€/kW]	$q_1, q_2$ [€]	$S^{\min}$ [kW]	$S^{\max}$ [kW]
PEME [?]	$e \rightarrow H_2$	1000	$1.5 \times 10^5$	0	$10^8$
SMR <sup>[12]</sup>	$NG \rightarrow H_2$	526, 235	$9.5 \times 10^6, 1.5 \times 10^7$	1000	$10^8$
	$NG \rightarrow e$				
SMR-CCS, $\phi = 0.54$	<sup>[12]</sup> $NG \rightarrow H_2$	621, 726	$1.1 \times 10^7, 1.8 \times 10^7$	1000	$10^8$
	$NG \rightarrow e$				
	$NG \rightarrow CO_2$				
SMR-CCS, $\phi = 0.90$	<sup>[12]</sup> $NG \rightarrow H_2$	940, 419	$1.7 \times 10^7, 2.7 \times 10^7$	1000	$10^8$
	$NG \rightarrow e$				
	$NG \rightarrow CO_2$				
Bio-SMR <sup>[19]</sup>	$b \rightarrow H_2$	947, 422	$1.7 \times 10^7, 2.7 \times 10^7$	1000	$10^8$
Gasifier <sup>[27]</sup>	$B \rightarrow H_2$	737, 329	$1.3 \times 10^7, 2.1 \times 10^7$	1000	$10^8$
CO <sub>2</sub> storage	$CO_2 \rightarrow CO_2$	0	0 ton	$10^9$ ton	

## D Network input data

- **Minimum and maximum size**

Firstly, each network is described by a minimum and maximum capacity. The maximum is set referring to[5]. In this paper, the capacities proposed are for liquid hydrogen:

$$V_{\text{Truck}} = 58 \text{ m}^3/\text{unit}$$

$$V_{\text{Railway}} = 128 \text{ m}^3/\text{unit}$$

Supposing that gaseous hydrogen is transported at a pressure of 300 bar and at a temperature of 25°C, the resulting density is  $\rho = 20 \text{ kg/m}^3$ . The following capacities for gaseous hydrogen are obtained:  $V_{\text{Truck}} = 1160 \text{ kg/unit}$

$$V_{\text{Railway}} = 2560 \text{ kg/unit}$$

Consequently, the maximum energy carried by the two networks are:

$$\text{Energy}_{\text{Truck}} = 38628 \text{ kWh/unit}$$

$$\text{Energy}_{\text{Railway}} = 85248 \text{ kWh/unit}$$

The maximum energy carried by railway is then multiplied by 10, because a train of 10 carriages is considered. These two energies are set to be transported hourly, following the temporal distribution of the demand, i.e one truck or one train per hour. Concerning the minimum energy transported, it is set to be one truck or one train per day, so the maximum capacities divided by 24 hours. Concerning the pipeline, the minimum energy transported is calculated setting a diameter of 20 cm with a flow velocity of 5 m/s. Instead, the maximum energy transported is considered with a diameter of 1 m and a flow velocity of 10 m/s. All these input parameters are summarized in the table below:

Network	Minimum size [kWh]	Maximum size [kWh]	$l$ [1/m]
Truck	1610	38628	$5 \times 10^{-7}$
Railway	35520	85248	$5 \times 10^{-7}$
Pipeline	1696	84823	$5 \times 10^{-7}$

**Table 6:** Minimum and maximum size for the selected networks.

- **Cost and CO<sub>2</sub> emissions coefficients**

Secondly, each network is characterized by three coefficients:

- Investment cost coefficient  $\alpha$
- Operational cost coefficient  $\beta$
- CO<sub>2</sub> emissions coefficient  $\gamma$

For the truck network,  $\alpha$  is expressed in €/kWh and represents how much one truck costs per unit of energy transported [5]. The cost for a truck comprises the tank unit cost, the cab cost and the undercarriage cost. About the railway network,  $\alpha$  is also expressed in €/kWh and comprises the tank unit cost and the undercarriage cost [5]. Concerning the pipeline,  $\alpha$  is expressed as €/kWh/m, so cost per unit of energy transported per unit length. This cost accounts for the material cost and the labor cost. Instead,  $\beta$  for every network is expressed in €/kWh/m. It accounts for the price of the fuel and for the fuel economy, diesel and electricity for truck and railway respectively. Concerning the pipeline,  $\beta$  is chosen to be equal to zero because the operational cost for a pipeline is negligible with respect to the investment cost. Finally,  $\gamma$  is expressed in ton<sub>CO<sub>2</sub></sub>/kWh/m, so the amount of emitted CO<sub>2</sub> per unit of energy transported per unit of distance covered.

Network	$\alpha_{\text{T,R}}$ [€/kWh]	$\alpha_{\text{P}}$ [€/kWh/m]	$\beta$ [€/kWh/m]	$\gamma$ [ton <sub>CO<sub>2</sub></sub> /kWh/m]
Truck	13[5]	-	$2 \times 10^{-8}$ [28]	$4 \times 10^{-12}$
Railway	6[5]	-	$3 \times 10^{-10}$ [29]	$2 \times 10^{-14}$ [29]
Pipeline	-	0.008[30]	0	$6 \times 10^{-15}$

**Table 7:** Cost and emissions coefficients for the selected networks.

## References

- [1] Paolo Gabrielli, Matteo Gazzani, Emanuele Martelli, and Marco Mazzotti. Optimal design of multi-energy systems with seasonal storage. *Applied Energy*, 219(June 2017):408–424, 2018.
- [2] Paris Agreement.
- [3] IPCC. Global Warming of 1.5 °C: Summary for Policymakers. Technical report, Intergovernmental Panel on Climate Change, 2018.
- [4] FAOSTAT.
- [5] A. Almansoori and N. Shah. Design and operation of a future hydrogen supply chain: Multi-period model. *International Journal of Hydrogen Energy*, 34(19):7883–7897, 2009.
- [6] SINTEF. Elegancy.
- [7] A C T Project Number, Low-carbon Economy, and C C S Era-net Act. ACT Project Number : ELEGANCY Project full title : Enabling a Low-Carbon Economy via Hydrogen and CCS Technical Specification. (1):1–23, 2018.
- [8] Sabine Kuster. *00 022-1800*. 2018.
- [9] Federal Statistical Office. Population’s transport behaviour.
- [10] Federal Statistical Office. Road vehicles - Stock, level of motorisation.
- [11] Tomtom Esri, DeLorme, HERE, USGS, Intermap, iPC, NRCAN, Esri Japan, METI, Esri China (Hong Kong), Esri (Thailand), MapmyIndia. ArcGIS Online.
- [12] IEAGHG R&D Programme. IEAGHG Technical Report February 2017 Techno - Economic Evaluation of SMR Based Standalone (Merchant) Hydrogen Plant with CCS. (February), 2017.
- [13] Hydrogen Europe. Electrolyzers.
- [14] Paolo Gabrielli, Matteo Gazzani, and Marco Mazzotti. Electrochemical conversion technologies for optimal design of decentralized multi-energy systems: Modeling framework and technology assessment. *Applied Energy*, 221(December 2017):557–575, 2018.
- [15] Marcelo Carmo, David L. Fritz, Jürgen Mergel, and Detlef Stolten. A comprehensive review on PEM water electrolysis. *International Journal of Hydrogen Energy*, 38(12):4901–4934, 2013.
- [16] Meng Ni, Dennis Y.C. Leung, Michael K.H. Leung, and K. Sumathy. An overview of hydrogen production from biomass. *Fuel Processing Technology*, 87(5):461–472, 2006.
- [17] Oliver Thees, Vanessa Burg, Matthias Erni, Gilliane Bowman, and Renato Lemm. Biomassepotenzial der Schweiz für die energetische Nutzung, Ergebnisse des Schweizerischen Energiekompetenzentrums SCCER BIOSWEET. page 299, 2017.
- [18] M. K. Cohce, M. A. Rosen, and I. Dincer. Efficiency evaluation of a biomass gasification-based hydrogen production. *International Journal of Hydrogen Energy*, 36(17):11388–11398, 2011.
- [19] and, , and and. Green Hydrogen Production from Raw Biogas: A Techno-Economic Investigation of Conventional Processes Using Pressure Swing Adsorption Unit. *Processes*, 6(3):19, 2018.
- [20] Alexander Körner. Technology Roadmap Hydrogen and Fuel Cells Technical Annex. page 30, 2015.
- [21] FSO. Population résidante permanente selon l’âge, par canton, district et commune, 2010-2017. Technical report, Swiss Federal Statistical Office, Bern, 2018.
- [22] FSO. Population’s travel behavior 2015. Technical report, Swiss Federal Statistical Office, 2017.
- [23] Andrew Simons and Christian Bauer. A life-cycle perspective on automotive fuel cells. *Applied Energy*, 157:884–896, 2015.

- [24] Energie360. [www.energie360.ch](http://www.energie360.ch), 2018.
- [25] Alice Chevrier. *Calculation of a dynamic carbon factor for the Swiss electricity grid*. PhD thesis, ETH Zurich, 2016.
- [26] Alberto Moro and Laura Lonza. Electricity carbon intensity in European Member States: Impacts on GHG emissions of electric vehicles. *Transportation Research Part D: Transport and Environment*, 64:5–14, oct 2018.
- [27] P Spath, A Aden, T Eggeman, M Ringer, B Wallace, and J Jechura. P. Spath, A. Aden, T. Eggeman, M. Ringer, B. Wallace, and J. Jechura. *Contract*, (May), 2005.
- [28] Global Petrol Price. Swiss diesel price.
- [29] Rapporto di gestione e di sostenibilità delle. 2016.
- [30] Nathan Parker. Using Natural Gas Transmission Pipeline Costs to Estimate Hydrogen Pipeline Costs. page 86, 2004.

## List of Figures

1	Global emissions pathway characteristics [3]. . . . .	1
2	Worldwide carbon dioxide emission by sector [4]. . . . .	2
3	Configuration of the overall hydrogen supply-chain system applied to Switzerland. . . . .	3
4	Ideal and schematic configuration of the system. . . . .	5
5	Realistic schematic configuration of the system. . . . .	6
6	Aggregated hydrogen demand for each cell (log10 scale). . . . .	6
7	ArcGIS configuration of the system. . . . .	7
8	Schematic representation of the investigated energy system. . . . .	8
9	Block diagram of a Steam Methane Reforming process [12]. . . . .	9
10	Block diagram an SMR with capture of CO <sub>2</sub> from shifted syngas using MDEA [12]. . . . .	10
11	Block diagram an SMR with capture of CO <sub>2</sub> from from SMR flue gas using MEA [12]. . . . .	10
12	Block diagram of a Polymer Electrolyte Membrane Electrolyzer process [14]. . . . .	11
13	Block diagram of a Biomass Gasification process for hydrogen production [18]. . . . .	12
14	Block diagram of a Steam Biomethane Reforming process for hydrogen production [19]. . . . .	13
15	Pareto front. . . . .	21
16	Network configuration in different Pareto points. . . . .	22
17	Network competition in three different Pareto points. . . . .	23
18	Minimum cost configuration of the system. . . . .	25
19	Sensitivity analysis on the energy loss parameter $l$ . . . . .	27
20	Total energy losses evolution of the system increasing the energy loss coefficient $l$ . . . . .	28
21	Total H <sub>2</sub> flow transported. . . . .	29
22	Configuration of the system with one unit/day as minimum railway size. . . . .	30
23	Configuration of the system with one unit/day as minimum railway size with modified connectivity matrix. . . . .	31
24	Configuration of the system with one carriage as minimum railway size changed the connectivity matrix. . . . .	31
25	(a) two unit/day as minimum size, (b) three unit/day as minimum size . . . . .	32
26	(a) Truck network with four units/day minimum size, (b) Total network with four/units as minimum size . . . . .	33
27	Sensitivity analysis on the truck minimum size. . . . .	34
28	Specific work of a compressor as a function of the pressure ratio $\pi$ [14]. . . . .	35
29	Minimum cost configuration with and without H <sub>2</sub> compression. . . . .	36
30	Influence of the H <sub>2</sub> compression on the operational cost and on the CO <sub>2</sub> emissions. . . . .	37
31	Linear and piece-wise affine approximation of the investment cost. . . . .	38
32	Minimum cost configuration with a piece-wise affine and linear approximation of the investment cost. . . . .	38
33	Minimum cost configuration with a piece-wise affine and linear approximation of the investment cost. . . . .	39
34	Pareto front with SMR and PEME technologies. . . . .	40
35	Optimal configurations of the system along the Pareto front. . . . .	41
36	Size of the technologies and energy imported from the grids along the Pareto front. . . . .	42
37	Impact of the emission factor of the electricity grid $\epsilon_e$ in the minimum emission configuration. . . . .	43
38	Impact of the emission factor of the electricity grid $\epsilon_e$ in the minimum emission configuration. . . . .	44
39	Pareto front with total H <sub>2</sub> demand satisfied by biomass potential. . . . .	46
40	Optimal configurations of the system along the Pareto front when the total H <sub>2</sub> demand can be satisfied by biomass technologies. . . . .	48
41	Activated connections, hydrogen flow and size of the installed technologies along the Pareto front with total H <sub>2</sub> demand satisfied by biomass technologies. . . . .	49
42	Biomass exploitation and decentralisation along the Pareto front. . . . .	49
43	Pareto front with 20% of H <sub>2</sub> demand satisfied by biomass potential. . . . .	50
44	Optimal configurations of the system along the Pareto front when the 20% of H <sub>2</sub> demand can be satisfied by biomass technologies. . . . .	51
45	Biomass exploitation and decentralisation along the Pareto front. . . . .	52
46	Pareto front with 0% of H <sub>2</sub> demand satisfied by biomass potential. . . . .	52

47	Minimum emissions configuration with 0% of H <sub>2</sub> demand satisfied by biomass potential. .	53
48	Pareto front with 0% of H <sub>2</sub> demand satisfied by biomass potential and with no PEME available. . . . .	54
49	Minimum emissions configuration with 0% of H <sub>2</sub> demand satisfied by biomass potential, without PEME. . . . .	55
50	Pareto fronts with the SMR technology, the SMR SMRCCS $\phi = 0.54$ and the SMRCCS $\phi = 0.89$ . . . . .	56
51	Optimal configurations of the system along the Pareto front when the 20% of H <sub>2</sub> demand can be satisfied by biomass technologies. . . . .	57
52	Realistic schematic configuration with the location of the two storages: the green color refers to Bern, while the pink color refers to Basel. . . . .	58
53	Pareto fronts with and without the possibility to store CO <sub>2</sub> in external storages. . . . .	59
54	Minimum emissions configuration of the system with the CO <sub>2</sub> storage located in Bern, with SMRCCS $\phi = 0.54$ as the capture technology. . . . .	59
55	Minimum emissions configuration of the system with the CO <sub>2</sub> storage located in Basel, with SMRCCS $\phi = 0.89$ as the capture technology. . . . .	60

## List of Tables

1	Truck network input parameters for dry biomass. . . . .	45
2	Parameters used to calculate hydrogen demand required for Swiss mobility within the realistic system configuration. . . . .	64
3	Carrier prices and carbon intensity. . . . .	64
4	Parameters describing the conversion performance of production technologies. . . . .	65
5	Parameters describing the cost coefficients of production technologies. . . . .	65
6	Minimum and maximum size for the selected networks. . . . .	66
7	Cost and emissions coefficients for the selected networks. . . . .	66